



---

# Automatic Dental Caries Detection in Bitewing Radiographs

---

## Author

Vincent Idah Majanga

## Supervisor

Prof. Serestina Viriri

*A thesis submitted to the University of KwaZulu-Natal, College of Agriculture,  
Engineering and Science, in fulfilment of the requirements for the degree of  
Doctor of Philosophy in Computer Science*

School of Mathematics, Statistics and Computer Science,  
University of KwaZulu-Natal, Durban, South Africa.

©{Vincent Idah Majanga} {2022}

## Declaration of Authorship

I, Vincent Idah Majanga, declare that this thesis titled, “Automatic Dental Caries Detection” and the work presented in it are my own. I declare that:

1. The research reported in this thesis, except where otherwise indicated or acknowledged, is my original work;
2. This thesis has not been submitted in full or in part for any degree or examination to any other university;
3. This thesis does not contain other persons’ data, pictures, graphs or other information, unless specifically acknowledged as being sourced from other persons;
4. This thesis does not contain other persons’ writing, unless specifically acknowledged as being sourced from other researchers. Where other written sources have been quoted, then:
  - (a) their words have been re-written, but the general information attributed to them has been referenced;
  - (b) where their exact words have been used, their writing has been placed inside quotation marks, and referenced;
5. This thesis does not contain text, graphics or tables copied and pasted from the Internet, unless specifically acknowledged, and the source being detailed in the thesis and in the References sections.

**Candidate:** Vincent Idah Majanga      **Signed** VIM      **Date:** 21/03/2022

As the candidate’s supervisors, we have approved this dissertation for submission.

**Supervisor:** Prof. Serestina Viriri      **Signed:**       **Date:** 21/03/2022

## List of Publications

I, Vincent Idah Majanga, declare that the following are publications from this thesis:

1. **V. Majanga, S. Viriri**, "Dental Images Segmentation Using Threshold Connected Component Analysis", *Computational Intelligence and Neuroscience*, vol. 2021, (2021). DOI: <https://doi.org/10.1155/2021/2921508>
2. **V. Majanga, S. Viriri**, "Automatic Blob Detection for Dental Caries", *Applied Sciences*, vol. 11, no. 19, 9232 (2021). DOI: <https://doi.org/10.3390/app11199232>
3. **V. Majanga, S. Viriri**, "Dropout Regularization for Automatic Segmented Dental Images", *Recent Challenges in Intelligent Information and Database Systems*, CCIS Springer, vol. 1371, pp. 254–265, (2021). DOI: [https://doi.org/10.1007/978-981-16-1685-3\\_21](https://doi.org/10.1007/978-981-16-1685-3_21)
4. **V. Majanga, S. Viriri**, "A Deep Learning Approach for Automatic Segmentation of Dental Images", *Mining Intelligence and Knowledge Exploration*, Springer, vol. 11987, pp. 143–15, (2020). DOI: [https://doi.org/10.1007/978-3-030-66187-8\\_14](https://doi.org/10.1007/978-3-030-66187-8_14)
5. **V. Majanga, S. Viriri**, "A Survey of Dental Caries Segmentation and Detection Techniques", *Computational and Mathematical Methods in Medicine*, (2022). (Under review).

## List of Abbreviations

**CT** Computed Tomograph

**CNN** Convolution Neural Network

**DNN** Deep Neural Network

**FCNN** Fully Convolution Neural Network

**ROI** Region Of Interest

**FPN** Feature Pyramid Network

**ResNet** Residual Network

**FCN** Fully Convolution Network

**FOF** First Order Features

**RLM** Run-Length Matrix

**GLCM** Gray Level Co-occurrence Matrix

**GTDM** Gray Tone Difference Matrix

**LBP** Local Binary Pattern

**LTP** Local Ternary Pattern

**mMG** Multiple Morphological Gradient

**RNN** Recurrent Neural Networks

**RELU** Rectified Linear Unit

**AlexNet** Alex Network

**LeNet** Le Network

**VGGNET** Visual Geometry Group Network

**GoogleNet** Google Network

**Inception v3** Inception Version 3

**LSM** Long Short Term Memory

**GRU** Gated Recurrent Unit

**MRF** Markov Random Field

**DBN** Deep Belief Networks

**CPU** Central Processing Unit

**GPU** Graphical Processing Unit

**U-Net** Universal Network

**PASCAL VOC** PASCAL Visual Object

**NORB** NYU Object Recognition Benchmark

**CIFAR** Canadian Institute For Advanced Research

**CSAIL** Computer Science Intelligence Laboratory

**MNIST** Modified National Institute of Standards and Technology

**MIT** Massachussets Institute of Technology

**X-rays** Radiographic images

# Abstract

Dental Caries is one of the most prevalent chronic disease around the globe. Distinguishing carious lesions has been a challenging task. Conventional computer aided diagnosis and detection methods in the past have heavily relied on visual inspection of teeth. These are only effective on large and clearly visible caries on affected teeth. Conventional methods have been limited in performance due to the complex visual characteristics of dental caries images, which consists of hidden or inaccessible lesions. Early detection of dental caries is an important determinant for treatment and benefits much from the introduction of new tools such as dental radiography. A method for the segmentation of teeth in bitewing X-rays is presented in this thesis, as well as a method for the detection of dental caries on X-ray images using a supervised model. The diagnostic method proposed uses an assessment protocol that is evaluated according to a set of identifiers obtained from a learning model. The proposed technique automatically detects hidden and inaccessible dental caries lesions in bitewing radiographs. The approach employed data augmentation to increase the number of images in the data set in order to have a total of 11,114 dental images. Image pre-processing on the data set was through the use of Gaussian blur filters. Image segmentation was handled through thresholding, erosion and dilation morphology, while image boundary detection was achieved through active contours method. Furthermore, the deep learning based network through the sequential model in Keras extracts features from the images through blob detection. Finally, a convexity threshold value of 0.9 is introduced to aid in the classification of caries as either present or not present. The relative efficacy of the supervised model in diagnosing dental caries when compared to current systems is indicated by the results detailed in this thesis. The proposed model achieved

a 97% correct diagnostic which proved quite competitive with existing models.



## **Dedication**

I dedicate this work to my father Francis Majanga and mother Dr. Eunice Majanga who made great sacrifices to see me succeed in life through good education.

My appreciation goes to God the Almighty, who has seen me through everything thus far.

# Acknowledgments

I would like to thank Prof. Serestina Viriri, who has been my supervisor throughout the duration of my doctoral degree. His kind advice, counsel, guidance and direction is what has made this work possible. Special thanks go to my family, the department of Computer Science UKZN and my friends Omran Salih, Solomon Omatayo, and Ashade Oladimeji for their continuous help and encouragement. Ultimately, I thank God for everything so far.

# Contents

<b>1</b>	<b>Introduction</b>	<b>1</b>
1.1	Tooth Anatomy . . . . .	2
1.2	Dental Caries . . . . .	2
1.3	Dental radiographs-X-rays . . . . .	5
1.4	Factors affecting Dental Caries. . . . .	6
1.5	Prevention of Caries . . . . .	7
1.6	Diagnosis of Caries . . . . .	8
1.7	Treatment of Caries . . . . .	8
1.8	Motivation . . . . .	10
1.9	Problem Statement . . . . .	11
1.10	Research Objectives . . . . .	12
1.11	Contributions . . . . .	12
1.12	Thesis Outline . . . . .	13
<b>2</b>	<b>Background and Related Work</b>	<b>15</b>
2.1	A survey of Dental Caries Segmentation and Detection Techniques . .	15

2.2	Introduction . . . . .	15
2.2.1	Summary . . . . .	49
<b>3</b>	<b>Teeth Segmentation</b>	<b>50</b>
3.1	Dental Images' Segmentation Using Threshold Connected Component Analysis. . . . .	50
3.2	Introduction . . . . .	50
3.3	Summary . . . . .	61
<b>4</b>	<b>Dental Caries Detection</b>	<b>62</b>
4.1	Automatic blob detection for dental caries. . . . .	62
4.2	Introduction . . . . .	62
4.3	Summary . . . . .	75
<b>5</b>	<b>Experimental Results and Discussion</b>	<b>76</b>
5.1	Introduction . . . . .	76
5.2	Dataset . . . . .	77
5.3	Caries Detection Framework . . . . .	77
5.4	Segmentation Results . . . . .	78
5.5	Caries Detection Results . . . . .	82
5.6	Conclusion . . . . .	85
<b>6</b>	<b>Conclusion and Future Work</b>	<b>87</b>
6.1	Conclusion . . . . .	87
6.2	Future Work . . . . .	88

# List of Tables

5.1	Overall comparison of Segmentation Methods. . . . .	82
5.2	Comparison of caries detection methods. . . . .	85

# List of Figures

1.1	Cross-section of the molar tooth [35]. . . . .	3
1.2	Periapical radiograph, Bitewing radiograph, Panoramic radiograph respectively [31]. . . . .	6
1.3	Computer aided system diagram as by [28] . . . . .	9
5.1	Images in the original dataset, images in the generated dataset after augmentation. . . . .	78
5.2	An overview of the caries detection framework. . . . .	79
5.3	Examples of the segmentation results in the dataset. . . . .	81
5.4	Examples of Gaussian filtered images. . . . .	83
5.5	Examples of all detected caries blobs . . . . .	84

# Chapter 1

## Introduction

Dental caries is a major human health problem globally and is a widely spread non-communicable disease. It is also the most prevalent condition according to the 2015 Global Burden of Disease study by [22]. The prevalence of dental caries continues to increase, mostly in low and middle-income countries, due to changes in living conditions and increased urbanization. This increase of cases is due to exposure to fluoride in water supply and inadequate oral hygiene products like toothpaste and tooth brushes. There is also poor access to oral health care services in the community. A majority of dental caries in these communities goes untreated, and severe cases can impair quality of life. For instance, caries may cause difficulties in eating and sleeping and, in advanced stages, may result in chronic infections and pain. Tooth decay is a frequent cause of absenteeism from school or work. In low-income communities, some people have resorted to extraction (pull out) caries in infected teeth when they cause discomfort or pain. Therefore, in order to keep dental caries under control, it is invaluable to treat it at its early stages before it advances.

## 1.1 Tooth Anatomy

The tooth is a small white structure found in the jaw bone of animals and human beings. In human beings, the number of teeth ranges from 20 primary teeth in children to 28-32 permanent teeth in adults. Furthermore, the tooth can be broken down into three main layers: the crown, neck and the root. The crown is the visible region above the gum line, while the neck connects the crown to the root. The root is the region inside the bone socket [35]. Additionally, each tooth comprises hard tissues that protect the soft tissues in the centre. The outermost layer of the tooth is the enamel. This is a hard tissue and beneath it is the dentin which is much softer than the enamel. The dental pulp is found at the centre of the tooth, and houses the blood vessels and tissue vessels for the tooth, as shown in Figure. 1.1.

## 1.2 Dental Caries

Dental caries is a tooth infection caused by bacteria that break down the hard tissues of a tooth. This infection is as a result of bacteria forming dental plaques that release acids when they come into contact with carbohydrates. Diet that includes fructose, sucrose and glucose accelerates the occurrence of dental caries. The acid released from the above process leads to de-mineralization of the tooth surface, and therefore caries occur when the rate of minerals is less than the rate of decay. There are various categories of dental caries and can be characterized using [4]. The protocol characterizes dental caries based on its location and also the affected tooth [23]. The categories are as follows:

**Class I-** dental caries on acclusal surfaces of posterior teeth, for instance, molars and incisors.

**Class II-** occurs on proximal surfaces of posterior teeth.



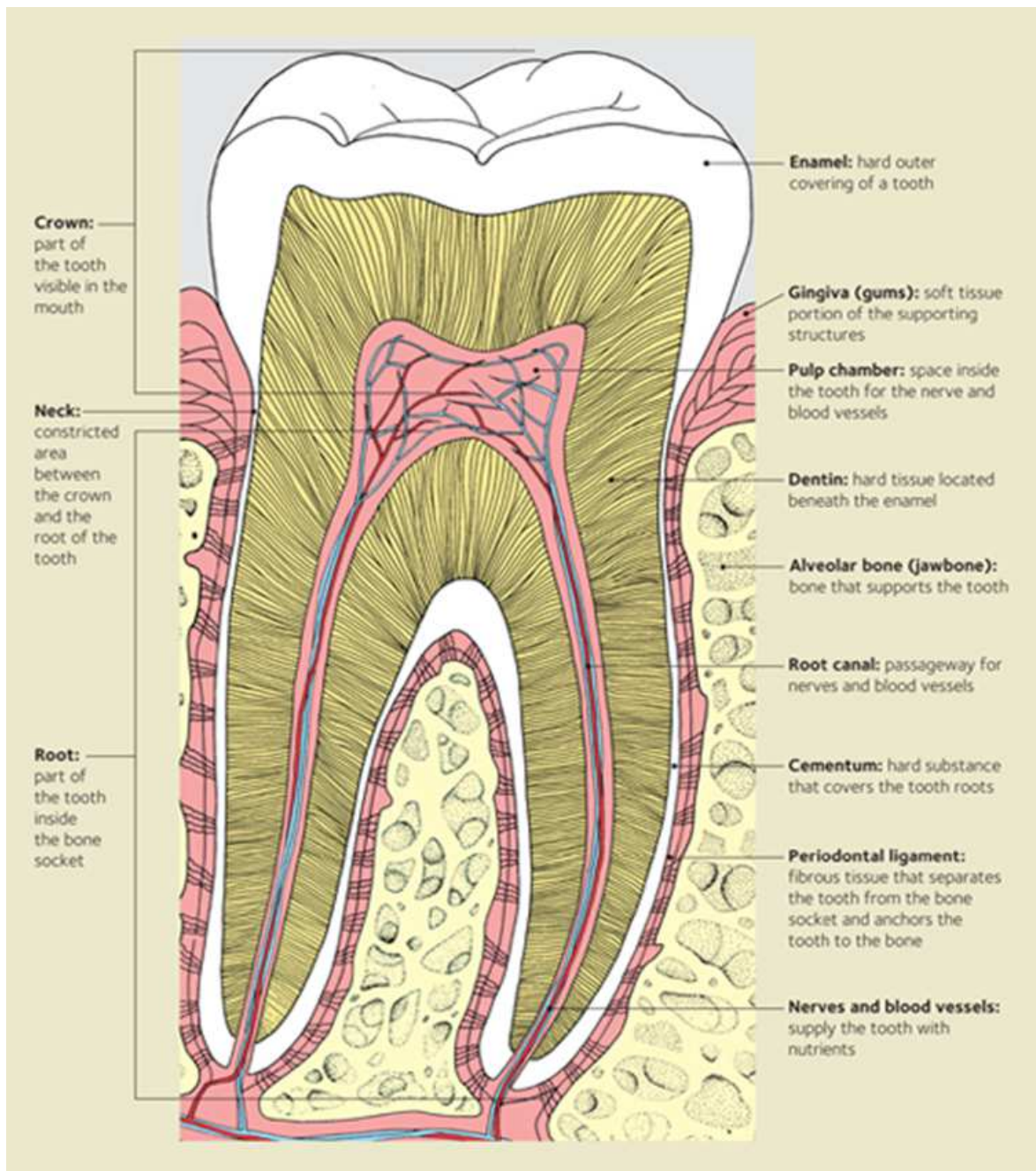


Figure 1.1: Cross-section of the molar tooth [35].

**Class III-** occurs on inter-proximal surfaces of anterior teeth, with no incisor edge involvement.

**Class IV-** occurs on inter-proximal surfaces of anterior teeth with incisor edge involvement.

**Class V-** occurs on the lingual or cervical third of the facial surface of the tooth.

**Class VI-** the caries occurs on the occlusal or incisor edge, worn away due to attrition.

From positional classification, caries can also be classified based on the severity of lesions on the tooth. This is done based on the amount of dentin and enamel that has been affected by the caries.

**Incipient caries** are caries that have a depth of less than half of the enamel of the tooth.

**Moderate caries** are caries that are more than halfway through the enamel but do not touch the dentin.

**Advanced caries** are caries that extend to the dentin region.

**Severe caries** are caries that extend more than halfway through the dentin and even reach the pulp.

Identification of caries under classes I, IV and VI can be done during clinical inspection, since the regions are visible orally. Caries that are not visible to the naked eye, such as those under classes II, III and V, can only be viewed by X-rays. The introduction of X-rays in the medical field has improved diagnosis of various ailments. In the dental field, radiographs have improved visual inspection of patient's teeth. X-rays have enabled professionals to be able to view previously unobservable regions of caries that would have otherwise gone untreated. Radiographs have proved to be very useful in their ability to diagnose dental caries and are still in use to date.

### 1.3 Dental radiographs-X-rays

There are varying degrees of information needed depending on the form of treatment required to diagnose a certain ailment. An X-ray or radiograph is a digital film that represents unobservable information not visible to the naked eye. Works by [19] explain three types of X-rays that are commonly used to diagnose dental health. There are two types of radiographs referred to as intra-oral and extra-oral, respectively [32]. **Intra-oral radiographs-** X-ray film captures radiographic images while inside the mouth, as seen in Figure. 1.2. This type is subdivided further to :

*Bitewing radiographs:-* this show details of upper and lower teeth inside the mouth.

*Periapical radiographs:-* show the complete tooth from the crown to the end of the root, and displays one tooth at a time in a single image.

*Occlusal radiographs:-* these show tooth development and its displacement.

**Extra-oral radiographs-** X-ray film captures radiographic images while outside the mouth. This type is subdivided further to:

*Panoramic radiograph:-* shows all teeth both in upper and lower jaws on a single image. Unlike periapical and bitewing radiographs, this type needs a specialized machine to view the back of a patients' head, and is also used to identify tumors, cysts and irregularities in the jaw region.

*Tomograph:-* shows a particular layer of the mouth while blurring out all other layers.

*Computed Tomograph (CT):-* this gives a 3D image of the interior structure of the mouth [1].

*Sialograph:-* has a visualization of the salivary glands following a dye injection in the mouth.

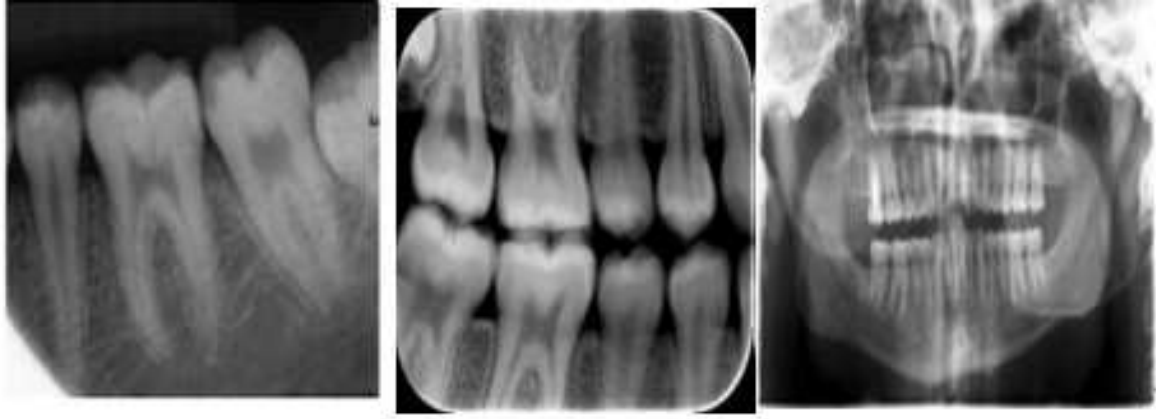


Figure 1.2: Periapical radiograph, Bitewing radiograph, Panoramic radiograph respectively [31].

## 1.4 Factors affecting Dental Caries.

[The biology, prevention, diagnosis and treatment of dental caries Scientific advances in the United States], show factors affecting caries namely, saliva, bacteria, diet, and hereditary.

**Bacteria-** this is shown by [16], how plaques form around the surface of the tooth, then come into contact with carbohydrates to form acids that dissolve the tooth structure. This concept formed the basic foundation of dental caries. There is no specific way of showing how bacteria affects the tooth, thus it is hard to control the dental caries disease. In method [5], explain how dental caries occur from bacteria associated with fermented carbohydrates, thus being referred to as a diet-bacteria disease. Researchers have associated the caries process with fermented carbohydrates, [30], show a relationship between sugar and caries leading to acids formed on the tooth's surface. Rather, [36], demonstrates how consumption of sweet snacks frequently is related to dental caries.

**Saliva-** plays a critical part in the well-being of soft and hard tissues of teeth inside

the mouth [14]. When the saliva flow rate is low, then this shows risk to dental caries. Further [18], explain how saliva flow measurement is an important risk assessment and management measure for dental caries.

## 1.5 Prevention of Caries

Dental caries can be prevented through various ways such as re-mineralization, fluoride, risk assessment, and the use of sealants.

**Sealants-** this can be done as [9], show how sealants are introduced over the specific carious region to stop the decay process on the tooth. These prevent food particles from collecting in the tooth pits, thus preventing caries.

**Re-mineralization-** this is done by hardening the tooth's enamel as explained by [10], to avoid dental caries to even take place.

**Fluoride-** this is found from excessive fluorosis in drinking water, [15] a practising dentist, associated with the enamel [2], showed its effects to the enamel of the tooth. As exhibited by [6], an optimal level of fluoride in water was found to prevent dental caries.

**Risk assessment-** this entails the prior determination of someone's developing dental caries during a specific period of time as [26], explain to enable easier management. Assessment is very useful in determining whether extra diagnostic measures are required. Information provided by [7], explain how assessment, assesses effectiveness of previous caries control measures and acts as a guide to treatment planning in the future. Further research has seen that caries can be prevented by saliva when fluoride application is combined with regular removal of forming dental plaques, realised by brushing teeth. Further contribution by [13], explain how saliva and small amounts of fluoride contributed to the hardening of the enamel and thus low risk of dental caries.

## 1.6 Diagnosis of Caries

Diagnosis of dental caries is done visually from either a clinical oral examination or radiographic image analysis methods.

**Clinical method-** this is described by [3] explicitly as the visual detection of dental caries from an oral examination. They used separators to visualize areas of interest and also used dental floss applied on these areas to detect roughness of the surfaces.

**Radiographic method-** the radiographs also known as X-rays are digital images and [38], introduced them in dentistry. Furthermore, [25], intensifies the use of dental radiographs in their research to detect caries. Images generated by [37], of higher diagnostic quality than those found from conventional films, are used to detect caries in bitewing X-rays.

## 1.7 Treatment of Caries

Treatment of caries can only be achieved through teeth restoration ways. Focus has been shifted from surgical ways to the management of caries via restoration of tooth structure development or implants. Emphasis on prevention by [17] of the disease, re-mineralization steps, and minimization and access to caries affected regions was to avoid further decay.

Dental radiographs or X-rays are the most vital form of representation when it comes to segmentation and detection of dental caries. These images are typically noisy and low in contrast due to the capture process involved. These low contrast images can affect visibility of caries due to the X-rays not fully penetrating the teeth. Therefore, there is need for image enhancement techniques to maintain diagnostic accuracy, and

this is by enhancing the contrast of the image while reducing noise levels. Recently, image processing is a very valuable tool in medical imaging. Computer aided diagnosis (CAD) systems have become an important tool in medical radiology, and have been used extensively in the detection of various diseases. Research has shown that the use of CAD system, has improved caries diagnosis compared to those of non-assisted assessments. Figure. 1.3 outlines the CAD system used by [28] in the detection of lung nodules.

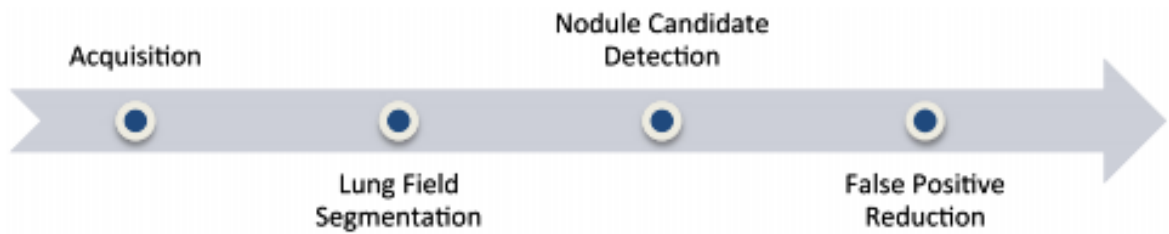


Figure 1.3: Computer aided system diagram as by [28]

The process begins with acquisition of images from different datasets and preprocessing them. This includes image enhancement and segmentation. The next stage is detection of possible lung nodules. For the purpose of this thesis, this will refer to caries lesions. Further, after the detection of possible caries, the CAD system attempts to reduce or rather eliminate false positives detected from the previous stage. Finally, the system classifies the lesions using a threshold value. Health-care professionals have started adopting CAD systems as part of their diagnostic process, due to their increased detection rate of dental caries in affected patients.

## 1.8 Motivation

Dental Caries is one of the chronic diseases around the globe. Distinguishing carious lesions has been a challenging task. Conventional computer aided diagnosis and detection systems have heavily relied on visual inspection of teeth. These are only effective on large and clearly visible caries on affected teeth. These conventional methods have been limited in performance due to the complex visual characteristics of dental caries images, which consists of hidden or inaccessible lesions. The introduction of dental radiography, is to detect hidden or inaccessible lesions that could not be done through conventional methods. Early detection of dental caries lesions is an important determinant of treatment measures and therefore is a beneficiary of the introduction of new tools, as emphasized by [27].

The fastest growing sectors in the health care industry are dental services and these consists the prevention, treatment and diagnosis of oral cavity diseases[29]. Most dentists use bite-wing radiographs to aid location of dental caries. They rely on information from these radiographs together with their patient’s medical history. Locating of dental caries is a challenging task and sometimes even experienced dentists miss the carious lesions, when just presented with bite-wing radiographs [33]. Traditionally, detection of dental caries relied on visual-tactile methods [20].

Sensitivity of visual-tactile methods is limited and especially done on posterior proximal tooth surfaces. Radio-graphical methods tend to have high sensitivity but require ionizing radiation as mentioned by [34]. The goal of this research is to obtain a method that automatically detects hidden and inaccessible dental caries in bitewing radiographs via a supervised learning model. The weaknesses of visual inspection of teeth have led to the increase in the use of dental radiographs for caries identification. Current models have predominantly focused on the segmentation of dental radiographs’ aspect than on the detection of caries aspect. The segmentation process



plays an important role in computer aided systems, and therefore aids faster identification and detection of carious lesions. Early identification and automatic detection of dental caries aids reducing the rate of infection and even prevents lesions from further advancement. Therefore, by combining existing methods and adapting them to come up with a new analytical model which can automatically process X-rays, segment, identify and later classify them as either having caries or not is of great importance. These combination leads to a novel caries detection approach with an efficient diagnostic potential. The novel approach aids the detection and location of dental caries significantly compared to existing models.

## 1.9 Problem Statement

From the literature discussed, there is limited research regarding caries identification and detection. Most existing methods dwell more on segmentation of caries lesions and less on the actual identification of specific locations, size, shapes, texture and color. The most challenging task is to locate unobservable regions of carious lesions on images, and this can only be aided by image preprocessing and a further post-processing of dental radiographs via deep learning. A novel supervised deep learning approach uses image analysis to identify, detect and diagnose the presence of dental caries. The area of the image is first subdivided into a region of interest, in the case of this research, individual teeth separated from the jaws. The region of interest is further subdivided into now a potential caries region via a threshold value to determine if caries is present or not. After this step, the model now eliminates false positive's caries regions and remains with only caries present. A deep learning model has faster diagnostic rates since it iterates a large database with enough images to be able to compare with. The threshold value and post-processing steps helps eliminate false positives before the caries detected images are analyzed with those in the training set, therefore they

won't have similar characteristics that may lead to wrong diagnosis.

## **1.10 Research Objectives**

The primary objective of this research is to model a deep learning approach for automatic dental caries detection. This automatic dental caries detection method uses a deep learning technique namely: blob detection to detect dental caries. It also uses image enhancement techniques used by current systems for pre-processing, segmentation and post-processing. The model segments dental images while maintaining both tooth edges and boundaries in order to obtain accurate results. The main goal of this thesis is to ensure that the proposed model gives a comparative or better diagnostic accuracy than those already implemented. The specific objectives which must be met include:

1. To segment teeth in dental X-rays using a threshold connected component analysis method.
2. To model a supervised deep learning framework for caries detection.

## **1.11 Contributions**

There are two major contributions of this research, namely: proposed hybrid segmentation method and a hybrid caries detection method based on dental image analysis. These contributions are described below:

1. A combination of region based and boundary based segmentation method. Segmentation is done through separation of various regions of interest from the larger image to locate objects. The boundary based method determines the line

of separation of edges or boundaries and locating discontinuities. Traditional segmentation methods determine the best candidate for separation through morphology or noise reduction on images. The region based method is implemented when the image only contains tooth structures with similar characteristics, in this case pixels on dental images. By using a weighted combination of the two methods, they are adapted to provide accurate results in all radiographic image types. Therefore, radiographic images can be accurately segmented while preserving crucial details needed for dental caries detection.

2. A deep learning caries detection approach based on image analysis. The detection approach uses images from the segmentation step to detect boundaries. Active contours method is used to find edge boundaries. Filters are then used to remove noise from the images and maintain their edge boundaries. Then later, blob detection and connectivity clustering model are used to detect and isolate caries candidates respectively. Lastly, a threshold value is used to select caries candidates and eliminate false positives from the detected caries candidates.

## **1.12 Thesis Outline**

The remainder of the thesis is organized as follows:

1. Chapter 2 - Background and Related Work contains a brief introduction of dental caries and how practical identification of caries is carried out. The rest of the chapter looks at existing research on deep learning dental segmentation and detection methods.
2. Chapter 3 - Teeth Segmentation contains a brief description of how teeth segmentation is going to be handled. The first part of this chapter looks at image

augmentation, enhancement techniques used to ensure sufficient data is available and ready for processing. The second part looks at thresholding and connected component analysis method used to isolate teeth from their background pixels, and from each other in X-rays. After this segmentation, boundary edge segmentation was handled via the active contour's method.

3. Chapter 4 - Dental Caries Detection covers a continuation from the previous chapter, where the edge boundaries of isolated individual teeth are used to isolate search space for caries detection. This chapter covers the final stage of the caries detection method, and details of methods used to isolate potential caries and evaluate them.
4. Chapter 5 - Results and Discussion covers results of the various methods implemented in the previous chapters, as well as a comparison of those results to similar existing methods.
5. Chapter 6 - Conclusion and Future Work concludes the thesis and discusses future work.

# Chapter 2

## Background and Related Work

### 2.1 A survey of Dental Caries Segmentation and Detection Techniques


### 2.2 Introduction

This paper provides a survey of both segmentation and detection methods of dental images, databases used, and evaluation protocols used in dental image analysis. The process of dental image analysis is important to improving medical imaging systems. In order to analyze dental images, we need access to image features. These image features can only be obtained through methods such as segmentation and feature extraction methods. For easier segmentation and detection of dental caries, prior knowledge of several tasks is needed. First, understanding the various sections of the tooth, and the specific position of the lesion on the tooth. Secondly, types of dental images used, for instance panoramic or bitewing radiographs, is also important. Further, which specific regions of interest are required to be able to choose the appropriate method for

segmentation and detection of caries. All these prior information is required to achieve high performance segmentation and detection of dental caries.

## Article

# A survey of Dental Caries Segmentation and detection Techniques.

Vincent Majanga <sup>1,†</sup> and Serestina Viriri <sup>1,†</sup> \* 

<sup>1</sup> School of Mathematics, Statistics and Computer Science; University of KwaZulu-Natal; Durban, 4000; South Africa

\* Correspondence: viriris@ukzn.ac.za

† These authors contributed equally to this work

**Abstract:** Dental caries detection, in the past, has been a challenging task given the amount of information got from various radio-graphic images. Several methods have been introduced to improve the quality of images for faster caries detection. Deep learning, has become the methodology of choice when it comes to analysis of medical images. This survey gives an in-depth look into the use of deep learning for object detection, segmentation and classification. It further looks into literature on segmentation and detection methods of dental images through deep learning. From the literature studied, we found out that methods were grouped according to the type of dental caries (proximal, enamel), type of X-ray images used (extra-oral, intra-oral), segmentation method (threshold-based, cluster-based, boundary-based and region-based). From the works reviewed, the main focus has been found to be on threshold-based segmentation methods. Most of the reviewed papers have preferred the use of intra-oral X-ray images rather than extra-oral X-rays images to perform segmentation on dental images of already isolated parts of the teeth. This paper presents an in-depth analysis of recent research in deep learning for dental caries segmentation and detection. It involves discussing the methods and algorithms used in segmenting and detecting dental caries. It also discusses various existing models used and how they compare with each other in terms of system performance and evaluation. We also discuss the limitations of these methods as well as future perspectives on how to improve their performance.

**Keywords:** Dental Segmentation; Bitewing images; Dental Caries; Deep learning; Dental Caries.

**Citation:** Majanga, V.; Viriri, S. A survey of Dental Caries Segmentation and detection Techniques.. *Journal Not Specified* **2021**, *1*, 0. <https://doi.org/>

Received:

Accepted:

Published:

**Publisher's Note:** MDPI stays neutral with regard to jurisdictional claims in published maps and institutional affiliations.

**Copyright:** © 2021 by the authors. Submitted to *Journal Not Specified* for possible open access publication under the terms and conditions of the Creative Commons Attribution (CC BY) license (<https://creativecommons.org/licenses/by/4.0/>).

## 1. Introduction

For easier segmentation and detection of dental caries, prior knowledge for several tasks is needed. First, understanding the various sections of the tooth and secondly, the specific position of the lesion on the tooth. An understanding of the types of dental images to be used for instance panoramic or bitewing radiographs is also needed. Furthermore, the specific regions or areas of interest which are required should be clear in order to be able to choose the suitable method for segmentation and detection of caries. All this information is required in order to achieve high performance segmentation and detection of dental caries.

### 1.1. Tooth Anatomy

The tooth is a small white structure found in the jaw bone of animals and human beings. In human beings, the number of teeth ranges from 20 primary teeth in children to 28-32 permanent teeth in adults. Further, the tooth can be broken down into three main layers: the crown, neck and root. The crown is the visible region above the gum line. The neck connects the crown to the root while the root is the region inside the bone socket. (Waugh et al. 2014). Additionally, each tooth comprises of hard tissues that protect the soft tissues in the centre. The outermost layer of the tooth is the enamel. This is a hard tissue beneath which is the dentin which is much softer than the enamel. The

37 dental pulp is found at the centre of the tooth and houses the blood vessels and tissue  
 38 vessels for the tooth.

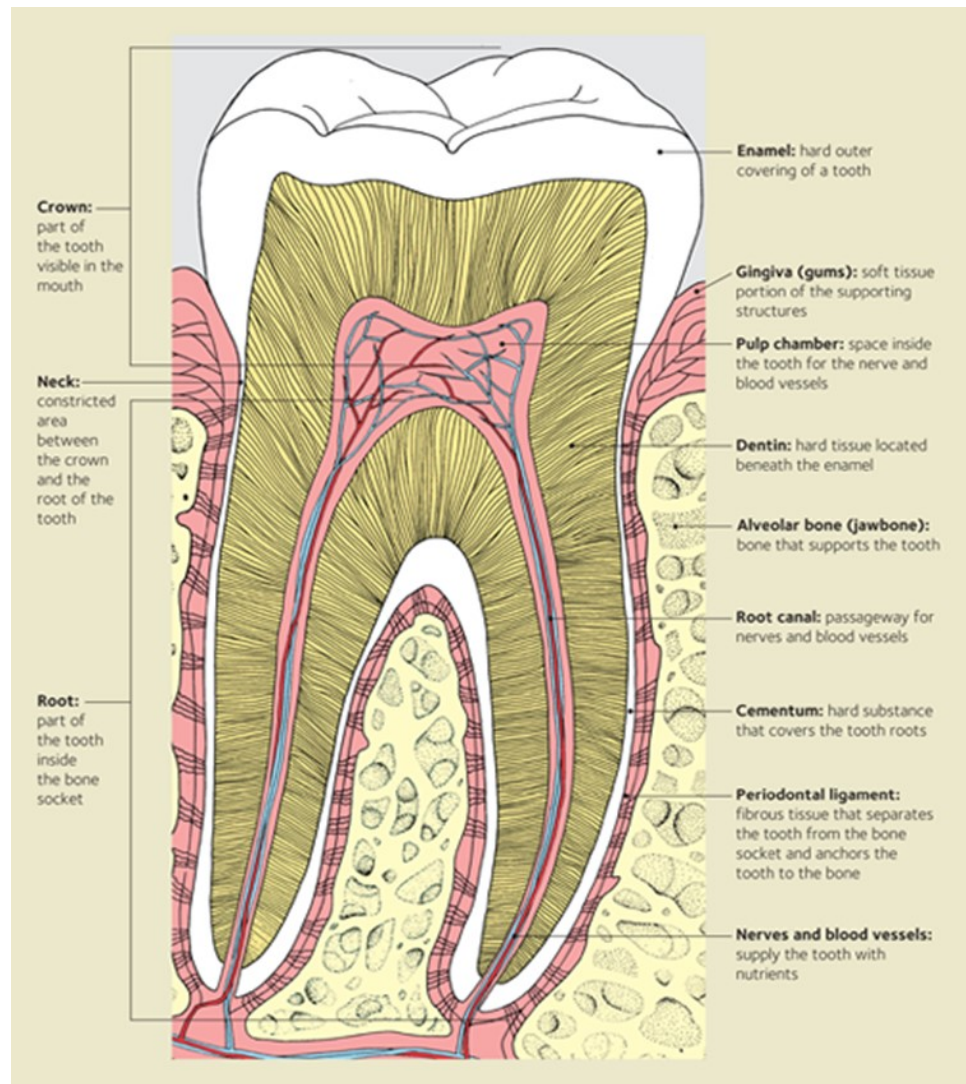


**Figure 1.** Cross section of the molar tooth (Waugh et al. 2014).

### 39 1.2. Dental Caries

40 Dental caries is a tooth infection caused by bacteria, that break down the hard tissues  
 41 of a tooth. This infection is as a result of bacteria forming dental plaques that release acids  
 42 when they come into contact with carbohydrates. Diet that includes fructose, sucrose  
 43 and glucose accelerate the occurrence of dental caries. The acid released from the above  
 44 process leads to de-mineralization of the tooth surface. Caries occur when the rate of de-



mineralization is less than the rate of decay. There are various categories of dental caries and these can be characterized (Black G.V. 1955). The protocol characterizes dental caries based on its location and also the affected tooth (Osterloh et al. 2016). The categories are as follows:

**Class I-** dental caries on occlusal surfaces of posterior teeth for instance, molars and incisors.

**Class II-** occurs on proximal surfaces of posterior teeth.

**Class III-** occurs on inter-proximal surfaces of anterior teeth with no incisor edge involvement.

**Class IV-** occurs on inter-proximal surfaces of anterior teeth with incisor edge involvement.

**Class V-** occurs on the lingual or cervical third of the facial surface of the tooth.

**Class VI-** the caries occurs on the occlusal or incisor edge worn away due to attrition.

From positional classification, caries can also be classified based on the severity of lesions on the tooth. This is done based on the amount of dentin and enamel that has been affected by the caries.

**Incipient caries** are caries that have a depth of less than half of the enamel of the tooth.

**Moderate caries** are caries that are more than halfway through the enamel but do not touch the dentin.

**Advanced caries** are caries that extend to the dentin region.

**Severe caries** are caries that extend more than halfway through the dentin and even reach the pulp.

Identification of caries under classes I, IV and VI can be done during clinical inspection, since the regions are visible orally. Caries that are not visible to the naked eye such as those under classes II, III and V, can only be viewed using X-rays. The introduction of X-rays in the medical field has greatly improved diagnosis of various ailments. In the dental field radio-graphy has improved the visual inspection of patient's teeth. X-rays have enabled professionals to be able to view previously unobservable regions of caries that would have gone untreated. Radio-graphs have proved to be very useful in their ability to diagnose dental caries and are still in use to date.

### 1.3. Dental radiographs-X-rays

There are varying degrees of information needed depending on the form of treatment required to diagnose a certain ailment. An X-ray or radiograph is a digital film that represents unobservable information not visible by the naked eye. Works by (Newman et al. 2011) explain three types of X-rays that are commonly used to diagnose dental health. There are two types of radiographs referred to as intra-oral and extra-oral respectively (Tikhe et al. 2016). **Intra-oral radiographs-** X-ray film captures radiographic images while inside the mouth. This type is subdivided further into:

*Bitewing radiographs:-* these show details of upper and lower teeth inside the mouth.

*Periapical radiographs:-* these show the complete tooth from the crown to the end of the root and displays one tooth at a time in a single image.

*Occlusal radiographs:-* these show tooth development and its displacement.

**Extra-oral radiographs-** X-ray film captures radiographic images while outside the mouth. This type is subdivided further into:

*Panoramic radiograph:-* shows all teeth both in upper and lower jaws on a single image. Unlike periapical and bitewing radiographs, this type needs a specialized machine to view the back of a patient's head and is also used to identify tumors, cysts and irregularities in the jaw region.



**Figure 2.** Periapical radiograph



**Figure 3.** Bitewing radiograph.



**Figure 4.** Panoramic radiograph ([Tangel et al. 2013](#)).

95 *Tomograph*:- shows a particular layer of the mouth while blurring out all other layers.

96 *Computed Tomograph (CT)*:- this gives a 3D image of the interior structure of the  
97 mouth ([Akarslan et al. 2008](#)).

98 *Sialograph*:- has a visualization of the salivary glands following a dye injection in  
99 the mouth.

## 100 **2. Deep Learning application areas.**

101 The introduction of deep learning systems has contributed to several application  
102 areas using medical images.

## 103 2.1. Digital microscopy and pathology

104 Deep learning methods have been very popular in these areas especially with  
 105 the growing availability of tissue specimen. In this domain, deep learning techniques  
 106 developed have had their main focus on three broad challenges. These are segmentation  
 107 of large organs, detecting, segmenting and classifying nuclei and also detecting and  
 108 classifying region of interest of lesions. Other areas where deep learning techniques  
 109 have contributed include, normalizing histopathology, color normalization in image  
 110 analysis. Work by (Janowczyk et al. 2017) introduces a method for normalizing stains on  
 111 histopathology images using auto encoders. Color normalization is further demonstrated  
 112 by (Vahadane et al. 2016), where they introduced the use of convolutional neural  
 113 networks(CNN) for tissue classification in stained images. **Brain** In this area , deep neural  
 114 networks (DNN) have been used for brain image analysis in several domains, most  
 115 notably the classification of Alzheimer’s disease. Other domains include segmentation  
 116 of brain tissues and anatomical structures for instance hippocampus. There is also the  
 117 segmentation and detection of brain tumor, lesions and micro-bleeds. There are other  
 118 tasks that require more anatomical information like white matter lesion segmentation,  
 119 and (Ghafoorian et al. 2016) tackled such scenarios. They lowered the sampling rate of  
 120 non-uniformed sampled patches so as to cover a larger part of the region of interest.

121 **Chest** Deep learning also has contributed to thoracic image analysis, both on tomog-  
 122 raphy and radiology. Deep neural networks have addressed the detection, characterization  
 123 and classifying nodules from radiology tests conducted. Computed tomography (CT)  
 124 scans have detected several diseases, including lung diseases from a single image. Chest  
 125 radiography is the most common radiology test and therefore uses a large set of images  
 126 that are used to train systems. These systems can be a combination of convolution neural  
 127 networks used for image analysis, and recurrent neural networks used for text analysis.

128 **Eye** Deep learning algorithms have also been introduced in the analysis of eye  
 129 images and have seen CNNs being employed to address the segmentation of anatomical  
 130 structures. These networks have also addressed the detection and segmentation of  
 131 retinal diseases, diagnosis and assessment of image quality. The work in (Gulshan et al.  
 132 2016) shows the performance of a Google Inception v3 network for diabetic retinopathy  
 133 detection and compares the results with that of seven ophthalmologists.

134 **Musculo-skeletal** In this domain, deep learning algorithms are used for identifi-  
 135 cation and segmentation of joints, bones and soft tissues in images. The method used  
 136 in (Mohamed et al. 2016) , is one of the applications that trained their system with  
 137 musculo-skeletal disc images , and had very good performance across several different  
 138 radiology scoring tasks.

139 **Breast** Research on breast imaging has resulted to (Kooi et al. 2016) , that shows  
 140 significant advances over the state of the art ,achieving performance of human readers  
 141 on the region of interest(ROI). The main task also is to detect breast cancer, and this  
 142 consists of several subtasks. These include detection and classification of lesions, micro  
 143 classification and cancer risk scores of images. The availability of huge amounts of image  
 144 data has made mammography easier to perform and the most common method used for  
 145 breast radiography.

146 **Abdomen** Research on the abdomen is localized on the segmentation of organs  
 147 mainly, pancreas, kidneys, liver(tumors), and bladder. The main radiograph used for  
 148 most organs is the CT radiograph, and MRI only for prostate analysis. The method  
 149 used by (Dou et al. 2017) , introduce a hybrid neural network used to extract features  
 150 that will be used further for classification. **Cardiac** Cardiac image analysis has embraced  
 151 deep learning, in segmentation, tracking, classification, and accessing image quality. The  
 152 MRI is used for radiographic testing. (Poudel et al. 2016) introduce the use of neural  
 153 networks to segment the left ventricle using the recurrent connection of U-network  
 154 architecture. (Kong et al. 2016) use neural networks to perform regression for identifying  
 155 some cardiac sequence on its model.

### 156 3. Factors affecting Dental Caries.

157 [The biology, prevention, diagnosis and treatment of dental caries Scientific ad-  
158 vances in the United States] , show factors affecting caries namely, saliva, bacteria, diet,  
159 and hereditary.

160 **Bacteria-** this is shown by (Miller et al. 1902) how plaques form around the surface  
161 of the tooth, then come into contact with carbohydrates to form acids that dissolve the  
162 tooth structure. This concept formed the basic foundation of dental caries. There is  
163 no specific way of how bacteria affects the tooth thus hard to control the dental caries  
164 disease. In method (Bowen et al. 1986) , explain how dental caries occurs from bacte-  
165 ria associating with fermented carbohydrates thus being referred to as a diet-bacteria  
166 disease. Researchers have associated the caries process with fermented carbohydrates,  
167 (Stephan1944 et al. ) , show a relationship between sugar and caries leading to acids  
168 formed on the tooth's surface. Rather (Weiss et al. 1960) , demonstrate how sweet snacks  
169 consumption frequently is related to dental caries.

170 **Saliva-** plays a critical part in the well-being of soft and hard tissues of teeth inside  
171 the mouth (Mandel et al. 1976) . When the saliva flow rate is low ,then this shows risk to  
172 dental caries. Further (Navazesh et al. 2003) , explain how saliva flow measurement is  
173 an important risk assessment and management measure for dental caries.

#### 174 3.1. Prevention of Caries

175 Dental caries can be prevented through various ways such as re-mineralization, fluoride,  
176 risk assessment, and the use of sealants.

177 **Sealants-** this can be done as (Griffin et al. 2008) , show how sealants are introduced  
178 over the specific carious region to stop the decay process on the tooth. These prevent  
179 food particles from collecting in the tooth pits thus preventing caries.

180 **Re-mineralization-** this is done by hardening the tooth's enamel as explained by  
181 (HEAD, J., 1912) , to avoid dental caries to even take place.

182 **Fluoride-** this is found from excessive fluorosis in drinking water , (Mckay F.S.,  
183 1928) a practicing dentist, associated with the enamel (Black, G.V., 1916) , showed its  
184 effects to the enamel of the tooth. Research from (Dean et al. 1950) , gave an optimal  
185 level of fluoride in water to prevent dental caries.

186 **Risk assessment-** this entails the prior determination of someone's developing  
187 dental caries during a specific period of time as (Reich et al. 1999) , explain to enable  
188 easier management. Assessment is very useful in determining whether extra diagnostic  
189 measures are required. Work by (Fontana et al. 2006) , explain how assessment assesses  
190 effectiveness of previous caries control measures and acts as a guide to treatment plan-  
191 ning in the future. Further research has seen that caries can be prevented by saliva  
192 when fluoride application is combined with regular removal of forming dental plaques,  
193 realised by brushing teeth. Research by (Koulourides et al. 1986) , explain how saliva  
194 and small amounts of fluoride contributed to the hardening of the enamel and thus low  
195 risk of dental caries.

#### 196 3.2. Diagnosis of Caries

197 Diagnosis of dental caries is done visually from either a clinical oral examination or  
198 radiographic image analysis methods.

199 **Clinical method-** this is described by (Black et al. 1917) and explicitly define it as  
200 the visual detection of dental caries from an oral examination. They used separators  
201 to visualize areas of interest and also used dental floss applied on these areas to detect  
202 roughness of the surfaces.

203 **Radiographic method-** the radiographs also known as X-rays are digital images  
204 and (Zero et al. 2009) , introduced them in dentistry. Work from (Raper et al. 1925) ,  
205 further intensified the use of dental radiographs in their research to detect caries. Works  
206 from (Wenzel et al. 2004) , generated images of higher diagnostic quality than those  
207 found from conventional films to detect caries in bitewing X-rays.

### 208 3.3. Treatment of Caries

209 Treatment of caries can only be achieved through teeth restoration ways. Focus  
210 has shifted from surgical ways to the management of caries via restoration of tooth  
211 structure development or implants. Research work from (Mirza et al. 2008) ,emphasize  
212 on prevention of the disease, re-mineralization steps, and minimize the access to caries  
213 affected regions to avoid further decay.

## 214 4. Image representation for dental segmentation and detection

215 The representation of dental images is done through the segmentation of various  
216 regions of interest from the larger image so as to locate objects. Segmentation of images  
217 is therefore partitioning of an image into several segments to be used to identify objects  
218 and their edges. Image segmentation can be categorized according to similarity and  
219 discontinuity properties. Discontinuity based methods are referred to as boundary  
220 based methods, while similarity based methods are referred to region based methods  
221 (Subramanyam et al. 2014).

222 Therefore the segmentation process is based on dividing an image into groups of  
223 similar characteristics and features. Mathematically , segmentation of an image  $R$  is a  
224 finite set of regions  $R_1...R_s$ .  $R = \cup i = 1 R_i R_i \cap R_{ji} \neq j$ .

### 225 4.1. Categories of Segmentation.

226 Research done by (Sezgin et al. 2004) and (Silva et al. 2018) , further categorizes  
227 segmentation methods according to various characteristics such as region, entropy,  
228 shape, threshold, pixels correlation among others. These characteristics were from  
229 thermal, X-ray images to aid analysis of specific points or regions of interest. Research  
230 studies show that dental image segmentation is classified as region-based, cluster-based,  
231 threshold-based, boundary-based, and watershed-based methods.

232 **Region-based:-** divides an image into several regions based on discontinuities of  
233 pixel intensity. (Lurie et al. 2012) , explain how segmentation of dental panoramic X-ray  
234 images , assist dentists to detect osteoporosis disease. Work by (Modi et al. 2011) , also  
235 use the region based approach in segmentation of bite-wing dental X-ray images.

236 **Threshold-based:-** this is done by choosing a threshold value from pixel intensities  
237 of an image. Then pixels that exceed the threshold value are placed into a region, while  
238 those that are below the threshold value are placed in an adjacent region. Threshold  
239 based segmentation is common in most of the reviewed articles , (Abaza et al. 2009),  
240 (Ajaz et al. 2013), (Azevedo et al. 2015) , (Wang et al. 2014), (Wang et al. 2015), (Xi et  
241 al. 2016), (Amer et al. 2015), (Tikhe et al. 2016), (Kaur et al. 2016) , (Lin et al. 2013),  
242 (Indraswari et al. 2015), (Razali2014).

243 **Cluster-based:-** is the automatic grouping of image data based on certain degrees  
244 of similarity between the data. The degree of similarity depends on the problem being  
245 solved. The algorithm used to perform clustering of data uses the automatically detected  
246 groups as initial parameters. Research by (Alsmadi et al. 2018) , perform jaw lesion  
247 segmentation using the fuzzy C means method. Works by (Tuan et al. 2017) , used a  
248 semi fuzzy supervised clustering algorithm to segment dental radio-graphs.

249 **Boundary-based:-** are used to find edge or point discontinuities on images. They  
250 detect color or pixel intensity discontinuities in the gray levels of the image. Active  
251 contours are used by (Icsin et al. 2016), (Niroshika et al. 2013) , (Hasan et al. 2016) ,  
252 as one of the approaches to segment images based on their boundaries. The approach  
253 performs segmentation by outlining an object from an image and is also referred to as  
254 the snake method. Level set method(LSM) is another approach for detecting boundaries  
255 in an image. It handles segmentation by performing geometric operations to detect  
256 contours with topology changes. Some of the work on boundary based segmentation  
257 include (Rad et al. 2013), (Kumar et al. 2017) , that used LSM to segment radio-graphic  
258 images.

259 **Watershed-based:-** is performed on a gray scale image and uses mathematical mor-  
 260 phology to segment adjacent regions in an image. , use Watershed based segmentation  
 261 was used by (Li et al. 2012) , on bitewing dental radiographs. It was also used by (Garg  
 262 et al. 2016) as a combination of the K-means clustering and the watershed method for  
 263 color based segmentation.

#### 264 4.2. Diagrammatic Representation

265 This section aims at giving pictorial representations of various segmentation meth-  
 266 ods. Methods by (Modi et al. 2011) , propose a novel way of finding region of interests  
 267 for both the gap valley and tooth isolation using edge intensity curves. They use the  
 268 region growing approach (Yau et al. 2008) , to detect the region of interest. They further  
 269 use canny edge detection algorithm (Sharifi et al. 2002) , to detect the edges of the  
 270 isolated teeth .

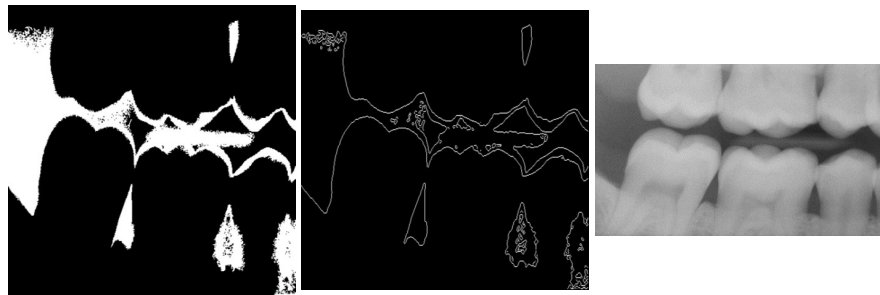


**Figure 5.** Left: Region growing approach, Central: Canny edge detected image, Right: Tooth isolation and gap valley using binary intensity integral curves (Modi et al. 2011).

271 (Tangel et al. 2013) proposed a dental classification of periapical images via the  
 272 fuzzy value which takes care of dental orientation problems such as missing teeth.  
 273 They also used the dental universal numbering system to categorize teeth into incisors,  
 274 canine, molar and premolar.

275 Segmentation of the images is done through multi scale aggregation (Tangel et al.  
 276 2012) , which deals with pixel distortions in image data. Integral projection is used to  
 277 detect horizontal individual teeth and this further is classified according to one of the four  
 278 incisor, molar, premolar and canine categories.

279 Additionally, (Chen et al. 2019) , propose the use of faster regions of a convolution  
 280 neural network to detect and number periapical dental images. A filtering algorithm is  
 281 used to delete overlapping boxes detected by the faster convolution network. A neural  
 282 network is introduced to detect missing teeth. A rule based teeth numbering system  
 283 is used to match labels of detected teeth boxes, to modify results that violate set rules.  
 284 Works by (Jader et al. 2018) , explain how they achieved instance segmentation through  
 285 the use of a mask region-based convolution neural network. This system is an extension  
 286 of (Ren et al. 2015) , that includes a section of convolution networks to achieve the task  
 287 of instance segmentation Figure 8.

288 Features are extracted from ResNet101, which then compose the feature pyramid  
 289 network (FPN). The FPN defines anchors and extracts regions of interest (ROI). The  
 290 Region proposal network is formed from a combination of anchors and the feature  
 291 pyramid network (FPN) Figure 8. Finally, regions of interest are aligned to same size  
 292 and further each fixed size is classified as tooth or a background (class scores). The fixed  
 293 size features are localized by regression of bounding box coordinates. Finally , pixels  
 294 are segmented by the fully convolutional network (FCN) (Hazirbas et al. 2016) , in each  
 295 detected mask as seen in Figure 9.



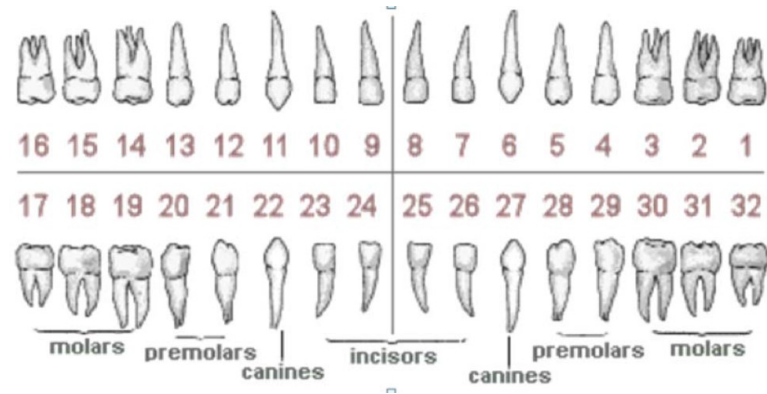


**Figure 6.** Dental universal numbering system (Tangel et al. 2013).

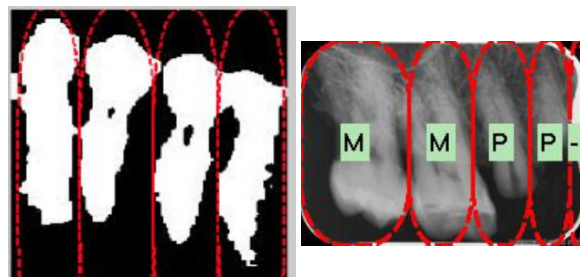


**Figure 7.** a. Horizontal integral projection of lower tooth, b. Classification result (Tangel et al. 2012).

296 A diagnostic system proposed by (Geetha et al. 2020) comprises of Laplacian  
 297 filtering, window based adaptive threshold, morphological operations, statistical feature  
 298 extraction and back propagation neural network. The back propagation neural network

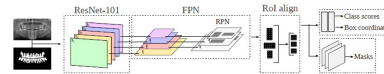


**Figure 8.** Training process of the segmentation system (Jader et al. 2018).

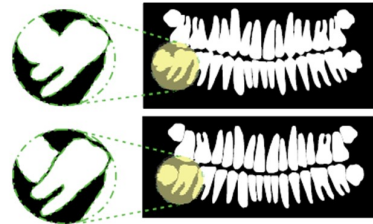


**Figure 9.** Process of separating the teeth.

is used to classify a tooth surface as normal or having dental caries. A study by (Jusman et al. 2020) analyzes feature extraction performance of dental caries image using Gray Level Cooccurrence Matrix (GLCM) algorithm for contrasted two types of caries based on the theory of GV Black, namely: dental caries Class 3 and Class 4.

A CNN model using a U-shaped deep CNN (U-Net) proposed by (Lee et al. 2021) for dental caries detection on bitewing radiographs and they investigated whether the model can improve clinicians' performance.

## 5. Feature Extraction Techniques for dental images.

Feature extraction on an image is done by the use of various methods depending on its texture, pixels, and color intensity. The method proposed by (Obuchowicz et al. 2020), evaluate the performance of various texture feature maps to recognize demineralization of caries. They used intra-oral image analysis that includes run-length matrices (RLM), first order features (FOF), co-occurrence matrices, gray tone matrices, local binary patterns and k-means clustering to transform images of confirmed caries cases. The



Table 1: Related works grouped by various categories and methods .

Category	Method	Related works
Region-based	Region growing approach	(Lurie et al. 2012), (Modi et al. 2011)
Threshold-based	Histogram-based threshold	(Abaza et al. 2009), (Ajaz et al. 2013), (Azevedo et al. 2015), (Wang et al. 2014), (Wang et al. 2015), (Xi et al. 2016), (Amer et al. 2015), (Tikhe et al. 2016), (Kaur et al. 2016), (Lin et al. 2013), (Indraswari et al. 2015), (Razali et al. 2014)
Cluster-based	Fuzzy C means	(Alsmadi et al. 2018), (Tuan et al. 2017)
Boundary-based	Active contours, Level set method	(Icsin et al. 2016), (Niroshika et al. 2013), (Hasan et al. 2016), (Rad et al. 2013), (Kumar et al. 2017)
Watershed-based	Watershed	(Garg et al. 2016), (Li et al. 2012)

performance from the different feature maps was compared to that of radio-graphic images by several radiologists. Feature maps are a product of extraction of features from an image by various methods techniques that include:

**First-order features (FOF):-** is a formalised description of the detection of probability of a particular intensity within data in an image, and this shape is used to determine image parameters such as contrast, sharpness and other objects. For instance, an image  $I$  with spatial resolution  $W * H$  and range intensity  $G$ , its histogram is defined as:

$$H(i) = \frac{1}{WH} \sum_{x=1}^W \sum_{y=1}^H \{1, I(x,y)=i \atop 0, otherwise\} i \in [0..G-1] \quad (1)$$

Several equations can be derived from the above equation namely mean, variance, entropy among others and can be represented as:

$$FOF_{mean} = \frac{1}{WH} \sum_{x=1}^W \sum_{y=1}^H I(x,y) \quad (2)$$

$$FOF_{variance} = \frac{1}{WH} \sum_{x=1}^W \sum_{y=1}^H (I(x,y) - FOF_{mean})^2 \quad (3)$$

$$FOF_{entropy} = \frac{1}{WH} - \sum_{i=1}^G H(i) \log(H(i) + \epsilon) \quad (4)$$

**Run-length matrix:-** this is defined by changes in the illumination of pixel values on an image, (Galloway et al. 1975), explain the coarse texture of pixels can be expressed by a larger section of similar color encoded as a matrix. Other works that have embraced this method include, (Eqbal et al. 2020), (Raj et al. 2019), (Deshmukh et al. 2018).

**Gray level co-occurrence matrix (GLCM):-** this according to (Haralick et al. 1973), shows texture relations between adjacent pixels in the image texture. The matrix is

328 calculated from entries that represent probabilities of coexisting gray tone pixels that  
 329 are next to each other, and the distance between the pixels is a feature parameter. Other  
 330 features that can be extracted by this matrix include , contrast, entropy, variance, sum  
 331 average and homogeneity. Related works include , (PS et al. 2016), (Korchiyne et al.  
 332 2014).

**Gray tone difference matrix(GTDM):-** this matrix according to (Amadasun et al. 1989) , is described as gray tone textural properties that is the difference in pixel intensity level  $I$  and illumination  $\bar{I}$  in a  $K * K$  neighborhood described as:

$$GLTDM(i) = \frac{1}{WH} \sum_{x=1}^W \sum_{y=1}^H |i - \bar{I}| \text{ where } \bar{I} = \frac{1}{M-1} \quad (5)$$

$$\sum_{m=-K}^K \sum_{n=-K}^K I(x+m, y+n), (m, n) \neq (0, 0) \quad (6)$$

333 Another method is , (Fekri et al. 2018) that combines GTDM, LBP and K-means clustering  
 334 for feature extraction.

335 **Laws' texture energy measures:-** according to (Laws, K., 1980) , this method is  
 336 utilised to set masks to calculate local energy of an image. These masks further detect  
 337 textural characteristics such as edges , spots, levels and ripples. Other works that use  
 338 this method include , (Orooji et al. 2018), (Ramapraha et al. 2017).

339 **Local binary patterns(LBP):-** detects small structures such as edges ,lines and spots  
 340 (Ojala et al. 1996) , on the skin, thus representing them as binary patterns. For pixel  
 341 inputs'  $(x_c, y_c)$  , a neighborhood of radius  $R$  and several evenly sampled points on  
 342 radius  $P$  are specified. The local binary pattern function is given by:

$$LBP_{P,R}(x_c, y_c) = \sum_{p=0}^{P-1} s[I(x_c, y_c) - I(x_p, y_p)].2^p \quad (7)$$

343 Here  $s[.]$  operator returns 1 for positive values and 0 for negative values.

344 Figure.10 shows , a  $3 * 3$  local binary operation concatenating all 8 bits to output a  
 345 binary number, which is converted to a decimal number. This decimal number is the  
 346 LBP code and is assigned to the center pixel. Other works that use LBP include, (Verma  
 347 et al. 2015) , (Liu et al. 2016).

348 **Clustering:-** this used k-means method to cluster pixels. The intensity of pixels  
 349 is taken into account, also prior information about the number of clusters should be  
 350 defined. Euclidean distance is the metric used when adding individual pixels to the  
 351 nearest cluster. A cluster value is set to the average value of all pixel intensities and this  
 352 procedure is iterated until a specified threshold is met (Min et al. 2018). Related works  
 353 include , (Li et al. 2018), (Edwards et al. 2018), (Zhao et al. 2019). Figure.11, shows the  
 354 feature maps of the extraction techniques discussed.

355 According to (Geetha et al. 2019) , they use a textural feature system for diagnosis of  
 356 dental caries in radiographs. This system introduced other feature extraction techniques  
 357 such as:

358 **Gabor Filters:-** originally introduced by (Gabor, D., 1946) , extracts edge like com-  
 359 ponents with very high frequency in a local region of an image. It is described as the best  
 360 texture descriptor due to its use in segmentation, object recognition, tracking of motion  
 361 and image registration. Spatial domain Gabor is defined as:

$$g(x, y) = \left( \frac{1}{2\pi\sigma_x\sigma_y} \right) \exp\left[ \frac{1}{2} \left( \frac{x^2}{\sigma_x^2} + \frac{y^2}{\sigma_y^2} \right) + 2\pi j W x \right] \quad (8)$$

362 Here  $\sigma_x$  and  $\sigma_y$  are standard deviations for  $(x, y)$  axis distribution, and the sinuisodal  
 363 frequency is denoted by  $W$ . Other related studies on Gabor filters include , (Avinash et  
 364 al. 2016), (Aguirre et al. 2018), (Hegde et al. 2018).

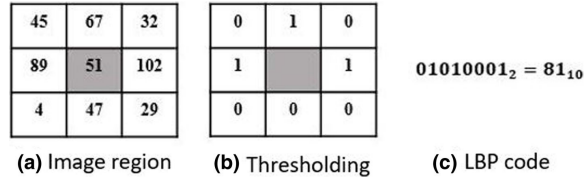


**Figure 10.** LBP operation given  $P=1$  and  $R=1$  (Ojala et al. 1996).

**Local ternary patterns:-** this from (Tan et al. 2010), show how LBP is extended to a three valued code from two values. The ternary code is got from comparing neighboring pixel values with a set threshold value  $\tau$ . Values that are within the threshold value are set to 0, those above it are set to +1, and those below the threshold value are set to -1.

The threshold function value is defined as:

$$f(x_i, x_c, \tau) = \begin{cases} 1 & \text{if } x_i \geq x_c + \tau \\ 0 & \text{if } |x_c - x_i| < \tau \\ -1 & \text{if } x_i \leq x_c - \tau \end{cases} \quad (9)$$

Here  $\tau$  is the set threshold,  $x_c$  is the value of the central pixel and  $x_i$  are the neighbouring pixels of  $x_c$ . Diagrammatically the process can be displayed by a Figure 12 LTP code for a 3\*3 matrix image region. Other related works include, (Murala et al. 2013), (Rabidas et al. 2016), (Deep et al. 2018).

**Morphological Gradient:-** method introduced by (Naam et al. 2016) is used to increase the intensity of boundary edges of an image. This method makes it easier to observe edge boundaries and other objects clearly (Naam et al. 2016), and identify dental caries on teeth. Other works that involve the mMG method include, (Liang et al. 2017), (Naqi et al. 2018), (Rakhlin et al. 2018). Multiple morphological gradient consists of several encryption elements that aid processing of images and include, gradient, multiple value, and threshold.

*Morphology gradient:* increases the intensity of the edges of objects in the image, and this is done by dilation subtracted by erosion morphology:  $(A \oplus B) - (A \ominus B)$ .

*Multiplier value:* is a constant value to enable the increase in pixel value on the image. This is defined as:

$$mv = \frac{\max(\max(A))}{w} \quad (10)$$

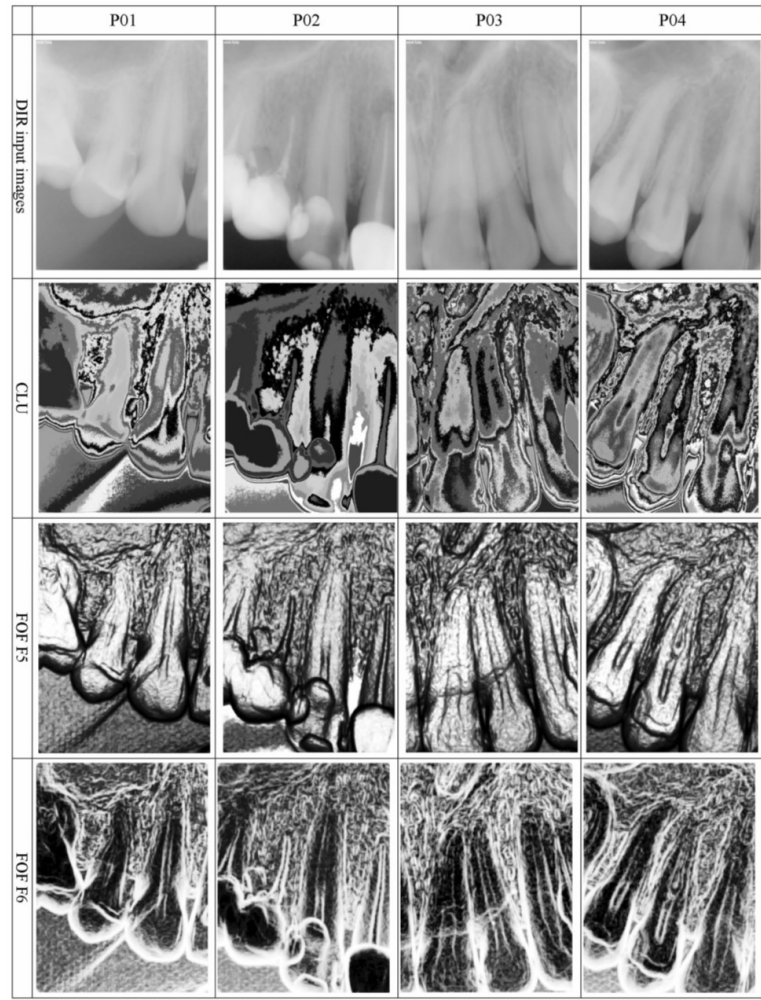


**Figure 11.** Intra-oral radio-graphs and their texture feature maps (Obuchowicz et al. 2020).

Here  $w$  is the bit depth.

*Threshold:* this is done by separating pixel values into two classes 0 or 1, that are dependent on a constant threshold value  $q$ . According to (Liang et al. 2017), thresholding is defined as:

$$T(A) = \begin{cases} 1, & A < q \\ 0, & A \geq q \end{cases} \quad (11)$$

Here  $0 < q \leq A_{max}$ .

A novel deep convolution layer network (CNN) with a long Short-Term Memory (LSTM) model proposed by (Singh et al. 2021) for the detection and diagnosis of dental caries on periapical dental images.

## 6. Deep learning methods and algorithms.

Research by (Litjens et al. 2017) explains how learning algorithms in machine learning are divided into, unsupervised and supervised learning algorithms.

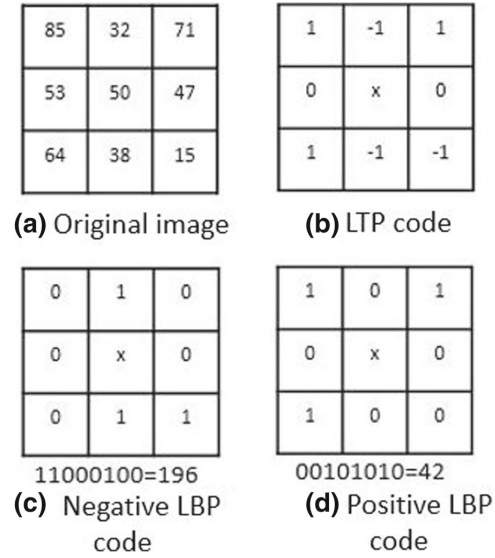


**Figure 12.** (a)..(d) LTP code with  $\tau \geq +15, \tau \leq -15$  and both positive and negative LBP codes.

#### 394 6.1. Learning algorithms

395 **Supervised learning**:- the model is represented with a dataset  $D = \{x, y\}_{n=1}^N$  of  
 396 input features  $x$  and  $y$ . The  $y$  can take different forms depending on the learning task for  
 397 instance, with classification  $y$  will be a scalar representing a class label. With regression  
 398 , it will take a vector of continuous variables. In dealing with a segmentation model,  
 399  $y$  can be a multi-dimensional label image, basically supervised training finds model  
 400 parameters  $\theta$  that best predict data given a loss function  $L(y, \hat{y})$ . This  $\hat{y}$  describes the  
 401 output of model obtained by feeding  $x$  to  $f(x; \theta)$  that represents the model.

402 **Unsupervised learning**:- are algorithms that are trained to find patterns , such as  
 403 data without labels for instance clustering and principle component analysis methods.  
 404 These algorithms can be performed on models with different loss functions.

#### 405 6.2. Neural networks.

These are networks that contribute to deep learning systems. Neural networks  
 comprise of neurons with some activation  $a$  and parameters  $\theta = \{W, \beta\}$ , where  $W$  is  
 weight and  $\beta$  set bias. Activation presents linear combination of input  $x$  to a neuron  
 and its parameters, followed by element on element (.) for non linearity, referred to as  
 the transfer function:  $a = \sigma(w^T + b)$ . Transfer functions for traditional neural networks  
 are sigmoid and the hyperbolic tangent function. Multi layered neural networks known  
 as perceptrons consist of several layers of these transformations :

$$f(x; \theta) = \sigma(W^L \theta (W^{L-1} \dots \sigma(W^0 x + b^0) + b^{L-1}) + b^L) \quad (12)$$

406 Here  $W^n$  is a matrix comprising of  $w_k$  rows with  $k$  as activation on the output. The  
 407  $n$  is the number of current layers, and  $L$  the final layer. Hidden layers are layers in  
 408 between the input layer and the output layer. When a network contains multiple hidden  
 409 layers it is referred to as a deep neural network.

Activation's done to the final layer which is the output layer of the network are mapped to a distribution over the number of classes  $P(y|x;\theta)$  through a softmax function:

$$P(y|x;\theta) = \text{softmax}(x;\theta) = \frac{e^{(W_i^L)^T x + (b_i)^L}}{\sum_{k=1}^K e^{(W_k^L)^T x + (b_k)^L}} \quad (13)$$

410 Here  $W_i^L$  is the weight of the output node associated with class  $i$ .

Stochastic gradient descent is the method used to fit parameters to the dataset  $D$ . A small subset of the dataset is used to optimize maximum likelihood and this in return minimize negative log-likelihood as:

$$\text{argmin}_{\theta} - \sum_{n=1}^N \log[P(y_n|x_n;\theta)]. \quad (14)$$

411 This further leads to binary cross entropy loss for two class problems and categorical  
412 cross entropy for multi class tasks. Deep neural networks gained popularity in 2006 and  
413 In method (Larochelle et al. 2007), they explain how they pre-trained DNNs layer by  
414 layer and fine tuned their stacked network to produce good evaluation performance.  
415 Currently the most used deep learning popular networks are the convolution and the  
416 recurrent networks.

#### 417 6.2.1. Convolution neural networks

418 These networks have weights that are shared in a manner that the network performs  
419 convolutions on images. This means that there is no redundancy in the the way the  
420 model learns separate detectors for the same object that occurs at different position on  
421 an image. It reduces the number of parameters to be used for learning. At each layer of  
422 the network the image is convolved with a set of  $K$  kernels  $W = (W_1, \dots, W_K)$ , with biases  
423  $\beta = (b_1, \dots, b_K)$  and each generating  $X_k$  feature map.

The features are subjected to a non-linear transform  $\sigma(\cdot)$  and the process iterated for every convolution layer  $l$  given by:

$$X_K^1 = \sigma(W_K^{l-1} * X^{l-1} + b_K^{l-1}). \quad (15)$$

424 The convolution neural network also have pooling layers that aggregate pixels  
425 and their neighbors using an invariant function which is the maximum operation.  
426 Aggregation is done to subsequent convolution layers and at the end of the stream, a  
427 regular network layer is added where weights are not shared. The network is trained by  
428 feeding activations to the output layer through a softmax function. Under the CNNs  
429 there exist common architectures that are widely used in the analysis of medical images  
430 and include:

431 **General classification architectures.**:- include networks such AlexNet (Krizhevsky2012).  
432 , unlike it's precursor LeNet (Lecun et al. 1998), consists of five convolution kernel layers  
433 employed in the input and output. AlexNet incorporated rectified linear units (RELU)  
434 as their activation function, and this has become the most common choice in CNNs.  
435 Further, there has been an interest in using smaller kernels instead of single layers of  
436 kernels with a large receptive field, this in return has less number of parameters. Re-  
437 search by (Simonyan et al. 2014), discussed the use of deeper neural networks that  
438 have small fixed size kernels in each layer of the 19- layer model referred to as VGG19  
439 network model. More complex building blocks have been introduced to deep networks,  
440 to improve efficiency in the training process, and also reduce the amount of parameters  
441 used. There is also (Goodfellow et al. 2014), GoogLeNet is a 22-layered network that uses  
442 inception blocks with a set of convolutions of different sizes. The ResNet architecture  
443 was introduced and consists of ResNet blocks which instead of learning a function, they  
444 learn mappings in each layer that is close to the identity function (Ren et al. 2015). There  
445 has been an increase in the use of these deep architectures due to their low memory



use and this even contributed to recent versions GoogleNet referred to as Inception v3 (Khosravi et al. 2018).

**Multi-stream architectures:-** are networks that accomodate multiple inputs in form of channels towards the input layer and then later merged at any point in the network. Image processing can be done by the use of multi-scale image analysis and classification for brain lesions (Kamnitsas et al. 2017). Multi-stream architecture (Couprie et al. 2013), used it for segmentation of natural images. Challenges of deep learning systems in the medical imaging domain is in adapting existing architectures for instance with different input formats (2D or 3D) data. Volume-tric data can be divided into slices and fed as different streams to a network to avoid a result of large amounts of parameters. These technique can still be used to perform knee cartilage segmentation (Prasoon et al. 2013). The same technique but for classification in the context of medical imaging (Setio et al. 2016).

**Segmentation architectures:-** are specific to the task of segmentation of medical images. Here CNNs are used to classify individual pixels with those in their neighborhood in an image. To avoid redundancy in the classification of the pixels, fully connected layers are re-written as convolutions and this helps the CNN to take in input images larger than what it was trained on and produce a likelihood map. The resultant fully CNN(fCNN) can then be applied to an entire volume of images. This further leads to low resolution of output compared to the input images due to pooling of layers. There is a technique that applies the FCNN to shifted versions of the input, and then stitching the result together to obtain a full resolution of the final output (Long et al. 2015). The FCNN was improved by proposing the U-net architecture that has convolutions in its down-sampling, and later an up-sampling task to increase the image size (Ronneberger et al. 2015). Another method added skip connections to U-net architecture to connect down-sampling and up-sampling of the convolution layers (Long et al. 2015). A similar approach was used by (Ciccek et al. 2016), for 3D data, and (Milletari et al. 2016), incorporated residual blocks and Dice loss layer to the U-net architecture instead of the commonly used cross-entropy.

### 6.2.2. Recurrent Neural Networks.

These networks were developed for discrete sequence analysis and have varied lengths for both inputs and outputs thus making them suitable for tasks such as machine translation. In a classification task, the model learns distribution over classes  $P(y|x_1...x_T; \theta)$  given sequence  $x_1...x_T$  as input.

The RNN has a hidden state  $h$  at time  $t$  which is the output of a non-linear mapping from  $x_t$  and previous state  $h_{t-1}$ :  $h_t = \sigma(Ex_t + Rh_{t-1} + b)$ . Here  $W, R$  are weight matrices that are shared over time. For a classification task, several fully connected layers are used and followed by a softmax to map the sequence over the classes as :

$$P(y|x_1...x_T; \theta) = \text{softmax}(h_T : W_{out}, b_{out}) \quad (16)$$

RNNs have similar problems of memory shortage as those of other deep neural networks. Several techniques have been developed such as the long short term memory(LSTM) cell (Hochreiter et al. 1997), to deal with the problem. A simplification of the LSTM is the gated recurrent unit(GRU) (Chung et al. 2014). RNNs are increasingly being adopted with promising results, for instance (Stollenga et al. 2015), in the human brain challenge.

### 6.3. Unsupervised models

Some of the unsupervised models reviewed include auto-encoders, restricted Boltzmann machines or deep belief networks.

### 6.3.1. Auto-encoders

These are networks trained to reconstruct input  $x$  on output  $y$  via a hidden layer  $h$ . They have a weight matrix  $W_{x,h}$  and bias  $b_{x,h}$  from input to hidden state and  $W_{h,x}$  with corresponding bias  $b_{h,x}$  from hidden state to reconstruction. The hidden activation is computed as:

$$h = \sigma(W_{x,h}x + b_{x,h}). \quad (17)$$

Here,  $h$  is smaller than  $x$  to prevent the model from learning the identity function. According to (Vincent et al. 2010), they introduced another solution to prevent the model from learning of the identity function. The model uses a de-noising auto-encoder that trains the model to reconstruct input from noise. Deep auto-encoders are realized by placing auto-encoder layers on top of each other, and in most cases the layers were trained individually. Examples of auto-encoders include:

**Variational auto-encoders:-** with these (Uzunova et al. 2019), introduce the use of conditional variational auto-encoders for pathology detection in medical images.

### 6.3.2. Adversarial networks

These are used for image generation tasks and include works from (Zhang et al. 2019) and (Korkinof et al. 2018).

### 6.3.3. Deep Belief Networks

These are a type of Markov random field (MRF) that constitute an input layer  $x = (x_1 \dots x_N)$  and a hidden layer  $h = (h_1 \dots h_M)$  that has a latent feature representation. Its connections are bi-directional and thus a generative model that can be sampled for new data points. An energy function can be defined for a state  $(x, h)$  of input and hidden layers as:

$$E(x, h) = h^T W_x - c^T x - b^T h \quad (18)$$

Here  $c$  and  $b$  are the bias terms. Further, the probability of the system is given by:

$$p(x, h) = \frac{1}{Z} \exp\{-E(x, h)\}. \quad (19)$$

This makes computing the partition function  $Z$  intractable, while conditioned inference in computing  $h$  conditioned on  $x$  is tractable and is given by:

$$P(h_j|x) = \frac{1}{1 + \exp(-b_j - W_j x)}. \quad (20)$$

The use of DBNs can be to fuse medical images (Kaur et al. 2019). DBNs also are used to extract high level features from medical images and effectively classify them (Khatami et al. 2016).

## 6.4. Software and Hardware

These are the processors and softwares used to handle the running of various deep learning techniques. They include GPU computing libraries such as CUDA and OpenCL, these being very fast processor units compared to the previously used CPUs. These GPUs work hand in hand with the available open source softwares that provide a platform to implement various operations of neural networks such as convolutions. Most popular packages include Caffe (Jia et al. 2014), TensorFlow (Abadi et al. 2016), Theano (Maclaurin et al. 2015), Torch (Collobert et al. 2011), that provide interfaces for implementing various operations in deep learning. They are also third party packages written on top of frameworks like Keras (Chollet et al. 2018) and Github (Zagalsky et al. 2015).



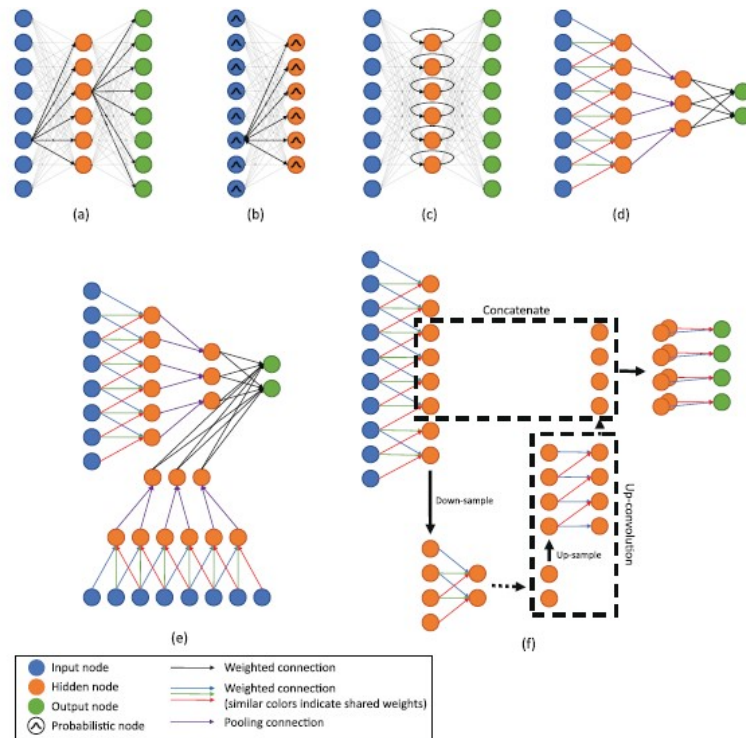


**Figure 13.** Representation of deep learning architectures:(a) Auto-encoder, (b) Deep Belief Networks, (c) recurrent neural network, (d) convolutional neural network, (e) multi-stream convolutional neural network, (f) U-net architecture (Litjens et al. 2017).

## 7. Deep learning uses in medical images.

These systems can be used in various tasks like segmentation, classification, detection and registration.

### 7.1. Classification

In this approach, one has a single or multiple inputs with a single variable as output. For instance, in a disease classification setup, one has the disease or not and diagnosis of the disease is based on a sample of the data set. Transfer learning is therefore realized and is defined as the use of pre-trained networks to cover very large data sets for deep networks training. Transfer learning can be used to fine-tune a pre-train network on medical images, and also for feature extraction on image data. These processes are beneficial in saving time used to train deep networks and enable extracted features to be analyzed faster. Object classification is usually done on a small part of the image and can be divided into two or more classes for analysis. For instance (Shen et al. 2015), used three CNNs, each taking a nodule patch as input and each feature output is

concatenated to form a final feature vector. Multi-stream CNNs are used to classify skin lesions with each stream working on different resolutions of the image (Kawahara et al. 2016).

## 7.2. Detection

Detection of objects and their respective regions of interest in images is an important part of diagnosis by medical practitioners. The task consists of localizing and identification of small regions in a full image. These systems are designed to automatically detect regions and decrease the reading time of human experts. An example of detection include (Naam et al. 2016) , explain the use of edge detection method to detect dental caries on dental images.

## 7.3. Segmentation.

Segmentation of various organs allow deep analysis of several parameters related to volume and shape, for example in skin or breast cancer analysis. It is always the first step before the detection process, and is defined as the identification of the pixels which make up the interior or exterior contour of the object of interest. There has been a wide variety of methods developed to segment images using deep learning medical images. Segmentation is needed to perform accurate segmentation on 3D CNNs using multi-stream networks with different scales (Ghafoorian et al. 2017).

## 7.4. Registration.

Registration is a common image analysis task in which coordinate transforms are calculated from one image to another. This is done iteratively assuming parametric transformations and a pred-determined metric is optimized. Deep networks can benefit from registration by estimating a similarity measure for two images to drive an iterative optimization , for instance (Simonovsky et al. 2016). They can also be used to predict transformation parameters using regression, for example (Rather et al. 2015).

## 8. Databases used by dental images.

There is need for efforts to build or come up with a public dataset to aid developing of algorithms to be used in the dental imaging area. In order for this to come to pass, researchers need to release data used in their papers, and this will lead to a repository that can reliably catalog and archive publicly dental imaging data. Several examples of datasets exist and include the Digital database for screening mammography(DDSM) (Lee et al. 2016) , that is used for mammogram image analysis and aids screening of breast cancer. There exists several databases that are used in dental imaging and this include:

**PASCAL VOC 2007:-** this is from the results from the pascal visual object classes challenge of 2007 (Everingham et al. 2010).

**Caltech101:-** this is a dataset of images to facilitate computer vision and its techniques (Fei et al. 2004) . This dataset is also applicable in image recognition and classification and contains a total of 9,146 images split into 101 distinct object categories.

**NORB:-** is used for experiments in 3D object recognition shapes (Lecun et al. 2004) . The dataset contains 50 toys belonging to five generic categories that include : air-planes,cars ,four legged animals, trucks.

**CIFAR-10/100:-** this consists of 60000 32\*32 colour images in 10 classes ,with 50000 training images and 10000 test images, (Krizhevsky, A. and Hinton, G., 2009).

**MNIST:-** acronym for modified national institute of standards and technology is a dataset of handwritten digits commonly used for training and testing data in the machine learning field. It contains 60000 training images and 10000 testing images (Deng, L., 2012).

**LabelMe:-** is a dataset and web based tool used for image annotation (Russell et al. 2008) , and was created by MIT computer science intelligence laboratory(CSAIL). It is

applicable in computer vision and is very dynamic, free and open to public contribution. It contains 187240 images , 62197 annotated images and 658992 labelled objects.

**ImageNet:-** is a large dataset used for visual object recognition, and has more than 20000 categories with each category containing several hundred images (Deng et al. 2009).

### Summary

Both MNIST and CIFAR-10/100 datasets are available for the public while the other datasets can be accessed by directly contacting the researchers. Dental datasets are difficult to find and thus researchers prefer to use available public datasets. ImageNet is one of the datasets that is used for evaluations by several dental imaging models like ResNets and VGGNets.

## 9. Evaluation protocols for dental images.

Deep learning techniques are used on problems having very large datasets with thousands of instances , and therefore they need a way to estimate the performance of a given data configuration and use this to compare with performances of other configurations. One of the ways is by splitting data (Adagbasa et al. 2019) , since very large datasets require long training times.

### 9.1. Splitting data.

The data is split into train and test data splits for instance with Keras library for deep learning provides two ways of handling the splitting of data. It can split your data into a validation set and evaluate the performance of your model on that validation set. This is done by setting the validation split(*validation\_split*) argument on the fit () function to a certain percentage of your training dataset such as: 30% for validation.

### 9.2. Manual k-fold cross validation

This is used as the standard evaluation method for machine learning techniques. This method splits the dataset into k-subsets and trains the model on all the subsets one after the other except one subset that is left out as the validation set. Evaluation is done on the left out subset which is the validation set, and the performance is averaged across all models created. The cross validation method is applicable on small deep learning models and is used with 5 or 10 folds. We also have (Sun et al. 2019) , as the train-test split method.

### 9.3. Train-Test split

:- this is achieved by splitting data into two parts the training and test set. The model is then fitted in the training set then use the fit model to make predictions on the test set and evaluate the skill of those predictions thus referred to as the train-test split. The train-test split skill is used as an estimate of how well the model performs especially when presented with new data. This method is preferred when you have very large data and slow model to train, thus the skill score for the model will be noisy because of the randomness in the data. The randomness of data makes the model flexible but makes it less stable for instance you get different results from training the same model. This can be controlled by introducing a random seed and repeating experiments multiple times. The use of random seed is basically just using the same randomness every time the model is being fit and evaluated. Get an average of the estimated model skill after running the experiments multiple times. We also have (Abdualgalil et al. 2020) , that also gives a description of the confusion matrix.

### 9.4. Confusion matrix

:- is an  $N * N$  matrix with  $N$  number of classes being predicted and is used mostly with class output models. The matrix consists of several metrics that include:

628 **Accuracy:-** total number of correct predictions.

629 **Precision or positive predictive value:-** is a proportion of positive correct predic-  
630 tions.

631 **Negative predictive value:-** is a proportion of negative correct predictions.

632 **Recall or Sensitivity:-** is a proportion of actual positive cases correctly identified.

633 **Specificity:-** is a proportion of actual negative cases correctly identified.

#### 634 9.5. F1-score

635 This is defined as the harmonic mean of the precision and recall values for a  
636 classification problem task.

637 The F1 score is given by:

$$F_1 = \left\{ \frac{\text{recall}^{-1} + \text{precision}^{-1}}{2} \right\}^{-1} = 2 \cdot \frac{\text{precision} \cdot \text{recall}}{\text{precision} + \text{recall}} \quad (21)$$

638 Harmonic mean is preferred from arithmetic mean because it takes care of extreme  
639 values for instance those in a binary classification model. The F1 score can also be  
640 adjusted to increase effectiveness by adding  $\beta$  as an adjustable parameter to get :

$$F_\beta = (1 + \beta^2) \cdot \frac{\text{precision} \cdot \text{recall}}{(\beta^2 \cdot \text{precision}) + \text{recall}} \quad (22)$$

### 641 10. Conclusion and Future work

642 From our survey , various techniques , methods and approaches have been dis-  
643 cussed that point towards the segmentation and detection of dental images. Various  
644 works that stem from the industry and academia have been mentioned and discussed  
645 regarding existing algorithms , segmentation and detection methods and also various  
646 protocols for evaluating performance. There are issues and encouraging future perspec-  
647 tives of study that have popped out from our discussions here and are highlighted below  
648 as:

- 649 • **Data availability and reliability.** Deep learning networks require large amount of  
650 data to be able to achieve meaningful and effective performance results. Due to the  
651 nature of dental images , there is need for hybrid datasets to aid good performance  
652 of the networks. There is need of public available datasets for dental images to  
653 make deep learning in the field possible.
- 654 • **Data standardization.** Many methods discussed here are handling the pre-processing  
655 step through manual methods such as, cropping the region of interest on an image.  
656 This methods contribute to the loss of some of key details from the images. Some  
657 networks end up dividing a whole image into sub-regions and this slows down the  
658 learning process that occurs one sub-region after the other. There are methods like  
659 down-sampling which might lead to deletion of important details and this seem to  
660 have been due to limitations in computational power. Deep learning approaches  
661 have seen increased learning on whole images rather than the need of manual  
662 manipulation of images at the pre processing stage, in order to get more general  
663 and accurate results.
- 664 • **Weight Regularization Methods.** Deep learning networks can also be improved by  
665 introducing weight regularization to improve their performance. The regularization  
666 of weights involves optimization of model hyper-parameters such as the learning  
667 rate and the dropout rate. Basically, weight regularization methods are introduced  
668 into networks for parameter optimization.
- 669 • **Hybrid approaches.** Deep networks can also be achieved by combining of several  
670 models or methods to form hybrid networks that will improve overall evaluation  
671 performance. The combination can be in any stage of the model, for instance  
672 combining two pre-processing techniques to come with a single one to enhance

image quality. This combination can also be handled by joining various attributes of different models to form one hybrid model that will enhance the training, extraction, detection and classification of objects.

Lastly, oral health care and follow up or recall from medical practitioners is very important for risk assessment and management of dental caries.

## References

- Waugh, A. and Grant, A., 2014. *Ross and Wilson Anatomy and physiology in health and illness* E-book. Elsevier Health Sciences.
- Black, G.V., 1955. *Operative dentistry* (Vol. 2). Medico-Dental Publishing Company.
- Osterloh, D. and Viriri, S., 2016, December. Unsupervised Caries Detection in Non-standardized Bitewing Dental X-Rays. In *International Symposium on Visual Computing* (pp. 649-658). Springer, Cham.
- Newman, M.G., Takei, H., Klokkevold, P.R. and Carranza, F.A., 2011. *Carranza's clinical periodontology*. Elsevier health sciences.
- Tikhe, S.V., Naik, A.M., Bhide, S.D., Saravanan, T. and Kaliyamurthie, K.P., 2016, February. Algorithm to identify enamel caries and interproximal caries using dental digital radiographs. In *2016 IEEE 6th International Conference on Advanced Computing (IACC)* (pp. 225-228). IEEE.
- Akarslan, Z.Z., Akdevelioglu, M., Gungor, K. and Erten, H., 2008. A comparison of the diagnostic accuracy of bitewing, periapical, unfiltered and filtered digital panoramic images for approximal caries detection in posterior teeth. *Dentomaxillofacial Radiology*, 37(8), pp.458-463.
- Tangel, M.L., Fatichah, C., Yan, F., Betancourt, J.P., Widyanto, M.R., Dong, F. and Hirota, K., 2013, June. Dental classification for periapical radiograph based on multiple fuzzy attribute. In *2013 Joint IFSA World Congress and NAFIPS Annual Meeting (IFSA/NAFIPS)* (pp. 304-309). IEEE.
- Janowczyk, A., Basavanthally, A. and Madabhushi, A., 2017. Stain normalization using sparse autoencoders (StaNoSA): application to digital pathology. *Computerized Medical Imaging and Graphics*, 57, pp.50-61.
- Vahadane, A., Peng, T., Sethi, A., Albarqouni, S., Wang, L., Baust, M., Steiger, K., Schlitter, A.M., Esposito, I. and Navab, N., 2016. Structure-preserving color normalization and sparse stain separation for histological images. *IEEE transactions on medical imaging*, 35(8), pp.1962-1971.
- Ghafoorian, M., Karssemeijer, N., Heskes, T., Van Uder, I.W.M., de Leeuw, F.E., Marchiori, E., van Ginneken, B. and Platel, B., 2016, April. Non-uniform patch sampling with deep convolutional neural networks for white matter hyperintensity segmentation. In *2016 IEEE 13th International Symposium on Biomedical Imaging (ISBI)* (pp. 1414-1417). IEEE.
- Gulshan, V., Peng, L., Coram, M., Stumpe, M.C., Wu, D., Narayanaswamy, A., Venugopalan, S., Widner, K., Madams, T., Cuadros, J. and Kim, R., 2016. Development and validation of a deep learning algorithm for detection of diabetic retinopathy in retinal fundus photographs. *Jama*, 316(22), pp.2402-2410.
- Mohamed, J., Nafizah, A.N., Zariyantey, A.H. and Budin, S.B., 2016. Mechanisms of diabetes-induced liver damage: the role of oxidative stress and inflammation. *Sultan Qaboos University Medical Journal*, 16(2), p.e132.
- Kooi, T., Gubern-Merida, A., Mordang, J.J., Mann, R., Pijnappel, R., Schuur, K., den Heeten, A. and Karssemeijer, N., 2016, June. A comparison between a deep convolutional neural network and radiologists for classifying regions of interest in mammography. In *International Workshop on Breast Imaging* (pp. 51-56). Springer, Cham.
- Dou, Q., Yu, L., Chen, H., Jin, Y., Yang, X., Qin, J. and Heng, P.A., 2017. 3D deeply supervised network for automated segmentation of volumetric medical images. *Medical image analysis*, 41, pp.40-54.

- 725 Poudel, R.P., Lamata, P. and Montana, G., 2016. Recurrent fully convolutional neural  
726 networks for multi-slice MRI cardiac segmentation. In *Reconstruction, segmentation,  
727 and analysis of medical images* (pp. 83-94). Springer, Cham.
- 728 Kong, B., Zhan, Y., Shin, M., Denny, T. and Zhang, S., 2016, October. Recognizing  
729 end-diastole and end-systole frames via deep temporal regression network. In *International conference on medical image computing and computer-assisted intervention* (pp.  
730 264-272). Springer, Cham.
- 731 Miller, W.D., 1902. The presence of bacterial plaques on the surface of teeth and  
732 their significance. *Dent Cosmos*, 44, pp.425-446.
- 733 Bowen, W.H., Birkhed, D., Granath, L. and McHugh, W.D., 1986. Dental caries:  
734 Dietary and microbiology factors. *Systemized prevention of oral disease: Theory and  
735 practice*, pp.19-41.
- 736 Stephan, R.M., 1944. Intra-oral hydrogen-ion concentrations associated with dental  
737 caries activity. *Journal of dental research*, 23(4), pp.257-266.
- 738 Weiss, R.L. and Trithart, A.H., 1960. Between-meal eating habits and dental caries  
739 experience in preschool children. *American Journal of Public Health and the Nations  
740 Health*, 50(8), pp.1097-1104.
- 741 Mandel, I.D. and Wotman, S., 1976. The salivary secretions in health and disease.  
742 *Oral sciences reviews*, (8), p.25.
- 743 NAVAZesh, M., 2003. How can oral health care providers determine if patients  
744 have dry mouth?. *The Journal of the american dental association*, 134(5), pp.613-618.
- 745 Griffin, S.O., Oong, E., Kohn, W., Vidakovic, B., Gooch, B.F. and CDC Dental Sealant  
746 Systematic Review Work Group, 2008. The effectiveness of sealants in managing caries  
747 lesions. *Journal of dental research*, 87(2), pp.169-174.
- 748 HEAD, J., 1912. A study of saliva and its action on tooth enamel in reference  
749 to its hardening and softening. *Journal of the American Medical Association*, 59(24),  
750 pp.2118-2122.
- 751 McKay, F.S., 1928. The relation of mottled enamel to caries. *The Journal of the  
752 American Dental Association* (1922), 15(8), pp.1429-1437.
- 753 Black, G.V., 1916. Mottled teeth: an endemic developmental imperfection of the  
754 enamel of the teeth heretofore unknown in the literature of dentistry. *Dental Cosmos*, 58,  
755 pp.129-156.
- 756 Dean, H.T., Arnold Jr, F.A., Jay, P. and Knutson, J.W., 1950. Studies on mass control  
757 of dental caries through fluoridation of the public water supply. *Public Health Reports*  
758 (1896-1970), pp.1403-1408.
- 759 Reich, E., Lussi, A. and Newbrun, E., 1999. Caries-risk assessment. *International  
760 dental journal*, 49(1), pp.15-26.
- 761 Fontana, M. and Zero, D.T., 2006. Assessing patients' caries risk. *The Journal of the  
762 American Dental Association*, 137(9), pp.1231-1239.
- 763 Koulourides, T., 1986. Implications of remineralization in the treatment of dental  
764 caries.
- 765 Black, G.V. and Black, A.D., 1917. *The pathology of the hard tissues of the teeth*  
766 (Vol. 1). Medico-Dental Publishing Company.
- 767 Zero, D.T., Fontana, M., Martínez-Mier, E.A., Ferreira-Zandoná, A., Ando, M.,  
768 González-Cabezas, C. and Bayne, S., 2009. The biology, prevention, diagnosis and  
769 treatment of dental caries: scientific advances in the United States. *The Journal of the  
770 American Dental Association*, 140, pp.25S-34S.
- 771 Raper, H.R., 1925. Practical clinical preventive dentistry based upon periodic  
772 roentgen-ray examinations. *The Journal of the American Dental Association* (1922),  
773 12(9), pp.1084-1100.
- 774 Wenzel, A., 2004. Bitewing and digital bitewing radiography for detection of caries  
775 lesions. *Journal of dental research*, 83(1<sub>suppl</sub>), pp.72 – 75.
- 776 Mirza, J. and Robertson, G., 2008. *Vital guide to Dental implants*. Vital, 6(1),  
pp.19-22.

- Subramanyam, R.B., Prasad, K.P. and Anuradha, B., 2014. Different image segmentation techniques for dental image extraction. *Int. J. Eng. Res. Appl*, 4(7), pp.173-177.
- Sezgin, M. and Sankur, B., 2004. Survey over image thresholding techniques and quantitative performance evaluation. *Journal of Electronic imaging*, 13(1), pp.146-166.
- Silva, G., Oliveira, L. and Pithon, M., 2018. Automatic segmenting teeth in X-ray images: Trends, a novel data set, benchmarking and future perspectives. *Expert Systems with Applications*, 107, pp.15-31.
- Lurie, A., Tosoni, G.M., Tsimikas, J. and Walker Jr, F., 2012. Recursive hierarchic segmentation analysis of bone mineral density changes on digital panoramic images. *Oral surgery, oral medicine, oral pathology and oral radiology*, 113(4), pp.549-558.
- Modi, C.K. and Desai, N.P., 2011, May. A simple and novel algorithm for automatic selection of ROI for dental radiograph segmentation. In 2011 24th Canadian Conference on Electrical and Computer Engineering (CCECE) (pp. 000504-000507). IEEE.
- Abaza, A., Ross, A. and Ammar, H., 2009, November. Retrieving dental radiographs for post-mortem identification. In 2009 16th IEEE International Conference on Image Processing (ICIP) (pp. 2537-2540). IEEE.
- Ajaz, A. and Kathirvelu, D., 2013, April. Dental biometrics: Computer aided human identification system using the dental panoramic radiographs. In 2013 International Conference on Communication and Signal Processing (pp. 717-721). IEEE.
- Azevedo, A.D.C.S., Alves, N.Z., Michel-Crosato, E., Rocha, M., Cameriere, R. and Biazevic, M.G.H., 2015. Dental age estimation in a Brazilian adult population using Cameriere's method. *Brazilian oral research*, 29(1), pp.1-9.
- Wang, L., Shi, F., Li, G., Gao, Y., Lin, W., Gilmore, J.H. and Shen, D., 2014. Segmentation of neonatal brain MR images using patch-driven level sets. *NeuroImage*, 84, pp.141-158.
- Wang, Y., Lin, C.L. and Miller, J.D., 2015. Improved 3D image segmentation for X-ray tomographic analysis of packed particle beds. *Minerals Engineering*, 83, pp.185-191.
- Xi, Y., Jin, Y., De Man, B. and Wang, G., 2016. High-kVp assisted metal artifact reduction for X-ray computed tomography. *IEEE Access*, 4, pp.4769-4776.
- Amer, Y.Y. and Aqel, M.J., 2015. An efficient segmentation algorithm for panoramic dental images. *Procedia Computer Science*, 65, pp.718-725.
- Kaur, G. and Rani, J., 2016. MRI brain tumor segmentation methods-a review. *Infinite Study*.
- Garg, I. and Kaur, B., 2016, March. Color based segmentation using K-mean clustering and watershed segmentation. In 2016 3rd International Conference on Computing for Sustainable Global Development (INDIACom) (pp. 3165-3169). IEEE.
- Lin, M., Chen, J.H., Wang, X., Chan, S., Chen, S. and Su, M.Y., 2013. Template-based automatic breast segmentation on MRI by excluding the chest region. *Medical physics*, 40(12), p.122301.
- Indraswari, R., Arifin, A.Z., Navastara, D.A. and Jawas, N., 2015, September. Teeth segmentation on dental panoramic radiographs using decimation-free directional filter bank thresholding and multistage adaptive thresholding. In 2015 International Conference on Information Communication Technology and Systems (ICTS) (pp. 49-54). IEEE.
- Razali, M.R.M., Ahmad, N.S., Hassan, R., Zaki, Z.M. and Ismail, W., 2014, December. Sobel and canny edges segmentations for the dental age assessment. In 2014 International Conference on Computer Assisted System in Health (pp. 62-66). IEEE.
- Alsmadi, M.K., 2018. A hybrid Fuzzy C-Means and Neutrosophic for jaw lesions segmentation. *Ain Shams Engineering Journal*, 9(4), pp.697-706.
- Tuan, T.M., 2017. Dental segmentation from X-ray images using semi-supervised fuzzy clustering with spatial constraints. *Engineering Applications of Artificial Intelligence*, 59, pp.186-195.
- Işın, A., Direkoğlu, C. and Şah, M., 2016. Review of MRI-based brain tumor image segmentation using deep learning methods. *Procedia Computer Science*, 102, pp.317-324.

- 831 Niroshika, U.A.A. and Meegama, R.G.N., 2013. Active Contour Model for the  
832 Detection of Sharp Corners in Image Boundaries.
- 833 Hasan, A.M., Meziane, F., Aspin, R. and Jalab, H.A., 2016. Segmentation of brain  
834 tumors in MRI images using three-dimensional active contour without edge. *Symmetry*,  
835 8(11), p.132.
- 836 Rad, A.E., Mohd Rahim, M.S., Rehman, A., Altameem, A. and Saba, T., 2013.  
837 Evaluation of current dental radiographs segmentation approaches in computer-aided  
838 applications. *IETE Technical Review*, 30(3), pp.210-222.
- 839 Kumar, R., Talukdar, F.A., Dey, N., Ashour, A.S., Santhi, V., Balas, V.E. and Shi, F.,  
840 2017. Histogram thresholding in image segmentation: A joint level set method and  
841 lattice boltzmann method based approach. In *Information Technology and Intelligent*  
842 *Transportation Systems* (pp. 529-539). Springer, Cham.
- 843 Yau, H.T., Lin, Y.K., Tsou, L.S. and Lee, C.Y., 2008. An adaptive region growing  
844 method to segment inferior alveolar nerve canal from 3D medical images for dental  
845 implant surgery. *Computer-Aided Design and Applications*, 5(5), pp.743-752.
- 846 Sharifi, M., Fathy, M. and Mahmoudi, M.T., 2002, April. A classified and compar-  
847 ative study of edge detection algorithms. In *Proceedings. International conference on*  
848 *information technology: Coding and computing* (pp. 117-120). IEEE.
- 849 Tangel, M.L., Fatichah, C., Widyanto, M.R., Dong, F. and Hirota, K., 2012. Mul-  
850 tiscale image aggregation for dental radiograph segmentation. *Journal of Advanced*  
851 *Computational Intelligence and Intelligent Informatics*, 16(3), pp.388-396.
- 852 Chen, H., Zhang, K., Lyu, P., Li, H., Zhang, L., Wu, J. and Lee, C.H., 2019. A deep  
853 learning approach to automatic teeth detection and numbering based on object detection  
854 in dental periapical films. *Scientific reports*, 9(1), pp.1-11.
- 855 Fekri-Ershad, S., 2018. Innovative Texture Database Collecting Approach and  
856 Feature Extraction Method based on Combination of Gray Tone Difference Matrixes,  
857 Local Binary Patterns, and K-means Clustering. *arXiv preprint arXiv:1803.04125*.
- 858 Jader, G., Fontineli, J., Ruiz, M., Abdalla, K., Pithon, M. and Oliveira, L., 2018,  
859 October. Deep instance segmentation of teeth in panoramic X-ray images. In 2018 31st  
860 SIBGRAPI Conference on Graphics, Patterns and Images (SIBGRAPI) (pp. 400-407).  
861 IEEE.
- 862 Ren, S., He, K., Girshick, R. and Sun, J., 2015. Faster r-cnn: Towards real-time object  
863 detection with region proposal networks. In *Advances in neural information processing*  
864 *systems* (pp. 91-99).
- 865 Hazirbas, C., Ma, L., Domokos, C. and Cremers, D., 2016, November. Fusetnet:  
866 Incorporating depth into semantic segmentation via fusion-based cnn architecture. In  
867 *Asian conference on computer vision* (pp. 213-228). Springer, Cham.
- 868 Li, Y., Shi, H., Jiao, L. and Liu, R., 2012. Quantum evolutionary clustering algorithm  
869 based on watershed applied to SAR image segmentation. *Neurocomputing*, 87, pp.90-98.
- 870 Obuchowicz, R., Nurzynska, K., Obuchowicz, B., Urbanik, A. and Piórkowski, A.,  
871 2020. Caries detection enhancement using texture feature maps of intraoral radiographs.  
872 *Oral Radiology*, 36(3), pp.275-287.
- 873 Galloway, M.M. and MM, G., 1975. Texture analysis using gray level run lengths.
- 874 Eqbal, S., Paliwal, R.K. and Yadava, R.L., 2020. FCM and SVM Based Medical Image  
875 Feature Extraction using Wavelet Transform. *Tathapi with ISSN 2320-0693 is an UGC*  
876 *CARE Journal*, 19(23), pp.24-32.
- 877 Raj, J.R.F., Vijayalakshmi, K. and Priya, S.K., 2019. Medical image denoising using  
878 multi-resolution transforms. *Measurement*, 145, pp.769-778.
- 879 Deshmukh, H.U. and Thorat, S.S., 2018. Tumor Detection from Brain MRI Image  
880 Using Neural Network Approach.
- 881 Haralick, R.M., Shanmugam, K. and Dinstein, I.H., 1973. Textural features for image  
882 classification. *IEEE Transactions on systems, man, and cybernetics*, (6), pp.610-621.



- PS, S.K. and Dharun, V.S., 2016. Extraction of texture features using GLCM and shape features using connected regions. *International Journal of Engineering and Technology*.
- Korchiyne, R., Farssi, S.M., Sbihi, A., Touahni, R. and Alaoui, M.T., 2014. A combined method of fractal and GLCM features for MRI and CT scan images classification. *arXiv preprint arXiv:1409.4559*.
- Amadasun, M. and King, R., 1989. Textural features corresponding to textural properties. *IEEE Transactions on systems, man, and Cybernetics*, 19(5), pp.1264-1274.
- Laws, K., 1980. Textured image segmentation [Ph. D. dissertation]. Los Angeles, CA: University of Southern California.
- Orooji, M., Alilou, M., Rakshit, S., Beig, N.G., Khorrami, M., Rajiah, P., Thawani, R., Ginsberg, J., Donatelli, C., Yang, M. and Jacono, F., 2018. Combination of computer extracted shape and texture features enables discrimination of granulomas from adenocarcinoma on chest computed tomography. *Journal of Medical Imaging*, 5(2), p.024501.
- Ramaprabha, P.S., Chitra, M.P. and Prem Kumar, M., 2017. Effective lesion detection of colposcopic images using active contour method.
- Ojala, T., Pietikäinen, M. and Harwood, D., 1996. A comparative study of texture measures with classification based on featured distributions. *Pattern recognition*, 29(1), pp.51-59.
- Geetha, V. and Aprameya, K.S., 2019. Textural analysis based classification of digital X-ray images for dental caries diagnosis. *Int J Eng Manuf (IJEM)*, 9(3), pp.44-45.
- Gabor, D., 1946. Theory of communication. Part 1: The analysis of information. *Journal of the Institution of Electrical Engineers-Part III: Radio and Communication Engineering*, 93(26), pp.429-441.
- Avinash, S., Manjunath, K. and Kumar, S.S., 2016, August. An improved image processing analysis for the detection of lung cancer using Gabor filters and watershed segmentation technique. In 2016 International Conference on Inventive Computation Technologies (ICICT) (Vol. 3, pp. 1-6). IEEE.
- Aguirre-Ramos, H., Avina-Cervantes, J.G., Cruz-Aceves, I., Ruiz-Pinales, J. and Ledesma, S., 2018. Blood vessel segmentation in retinal fundus images using Gabor filters, fractional derivatives, and Expectation Maximization. *Applied Mathematics and Computation*, 339, pp.568-587.
- Hegde, M. and Sivakumar, P.A., 2018. Development and implementation of vlsi reconfigurable architecture for gabor filter in medical imaging application. *International Journal of Engineering and Management Research (IJEMR)*, 8(3), pp.71-76.
- Verma, M. and Raman, B., 2015. Center symmetric local binary co-occurrence pattern for texture, face and bio-medical image retrieval. *Journal of Visual Communication and Image Representation*, 32, pp.224-236.
- Li, F., Liu, M. and Alzheimer's Disease Neuroimaging Initiative, 2018. Alzheimer's disease diagnosis based on multiple cluster dense convolutional networks. *Computerized Medical Imaging and Graphics*, 70, pp.101-110.
- Edwards, S., Brown, S. and Lee, M., 2018. Automated 3-D Tissue Segmentation Via Clustering. *Journal of Biomedical Engineering and Medical Imaging*, 5(2), pp.08-08.
- Zhao, K., Zhou, L., Qian, P., Ding, Y., Jiang, Y., Chen, Y., Zheng, J., Su, K.H. and Muzic, R.F., 2019. A transfer fuzzy clustering and neural network based tissue segmentation method during PET/MR attenuation correction. *Journal of Medical Imaging and Health Informatics*, 9(7), pp.1491-1497.
- Liu, L., Lao, S., Fieguth, P.W., Guo, Y., Wang, X. and Pietikäinen, M., 2016. Median robust extended local binary pattern for texture classification. *IEEE Transactions on Image Processing*, 25(3), pp.1368-1381.
- Tan, X. and Triggs, B., 2010. Enhanced local texture feature sets for face recognition under difficult lighting conditions. *IEEE transactions on image processing*, 19(6), pp.1635-1650.

- 936 Murala, S. and Wu, Q.J., 2013. Local ternary co-occurrence patterns: a new feature  
937 descriptor for MRI and CT image retrieval. *Neurocomputing*, 119, pp.399-412.
- 938 Deep, G., Kaur, L. and Gupta, S., 2018. Local mesh ternary patterns: a new descrip-  
939 tor for MRI and CT biomedical image indexing and retrieval. *Computer Methods in*  
940 *Biomechanics and Biomedical Engineering: Imaging Visualization*, 6(2), pp.155-169.
- 941 Rabidas, R., Midya, A., Sadhu, A. and Chakraborty, J., 2016, March. Benign-  
942 malignant mass classification in mammogram using edge weighted local texture features.  
943 In *Medical Imaging 2016: Computer-Aided Diagnosis* (Vol. 9785, p. 97851X). Interna-  
944 tional Society for Optics and Photonics.
- 945 Naam, J., Harlan, J., Madenda, S. and Wibowo, E.P., 2016. The algorithm of image  
946 edge detection on panoramic dental X-ray using multiple morphological gradient (mMG)  
947 method. *International Journal on Advanced Science, Engineering and Information*  
948 *Technology*, 6(6), pp.1012-1018.
- 949 Naam, J., Harlan, J., Madenda, S. and Wibowo, E.P., 2016. Identification of the  
950 proximal caries of dental x-ray image with multiple morphology gradient method.  
951 *International Journal on Advanced Science, Engineering and Information Technology*,  
952 6(3), pp.343-346.
- 953 Liang, Y., Sun, L., Ser, W., Lin, F., Tay, E.Y., Gan, E.Y., Thng, T.G. and Lin, Z.,  
954 2017. Hybrid threshold optimization between global image and local regions in image  
955 segmentation for melasma severity assessment. *Multidimensional Systems and Signal*  
956 *Processing*, 28(3), pp.977-994.
- 957 Rakhlin, A., Shvets, A., Iglovikov, V. and Kalinin, A.A., 2018, June. Deep convo-  
958 lutional neural networks for breast cancer histology image analysis. In *International*  
959 *Conference Image Analysis and Recognition* (pp. 737-744). Springer, Cham.
- 960 Naqi, S.M., Sharif, M., Yasmin, M. and Fernandes, S.L., 2018. Lung nodule detection  
961 using polygon approximation and hybrid features from CT images. *Current Medical*  
962 *Imaging*, 14(1), pp.108-117.
- 963 Min, E., Guo, X., Liu, Q., Zhang, G., Cui, J. and Long, J., 2018. A survey of clustering  
964 with deep learning: From the perspective of network architecture. *IEEE Access*, 6,  
965 pp.39501-39514.
- 966 Litjens, G., Kooi, T., Bejnordi, B.E., Setio, A.A.A., Ciompi, F., Ghafoorian, M., Van  
967 Der Laak, J.A., Van Ginneken, B. and Sánchez, C.I., 2017. A survey on deep learning in  
968 medical image analysis. *Medical image analysis*, 42, pp.60-88.
- 969 Larochelle, H., Erhan, D., Courville, A., Bergstra, J. and Bengio, Y., 2007, June. An  
970 empirical evaluation of deep architectures on problems with many factors of variation.  
971 In *Proceedings of the 24th international conference on Machine learning* (pp. 473-480).
- 972 Krizhevsky, A., Sutskever, I. and Hinton, G.E., 2012. Imagenet classification with  
973 deep convolutional neural networks. In *Advances in neural information processing*  
974 *systems* (pp. 1097-1105).
- 975 LeCun, Y., Bottou, L., Bengio, Y. and Haffner, P., 1998. Gradient-based learning  
976 applied to document recognition. *Proceedings of the IEEE*, 86(11), pp.2278-2324.
- 977 Simonyan, K. and Zisserman, A., 2014. Very deep convolutional networks for  
978 large-scale image recognition. *arXiv preprint arXiv:1409.1556*.
- 979 Goodfellow, I.J., Shlens, J. and Szegedy, C., 2014. Explaining and harnessing adver-  
980 sarial examples. *arXiv preprint arXiv:1412.6572*.
- 981 Khosravi, P., Kazemi, E., Imielinski, M., Elemento, O. and Hajirasouliha, I., 2018.  
982 Deep convolutional neural networks enable discrimination of heterogeneous digital  
983 pathology images. *EBioMedicine*, 27, pp.317-328.
- 984 Kamnitsas, K., Ledig, C., Newcombe, V.F., Simpson, J.P., Kane, A.D., Menon, D.K.,  
985 Rueckert, D. and Glocker, B., 2017. Efficient multi-scale 3D CNN with fully connected  
986 CRF for accurate brain lesion segmentation. *Medical image analysis*, 36, pp.61-78.
- 987 Couprie, C., Farabet, C., Najman, L. and LeCun, Y., 2013. Indoor semantic segmen-  
988 tation using depth information. *arXiv preprint arXiv:1301.3572*.

- 989 Prason, A., Petersen, K., Igel, C., Lauze, F., Dam, E. and Nielsen, M., 2013, September. Deep feature learning for knee cartilage segmentation using a triplanar convolutional neural network. In International conference on medical image computing and computer-assisted intervention (pp. 246-253). Springer, Berlin, Heidelberg.
- 990  
991  
992  
993 Setio, A.A.A., Ciompi, F., Litjens, G., Gerke, P., Jacobs, C., Van Riel, S.J., Wille, M.M.W., Naqibullah, M., Sánchez, C.I. and van Ginneken, B., 2016. Pulmonary nodule detection in CT images: false positive reduction using multi-view convolutional networks. *IEEE transactions on medical imaging*, 35(5), pp.1160-1169.
- 994  
995  
996  
997 Long, J., Shelhamer, E. and Darrell, T., 2015. Fully convolutional networks for semantic segmentation. In Proceedings of the IEEE conference on computer vision and pattern recognition (pp. 3431-3440).
- 998  
999  
1000 Ronneberger, O., Fischer, P. and Brox, T., 2015, October. U-net: Convolutional networks for biomedical image segmentation. In International Conference on Medical image computing and computer-assisted intervention (pp. 234-241). Springer, Cham.
- 1001  
1002  
1003 Çiçek, Ö., Abdulkadir, A., Lienkamp, S.S., Brox, T. and Ronneberger, O., 2016, October. 3D U-Net: learning dense volumetric segmentation from sparse annotation. In International conference on medical image computing and computer-assisted intervention (pp. 424-432). Springer, Cham.
- 1004  
1005  
1006  
1007 Milletari, F., Navab, N. and Ahmadi, S.A., 2016, October. V-net: Fully convolutional neural networks for volumetric medical image segmentation. In 2016 fourth international conference on 3D vision (3DV) (pp. 565-571). IEEE.
- 1008  
1009  
1010 Hochreiter, S. and Schmidhuber, J., 1997. Long short-term memory. *Neural computation*, 9(8), pp.1735-1780.
- 1011  
1012 Chung, J., Gulcehre, C., Cho, K. and Bengio, Y., 2014. Empirical evaluation of gated recurrent neural networks on sequence modeling. *arXiv preprint arXiv:1412.3555*.
- 1013  
1014 Stollenga, M.F., Byeon, W., Liwicki, M. and Schmidhuber, J., 2015. Parallel multi-dimensional lstm, with application to fast biomedical volumetric image segmentation. In Advances in neural information processing systems (pp. 2998-3006).
- 1015  
1016  
1017 Vincent, P., Larochelle, H., Lajoie, I., Bengio, Y., Manzagol, P.A. and Bottou, L., 2010. Stacked denoising autoencoders: Learning useful representations in a deep network with a local denoising criterion. *Journal of machine learning research*, 11(12).
- 1018  
1019  
1020 Uzunova, H., Schultz, S., Handels, H. and Ehrhardt, J., 2019. Unsupervised pathology detection in medical images using conditional variational autoencoders. *International journal of computer assisted radiology and surgery*, 14(3), pp.451-461.
- 1021  
1022  
1023 Zhang, H., Goodfellow, I., Metaxas, D. and Odena, A., 2019, May. Self-attention generative adversarial networks. In International Conference on Machine Learning (pp. 7354-7363).
- 1024  
1025  
1026 Korkinof, D., Rijken, T., O'Neill, M., Yearsley, J., Harvey, H. and Glocker, B., 2018. High-resolution mammogram synthesis using progressive generative adversarial networks. *arXiv preprint arXiv:1807.03401*.
- 1027  
1028  
1029 Kaur, M. and Singh, D., 2019. Fusion of medical images using deep belief networks. *Cluster Computing*, pp.1-15.
- 1030  
1031 Khatami, A., Khosravi, A., Lim, C.P. and Nahavandi, S., 2016, October. A wavelet deep belief network-based classifier for medical images. In International Conference on Neural Information Processing (pp. 467-474). Springer, Cham.
- 1032  
1033  
1034 Jia, Y., Shelhamer, E., Donahue, J., Karayev, S., Long, J., Girshick, R., Guadarrama, S. and Darrell, T., 2014, November. Caffe: Convolutional architecture for fast feature embedding. In Proceedings of the 22nd ACM international conference on Multimedia (pp. 675-678).
- 1035  
1036  
1037  
1038 Abadi, M., Barham, P., Chen, J., Chen, Z., Davis, A., Dean, J., Devin, M., Ghemawat, S., Irving, G., Isard, M. and Kudlur, M., 2016. Tensorflow: A system for large-scale machine learning. In 12th USENIX symposium on operating systems design and implementation (OSDI 16) (pp. 265-283).
- 1039  
1040  
1041

- Maclaurin, D., Duvenaud, D. and Adams, R.P., 2015. Autograd: Effortless gradients in numpy. In ICML 2015 AutoML Workshop (Vol. 238, p. 5).
- Collobert, R., Kavukcuoglu, K. and Farabet, C., 2011. Torch7: A matlab-like environment for machine learning. In BigLearn, NIPS workshop (No. CONF).
- Chollet, F., 2018. Introduction to Keras. March 9th.
- Deep, G., Kaur, L. and Gupta, S., 2018. Local mesh ternary patterns: a new descriptor for MRI and CT biomedical image indexing and retrieval. *Computer Methods in Biomechanics and Biomedical Engineering: Imaging Visualization*, 6(2), pp.155-169.
- Zagalsky, A., Feliciano, J., Storey, M.A., Zhao, Y. and Wang, W., 2015, February. The emergence of github as a collaborative platform for education. In *Proceedings of the 18th ACM Conference on Computer Supported Cooperative Work Social Computing* (pp. 1906-1917).
- Shen, W., Zhou, M., Yang, F., Yang, C. and Tian, J., 2015, June. Multi-scale convolutional neural networks for lung nodule classification. In *International Conference on Information Processing in Medical Imaging* (pp. 588-599). Springer, Cham.
- Kawahara, J., BenTaieb, A. and Hamarneh, G., 2016, April. Deep features to classify skin lesions. In *2016 IEEE 13th international symposium on biomedical imaging (ISBI)* (pp. 1397-1400). IEEE.
- Ghafoorian, M., Karssemeijer, N., Heskes, T., Bergkamp, M., Wissink, J., Obels, J., Keizer, K., de Leeuw, F.E., van Ginneken, B., Marchiori, E. and Platel, B., 2017. Deep multi-scale location-aware 3D convolutional neural networks for automated detection of lacunes of presumed vascular origin. *NeuroImage: Clinical*, 14, pp.391-399.
- Simonovsky, M. and Komodakis, N., 2016. Onionnet: Sharing features in cascaded deep classifiers. *arXiv preprint arXiv:1608.02728*.
- Rather, A.M., Agarwal, A. and Sastry, V.N., 2015. Recurrent neural network and a hybrid model for prediction of stock returns. *Expert Systems with Applications*, 42(6), pp.3234-3241.
- Lee, R.S., Gimenez, F., Hoogi, A. and Rubin, D., 2016. Curated breast imaging subset of DDSM. *The Cancer Imaging Archive*, 8.
- Everingham, M., Van Gool, L., Williams, C.K., Winn, J. and Zisserman, A., 2010. The pascal visual object classes (voc) challenge. *International journal of computer vision*, 88(2), pp.303-338.
- Fei-Fei, L., Fergus, R. and Perona, P., 2004, June. Learning generative visual models from few training examples: An incremental bayesian approach tested on 101 object categories. In *2004 conference on computer vision and pattern recognition workshop* (pp. 178-178). IEEE.
- LeCun, Y., Huang, F.J. and Bottou, L., 2004, June. Learning methods for generic object recognition with invariance to pose and lighting. In *Proceedings of the 2004 IEEE Computer Society Conference on Computer Vision and Pattern Recognition, 2004. CVPR 2004.* (Vol. 2, pp. II-104). IEEE.
- Krizhevsky, A. and Hinton, G., 2009. Learning multiple layers of features from tiny images.
- Deng, L., 2012. The mnist database of handwritten digit images for machine learning research [best of the web]. *IEEE Signal Processing Magazine*, 29(6), pp.141-142.
- Russell, B.C., Torralba, A., Murphy, K.P. and Freeman, W.T., 2008. LabelMe: a database and web-based tool for image annotation. *International journal of computer vision*, 77(1-3), pp.157-173.
- Deng, J., Dong, W., Socher, R., Li, L.J., Li, K. and Fei-Fei, L., 2009, June. Imagenet: A large-scale hierarchical image database. In *2009 IEEE conference on computer vision and pattern recognition* (pp. 248-255). Ieee.
- Adagbasa, E.G., Adelabu, S.A. and Okello, T.W., 2019. Application of deep learning with stratified K-fold for vegetation species discrimination in a protected mountainous region using Sentinel-2 image. *Geocarto International*, pp.1-21.

- 1095 Sun, X., Gossmann, A., Wang, Y. and Bischt, B., 2019, December. Variational  
1096 resampling based assessment of deep neural networks under distribution shift. In 2019  
1097 IEEE Symposium Series on Computational Intelligence (SSCI) (pp. 1344-1353). IEEE.
- 1098 Abdualgalil, B. and Abraham, S., 2020, February. Applications of Machine Learning  
1099 Algorithms and Performance Comparison: A Review. In 2020 International Conference  
1100 on Emerging Trends in Information Technology and Engineering (ic-ETITE) (pp. 1-6).  
1101 IEEE.
- 1102 Garcia-Garcia, A., Orts-Escolano, S., Oprea, S., Villena-Martinez, V. and Garcia-  
1103 Rodriguez, J., 2017. A review on deep learning techniques applied to semantic segmen-  
1104 tation. arXiv preprint arXiv:1704.06857.
- 1105 Bergstra, J. and Bengio, Y., 2012. Random search for hyper-parameter optimization.  
1106 The Journal of Machine Learning Research, 13(1), pp.281-305.
- 1107 Geetha, V., Aprameya, K.S. and Hinduja, D.M., 2020. Dental caries diagnosis in  
1108 digital radiographs using back-propagation neural network. Health information science  
1109 and systems, 8(1), pp.1-14.
- 1110 Jusman, Y., Tamarena, R.I., Puspita, S., Saleh, E. and Kanafiah, S.N.A.M., 2020, Au-  
1111 gust. Analysis of Features Extraction Performance to Differentiate of Dental Caries Types  
1112 Using Gray Level Co-occurrence Matrix Algorithm. In 2020 10th IEEE International  
1113 Conference on Control System, Computing and Engineering (ICCSCE) (pp. 148-152).  
1114 IEEE.
- 1115 Lee, S., Oh, S.I., Jo, J., Kang, S., Shin, Y. and Park, J.W., 2021. Deep Learning for  
1116 Early Dental Caries Detection in Bitewing Radiographs.
- 1117 Singh, P. and Sehgal, P., 2021. GV Black dental caries classification and preparation  
1118 technique using optimal CNN-LSTM classifier. Multimedia Tools and Applications,  
1119 80(4), pp.5255-5272.

Table 2: Works grouped by feature extraction method.

Feature Extraction Method	Related works
FOF	(Obuchowicz et al. 2020)
Run-length matrix	(Galloway et al. 1975), (Eqbal et al. 2020), (Raj et al. 2019), (Deshmukh et al. 2018)
LBP	(Ojala et al. 1996), (Verma et al. 2015), (Liu et al. 2016)
Clustering	(Min et al. 2018), (Li et al. 2018), (Edwards et al. 2018), (Zhao et al. 2019)
Laws texture energy measures	(Laws, K., 1980), (Orooji et al. 2018), (Ramaprabha et al. 2017)
GLCM	(Haralick et al. 1973), (PS et al. 2016), (Korchiyne et al. 2014)
GTDM	(Amadasun et al. 1989), (Fekri et al. 2018)
Gabor Filters	(Gabor, D., 1946), (Avinash et al. 2016), (Aguirre et al. 2018), (Hegde et al. 2018)
LTP	(Tan et al. 2010), (Murala et al. 2013), (Rabidas et al. 2016), (Deep et al. 2018)
Multiple morphology Gradient(mMG)	(Naam et al. 2016), (Naam et al. 2016), (Liang et al. 2017), (Naqi et al. 2018), (Rakhlin et al. 2018)

### 2.2.1 Summary

In this paper, we present a survey of deep learning methods used or related to segmentation and detection of dental caries. We also discussed various dataset benchmarks available to these methods. Further, we have summarized the performance of evaluation protocols used in deep learning dental segmentation and detection. Therefore, the choice of segmentation method to use depends on similarities and discontinuities of regions of interest on an image. Additionally, the choice of detection method to use depends on texture, pixels and color intensity characteristics on an image.

## Chapter 3

# Teeth Segmentation

### 3.1 Dental Images' Segmentation Using Threshold Connected Component Analysis.

### 3.2 Introduction

This paper discusses how dental images were segmented through a combination of thresholding and connected component analysis. Segmentation of dental radiographs into individual teeth is the most important part in any method that is to be used for analysis. Correct separation of individual teeth in turn yield accurate results. From the previous discussion on existing segmentation methods, it is difficult to choose one that suit one specific task. Therefore, important factors to consider when deciding a segmentation method include: noise levels on image and X-ray artefacts. Thresholding is the method of choice to implement segmentation on dental radiographs, due to the low noise levels of the dataset being analyzed as well as the various artefacts present. In this chapter, the adopted segmentation method is presented, as well as the pre-



processing steps involved to maximize efficiency.

## Research Article

# Dental Images' Segmentation Using Threshold Connected Component Analysis

Vincent Majanga  and Serestina Viriri 

*School of Mathematics, Statistics and Computer Science, University of KwaZulu-Natal, Durban 4000, South Africa*

Correspondence should be addressed to Serestina Viriri; [viriris@ukzn.ac.za](mailto:viriris@ukzn.ac.za)

Received 30 August 2021; Revised 3 November 2021; Accepted 24 November 2021; Published 14 December 2021

Academic Editor: Simone Ranaldi

Copyright © 2021 Vincent Majanga and Serestina Viriri. This is an open access article distributed under the Creative Commons Attribution License, which permits unrestricted use, distribution, and reproduction in any medium, provided the original work is properly cited.

Recent advances in medical imaging analysis, especially the use of deep learning, are helping to identify, detect, classify, and quantify patterns in radiographs. At the center of these advances is the ability to explore hierarchical feature representations learned from data. Deep learning is invaluable becoming the most sought out technique, leading to enhanced performance in analysis of medical applications and systems. Deep learning techniques have achieved great performance results in dental image segmentation. Segmentation of dental radiographs is a crucial step that helps the dentist to diagnose dental caries. The performance of these deep networks is however restrained by various challenging features of dental carious lesions. Segmentation of dental images becomes difficult due to a vast variety in topologies, intricacies of medical structures, and poor image qualities caused by conditions such as low contrast, noise, irregular, and fuzzy edges borders, which result in unsuccessful segmentation. The dental segmentation method used is based on thresholding and connected component analysis. Images are preprocessed using the Gaussian blur filter to remove noise and corrupted pixels. Images are then enhanced using erosion and dilation morphology operations. Finally, segmentation is done through thresholding, and connected components are identified to extract the Region of Interest (ROI) of the teeth. The method was evaluated on an augmented dataset of 11,114 dental images. It was trained with 10 090 training set images and tested on 1024 testing set images. The proposed method gave results of 93% for both precision and recall values, respectively.

## 1. Introduction

Dental caries is the most widespread chronic disease affecting teeth worldwide. Recently, there has been a decline in the rates of large cavity lesions, but still early lesions can be identified in most people [1]. Most of conventional caries detection methods rely on inspecting teeth visually. These methods are effective for large, clearly visible carious lesions as well as those partially visible but can be viewed by a handheld mirror [2]. The introduction of dental radiography is to detect hidden or inaccessible lesions that could not be otherwise done through conventional methods. Early detection of dental caries lesions is an important determinant of treatment measures and is therefore a beneficiary of the introduction of new tools [3]. The fastest growing sectors in

the health care industry are dental services which consist of prevention, treatment, and diagnosis of oral cavity diseases [4]. Most dentists use bitewing radiographs to aid in the location of dental caries. They rely on information from these radiographs together with their patients' medical history. Locating of dental caries is a challenging task and sometimes even the experienced dentists miss the carious lesions when they are just presented with bitewing radiographs [5]. Traditionally, detection of dental caries relied on visual-tactile methods [6]. Sensitivity of visual-tactile methods is limited and especially done on posterior proximal teeth surfaces. Radiographic methods tend to have high sensitivity but require ionizing radiation [7].

Surveys have been carried out on various segmentation and feature extraction methods [8] that are used in

preprocessing. A novel possibilistic exponential fuzzy C-means clustering algorithm proposed in [9] is used for segmenting medical images.

Analysis of dental radiographs requires some processing of the images so as to obtain useful information. The most invaluable image processing procedure or step is referred to as image segmentation. The representation of dental images is done through the segmentation of various regions of interest from the larger image so as to locate objects. Segmentation of images is therefore partitioning of an image into several segments to be used to identify objects and their edges. Image segmentation can be categorized according to similarity and discontinuity properties. Discontinuity-based methods are referred to as boundary-based methods, while similarity-based methods are referred to as region-based methods [10].

Image segmentation is the process of dividing an image into groups of similar characteristics and features. Mathematically, segmentation of an image  $R$  is a finite set of regions  $R_1 \dots R_s$ ,  $R = \cup_i R_i$  and  $R_i \cap R_j = \emptyset$ . Research work in [11, 12] categorizes segmentation methods according to various characteristics, namely, region, entropy, shape, threshold, and pixels' correlation, among others. These characteristics were from thermal, X-ray images to aid analysis of specific points or regions of interest. Dental image segmentation is also classified as region-based, cluster-based, threshold-based, boundary-based, and watershed-based methods.

Recent advances in medical imaging analysis, especially the use of deep learning, have implemented connected component analysis to help identify, detect, classify, and quantify patterns in radiographs. At the center of these advances is the ability to explore hierarchical feature representations learned from data. Connected component analysis is pivotal to many image processing pipelines [13]. It is handled by dividing an image into foreground and background pixel objects. Then, for further processing, foreground pixels are connected to each other and extracted, while background pixels are connected together to form edges boundaries on images. Connected component analysis is used after the image has been preprocessed, and thresholding has taken place.

This paper has identified several major limitations that hinder better performances of segmentation techniques with regard to dental images. First limitation is the limited amount of dental images available for training deep learning systems. Another issue is that most dental images used are characterized with low contrast, false or fuzzy edge borders, and noise. In addition, dental images are mostly multisized, multiresolution, and multiscaled in nature. Lastly, most existing segmentation techniques require expensive computational power resources which then limit their practicability.

This proposed method is built to sort the issues or limitations aforementioned. Due to the limitation in dental images, the available 120 images have been augmented to give 11,114 images in the dataset. The augmented dataset images are then preprocessed via the Gaussian blur to remove noise. Thereafter, the erosion and dilation

morphology operations are used to accentuate image pixels on the image. Lastly, segmentation is done by thresholding the pixel components connected and identified to extract the ROI of teeth. The method was trained on 10 090 training set images and tested on 1024 testing set images. An experimental analysis was done and the performance compared to state-of-the-art methods. The proposed method outperformed all of the methods in accuracy evaluation metrics. Figure 1 shows a flow diagram of the proposed method.

## 2. Related Works

Most of the deep learning networks methods have achieved great success in segmentation of medical images. Segmentation of medical images is one of the crucial tasks in computer vision. Various researchers have proposed and developed various techniques based on deep learning networks for dental images. Some of them have been reviewed in this paper, namely, thresholding, deep convolution neural networks, and connected component analysis.

A method of identifying dead unrecognizable people is proposed in [14] using panoramic dental images. A survey of diagnosis of dental image diseases using soft computing techniques is proposed in [15]. A deep recent literature is provided in [16] covering efforts on semantic and instance segmentation. A survey of the use of the U-Net architecture is provided in [17] which is widely used in biomedical image segmentation to address the automation of identification and detection of target regions.

Soft computing techniques proposed in [18] are used to improve performance of watermarking algorithms and applications of the same. Soft computing techniques also have been adopted for segmenting images and synergistically provide malleable information competent enough to manipulate real-life circumstances. Methodologies provided in [19] are used to feat lenience for roughness, ambiguity, imprecise acumen, and partial veracity for the sake of attaining compliance and economical results.

There is also the use of the Otsu thresholding and connected component analysis proposed in [20] for the segmentation of periapical dental images to aid automated forensic identification. Connected component analysis is used to extract the region of interest (ROI) of the segmented teeth. Estimation of tooth axis in some of the existing methods requires segmenting the tooth volume from computed tomograph (CT) images; then, estimation is done from that segmented tooth volume. Poor segmentation leads to poor axis estimation [21]; thus, the estimation of molar teeth axis from two projection images is proposed rather than the segmented volume.

Connected component analysis can also be done on a set of gray levels of an image. A maximally stable extremal region (MSER) algorithm is proposed to handle this analysis. Maximal intensity regions appear to grow and merge at different intensity thresholds, while stability is achieved via finding extremal regions which are virtually unchanged over a range of threshold selection, and thus, regional intensity variation aids cyst boundary extraction in dental radiographs [22]. CNNs have been used to study consistent

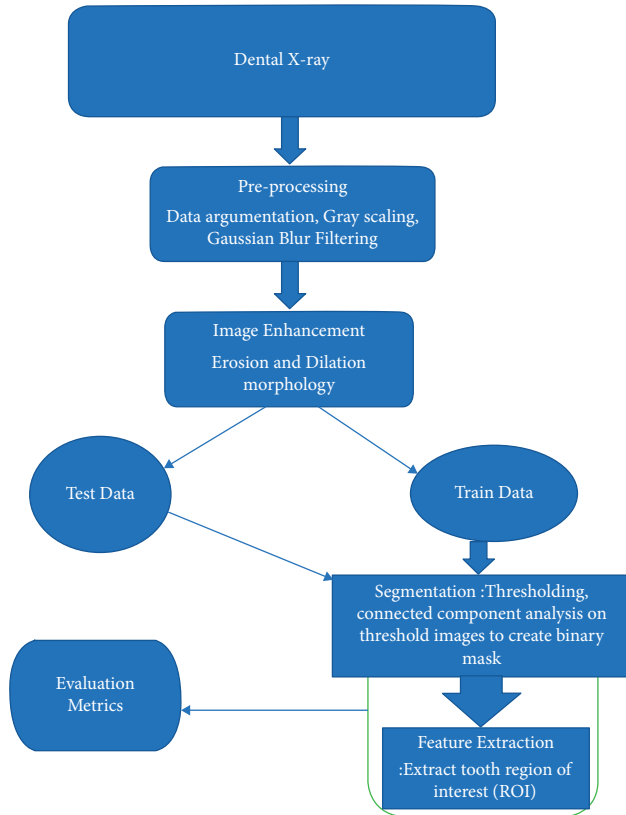


FIGURE 1: Flow diagram of the proposed segmentation method.

intensity patterns of organs at risks (OAR) from training CT images and even segment them in test CT images.

Training CNNs on CT images helps extract positive intensity patches that belong to OAR of interest and negative intensity patches that belong to surrounding structures. The patches were passed through CNN layers and image features; namely, edges, corners, and end points were captured and combined into more complex high-order features that describe the OAR efficiently. The trained network was applied to classify voxels in a ROI in the test images to obtain a corresponding OAR as a segmented image result [23].

Segmentation is a challenging task in the analysis of dental images. One of the most invaluable and yet largely unsolved issues of the level set method (LSM) is its initial contour generation. A new level set segmentation method in [24] proposes initial contour generation via morphological image information and intelligent level set segmentation through motion filtering and backpropagation of the neural network.

Early detection of dental cavity is invaluable and thus lifesaving. Ahmed et al. [25] present a caries detection method that applies *K*-means clustering and threshold method for segmentation of CT images. This is in order to construct a 3D view of the carious lesion which is an integral part of the diagnosis of dental caries. CT images have been extensively used in dental imaging diagnostics, and therefore, it is possible to use 3D data from the CT images to reconstruct 2D panoramic dental radiographs that provide a longitudinal view of the jaw bone, avoiding additional

exposure to X-rays. An automatic method, introduced in [26], is used for reconstructing 2D panoramic dental images based on 3D CT images, using Bezier curves and optimization techniques, and obtained very smooth panoramic images with good contrast.

Teeth segmentation is a critical task for effective caries detection as most carious lesions usually occur around tooth boundaries, and dental images are often subject to low contrast, noise, and uneven illumination. An effective way is introduced in [27] to segment individual teeth in periapical radiographs. The method performs image enhancement via adaptive power law transformation, local singularity using Holder exponent, tooth recognition via Otsu thresholding, connected component analysis, and, lastly, tooth delineation via snake boundary tracking and morphological operations.

The accuracy of the segmentation process determines the success or failure of the final analysis process. In order to diagnose problems with wisdom teeth, Amer and Aqel [28] propose an automatic method that prepares panoramic images for segmentation, and then, a segmentation algorithm is implemented followed by a postprocessing stage, as shown by Figure 2. The preprocessing step includes contrast enhancement, Otsu thresholding, morphology operations, and connected component labeling. A segmentation algorithm was used to extract the ROI, while histogram equalization was used in the postprocessing of panoramic images.

Teeth segmentation is important in highly automated postmortem identification. Automating the process of postmortem identification using dental images has received increased attention from researchers. A mathematical morphology is offered in [29] to bitewing teeth segmentation so as to aid postmortem identification of individuals. They also propose grayscale contrast transformation and removing noise via filters for image enhancement. Next, thresholding is used to isolate teeth from the background and then group the thresholded image using connected component labeling of both background and foreground pixels to get the ROI. Finally, the connected components were refined and analyzed based on their geometric properties, and then, unqualified objects were eliminated.

An automatic approach in [30] is introduced to detect dental arches on panoramic images. They use local entropy thresholding to binarize CT images because teeth have high intensities than their surrounding areas on images. They then use connected component labeling to partially remove metal artifacts and morphological dilation to close gaps between teeth so that the mandible region is one connected piece. Finally, the thinning result gives a rough dental arch shape, and this result is exploited by a curve fitting method to get a mathematically represented dental arch.

The proposed technique uses the connected component analysis to aid teeth segmentation on dental images. Connected analysis or labeling is the process of grouping object elements of a digital image by assigning the same label to adjacent elements. This facilitates further image analysis tasks: regions can be counted and can be individually manipulated and their properties can be measured. Object labeling is important not only when dealing with large-sized

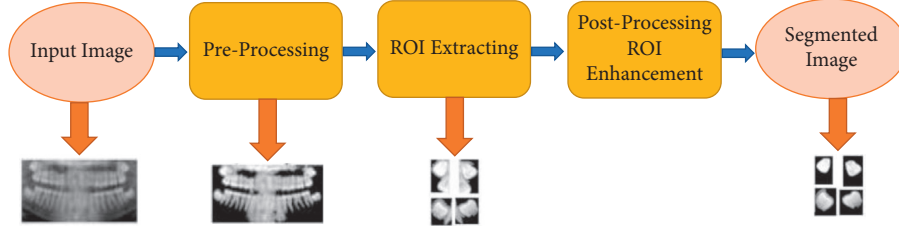


FIGURE 2: Stages of the segmentation method with expected results from each stage [28].

images to single out and count individual regions but also when counting the number of objects in small neighborhoods. This is quite invaluable especially when designing topology preserving removal operations for thinning transformations. In 2D images, the 4-way and 8-way connected components in the special case of a  $3 \times 3$  neighborhood can be counted. The proposed technique used the 8-way connected component analysis for segmentation of dental images and is discussed in Section 3.

### 3. The Proposed Method

The proposed method proposes preprocessing and segmentation of the dental images, as shown by Figure 1, and handled by the following steps.

**3.1. Dataset Preparation: Augmentation.** With the insufficient number of dental images for research, it is impossible to derive intelligent decisions by neural networks. Deep learning networks need huge amounts of data for training and testing purposes to achieve good evaluation performance. Image augmentation is highly prescribed and involves artificially creating training images through different ways of processing or a combination of multiple processing ways on the images present. One hundred and twenty images were subjected to data augmentation techniques, namely, image shifts via the width shift range and height shift range and rotation arguments to give 11,114 images after augmentation. The data augmentation process, as discussed in [31], can be described through the following steps:

(1) *Flips.* Horizontal and vertical flips for each image in the training set. Horizontal flips are commonly used in natural images, and vertical flips are used to capture invariance to vertical reflection in medical images.

(2) *Scaling.* We scale each one in either the  $x$  or  $y$  direction; specifically, we apply an affine transformation,  $A = (sx \ 0 \ 0 \ sy)$ .

(3) *Rotations.* The following affine transformation is obtained:

$$A = (\cos \theta \ \sin \theta \ -\sin \theta \ \cos \theta), \quad (1)$$

where  $\theta$  is between  $10$  and  $175^\circ$  and is applied.

**3.2. Image Enhancement.** Dataset preparation is first done through data augmentation; then, image enhancement is handled by improving contrast, brightness adjustment, and scaling so as to compensate the nonuniformity caused by image illumination. This is done through filtering and morphology operations. Filtering is done through the use of Gaussian blur filters to remove noise and is shown by Figure 3.

After image filtering, morphology operations that include erosion and dilation were used to diminish foreground features while accentuating background features, as shown in Figure 4.

**3.3. Thresholding.** Morphology operations in the image enhancement process was to separate teeth from the background. It is followed by image thresholding; this is used to obtain the general outline of individual teeth in the X-ray and is shown by Figure 5.

**3.4. Connected Component Analysis.** The 8-way clustering method was introduced to combine components of the same properties and neighborhood. This was after image pre-processing, image enhancement, morphology operations, and thresholding. With this method, image pixels were grouped into connected darker and brighter binary mask regions. Darker regions were combined and connected together to form the background, while brighter pixels were combined to form the foreground binary mask. This component connected analysis was used to extract the ROI shown by Figure 6.

The detection of these darker or brighter regions was influenced by the (LoG) Laplacian of Gaussian approach, which is a convolution kernel of the form

$$LoG = \frac{x^2 + y^2 - 2\sigma^2}{\sigma^4} e^{-x^2 - y^2 / 2\sigma^2}, \quad (2)$$

where  $\sigma$  is the width of the kernel. The masking procedure increases segmentation accuracy. Figure 7 shows segmentation results after the use of connected component analysis to extract the ROI on dental images.

## 4. Experiments and Results

The method was evaluated on an augmented dataset of 11,114 dental images. The dataset was split into two, the train set of 10 090 images and the test set of 1024 images. The method was trained on 10 090 train images and tested on

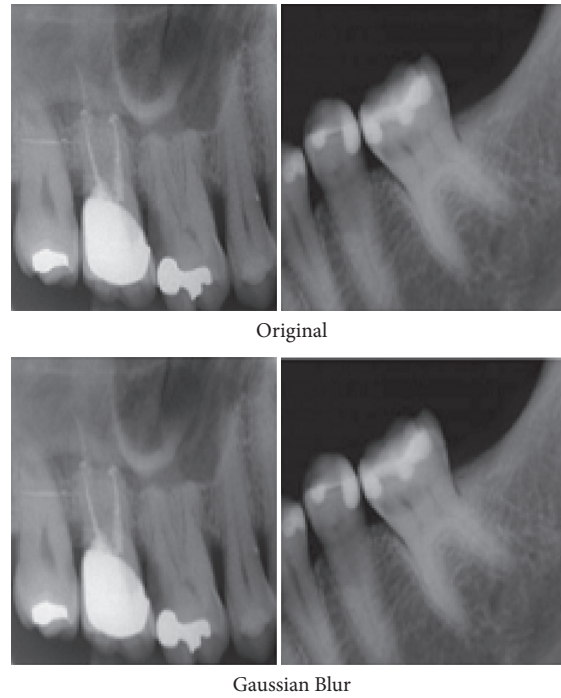


FIGURE 3: Original images and images after filtering by Gaussian blur filters.

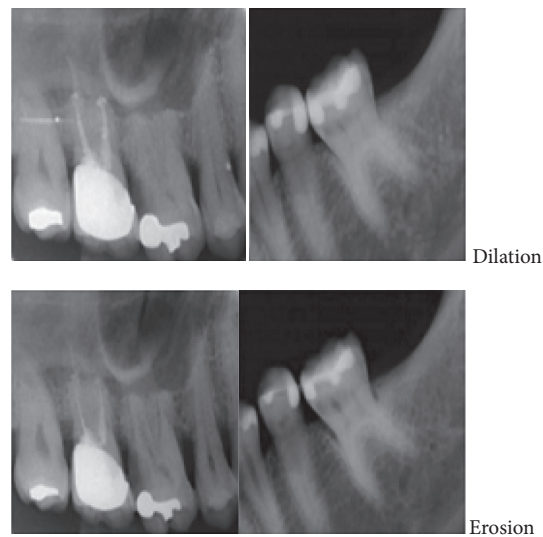


FIGURE 4: Images after erosion and dilation morphology operations.

1024 test images. The success rate of the segmentation methods covered in this paper is from separating individual teeth from different jaw regions on an image. The success rate is measured on to how it clearly shows tooth edge boundaries and individual teeth on images throughout the whole dataset.

Teeth separation is correctly considered if the separation did not cause division of the teeth. Teeth, which were already partial as a result of being at the edge of the radiograph, are considered correctly separated if no further partiality was caused. Teeth that were not correctly segmented were either as a result of poor image contrast, where enhancement

techniques could not salvage a distinction between teeth and nontooth structures. It should be noted that the proposed segmentation method after optimization exhibited better results than compared existing implementations. Table 1 provides a comparison of the proposed method to other implementations of connected component analysis. Results obtained from the proposed segmentation method indicate a noticeable improvement on existing models. Figure 7 shows some image examples of the segmentation results.

Figure 8 shows training and validation accuracy graphs of the proposed threshold connected analysis segmentation method on our augmented dataset.

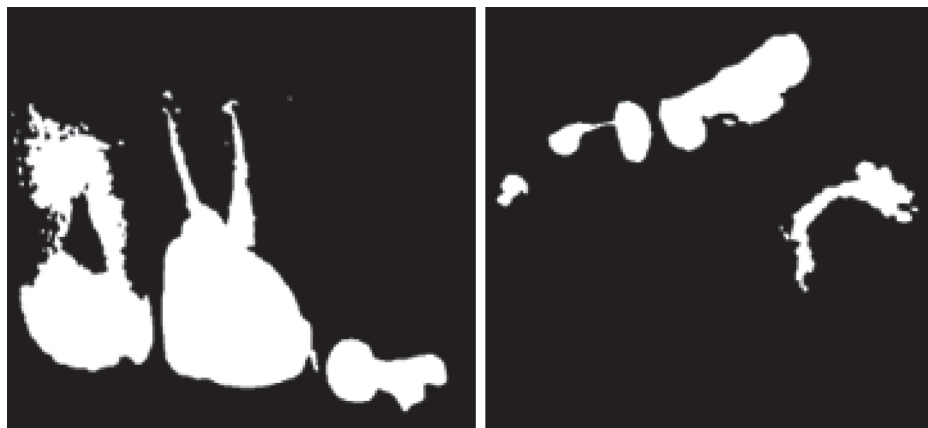


FIGURE 5: Images after thresholding.



FIGURE 6: Masked image from the 8-way component connected clustering method.

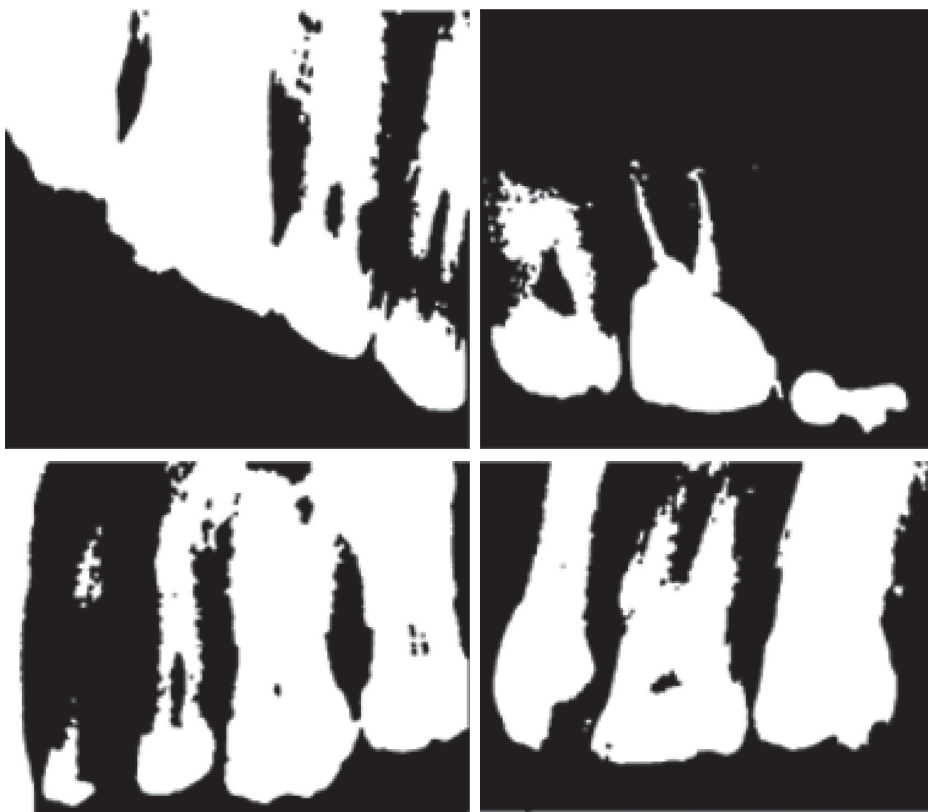


FIGURE 7: Segmentation results of the proposed method.



TABLE 1: Overall comparison of segmentation methods.

Methods	Types of images	Accuracy (%)
Fuzzy C-means clustering algorithm [9]	Breast tumours' images	97.4
Local singularity analysis [27]	Periapical images	89.59
Bezier function optimization [26]	Panoramic images	91.0
Intelligent level set [24]	Periapical images	90.0
Neck segmentation using CNNs [23]	CT images	89.5
<b>Proposed segmentation method</b>	<b>Bitewing images</b>	<b>93.0</b>

The statement in bold highlights the contribution made in this paper. It is meant to distinguish the current work from related works in the literature.

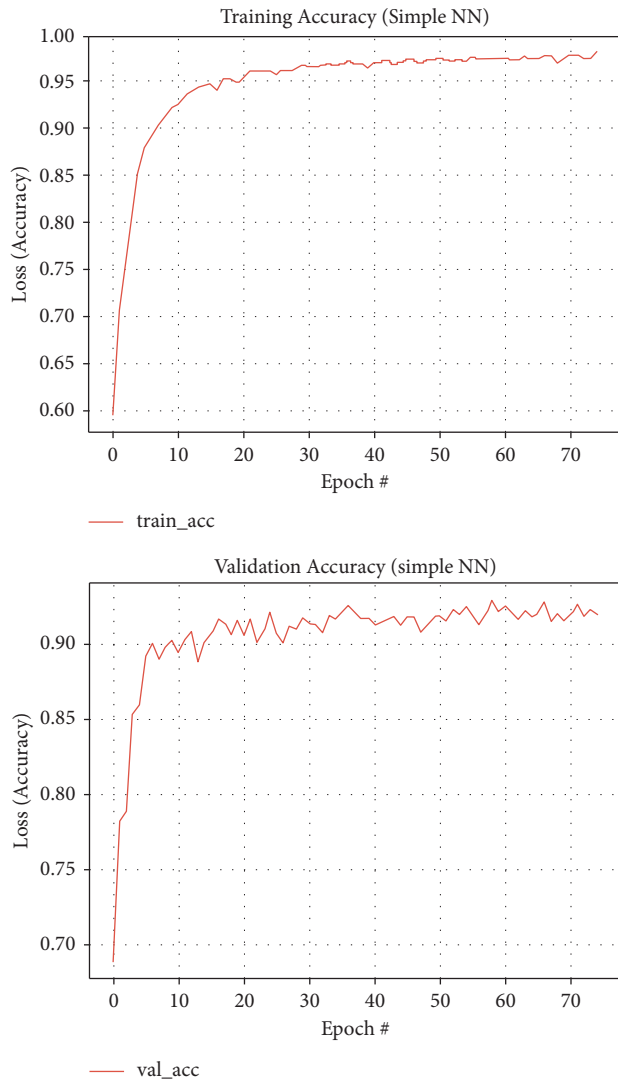


FIGURE 8: Training and validation accuracy graph curves for threshold connected component analysis segmentation method, respectively.

## 5. Conclusion and Future Work

Deep learning methods have been used for medical imaging and are now invaluable to the segmentation and detection of dental caries on dental imaging. In segmentation, regions of interest are segmented from the larger image to locate objects of similar characteristics and features. Segmentation

is also the partitioning of an image into several segments from the larger image so as to locate objects and their edges. Dental image segmentation can be categorized based on similarity, namely, region-based methods, and discontinuities, namely, boundary-based methods. Several works by different authors have been reviewed to expound more on the various segmentation methods and their use.

Soft computing approaches such as fuzzy logic, artificial neural network, and genetic algorithm have been emphasized and used for image segmentation. Contribution in [32] presents state-of-the-art elaboration of almost all dimensions associated with image segmentation. They encapsulate various aspects such as emerging topics, methods, evaluation parameters, problems associated with different types of images, databases, segmentation applications, and other resources that can be advantageous to researchers in developing new methods for segmentation.

The proposed paper here has discussed the proposed threshold connected component (TCC) segmentation method used. This segmentation method used preprocessing methods that include augmentation, and image enhancement methods and thresholding were discussed and implemented to make sure accurate segmentation is achieved. Thresholding was used to obtain the general outline of teeth, and then, connected component analysis by the 8-way clustering method was used. This clustering method was used to group pixels as either dark or bright pixel masks to allow separation of teeth from the background of the whole image.

Dental image datasets are hard to find publicly; thus, there is a need for data augmentation. Evaluating performance of these deep learning methods takes longer periods due to large volumes of data and thus longer training and testing time. Several evaluation protocols for performance evaluation have been introduced to reduce the time taken for training and testing networks. Therefore, it is important to use established protocols to evaluate performance of models, networks, and methods ability to meet expectations or goals through various measurements.

There are major observations from earlier research work in the segmentation and detection of dental caries which help in making justifiable conclusions. Some of those observations that we deem very important include

- (i) It was observed that existing work mostly employed a preprocessing step on the dental images to prepare the images for the next steps that follow
- (ii) It was also observed that the image processing method used for segmentation of dental caries had a



ripple effect on the performance of the deep learning system used

- (iii) It was also observed that the performance of deep learning methods was dependent on the size of the dataset and image variability
- (iv) Data augmentation plays a big role in boosting the performance of deep learning methods especially those on not-too large datasets
- (v) It was also observed that dental images' segmentation work use panoramic radiographs and Otsu thresholding for most connected component analysis

Therefore, it can be concluded that the proposed method provides a new approach to solve teeth segmentation problems. The method offers a robust way for providing sufficient data for deep learning in datasets through data augmentation. It also aids both individual teeth separation and edge boundary detection which makes it easier for both supervised and unsupervised learning models to correctly process teeth in the dataset. The success rate of the proposed method on the given supervised model provides a potential avenue for future work using unsupervised models thus leading to even better results.

Image analysis has been used by the proposed caries detection model in this thesis to determine presence of dental caries in dental radiographs. The final results depend heavily on the quality of the image by the time it reaches the diagnostic method. Weight regularization methods at the segmentation stage could improve the final result, and future work will look at how to implement such optimizations. The dataset that was used was relatively noise free; thus, minimal preprocessing needed to be implemented for noise removal. The dataset had few images for processing, and there was need to add more images through various processing methods, which will aid deep learning by the model. There are a series of encouraging future perspectives of study that may see improvement in dental segmentation and detection of dental caries. Among them are

- (i) Data availability and reliability: deep learning networks require large amount of data to be able to achieve meaningful and effective performance results. Due to the nature of dental images, there is need for hybrid datasets to aid good performance of the networks. There is need of public available datasets for dental images to make deep learning possible.
- (ii) Data standardization: many methods discussed in this research are handling image preprocessing via manual methods such as cropping regions of interest on an image. These methods contribute to loss of some key details from the images. Some networks end up dividing a whole image into subregions and this ends up slowing down the learning process that occurs one subregion after the other. Other methods such as downsampling lead to deletion of important image details, and this is due to limitations in

computational power. Deep learning approaches have seen an increase in learning of whole images rather than the manual manipulation of images via preprocessing, so as to get more general and accurate results.

- (iii) Weight regularization methods: deep learning methods and networks can also be improved by the introduction of weight regularization to improve their performance. The regularization of weights involves optimization of model hyperparameters such as the learning rate and the dropout rate. Basically, weight regularization methods are introduced into networks for parameter optimization.
- (iv) Hybrid approaches: deep learning methods can be further improved by combining several models or techniques to form hybrid ones that will eventually improve the overall evaluation performance. The combination can be at any stage of the model, for instance, combining two or more preprocessing techniques to come up with a single step to enhance image quality. The combination can also be handled by joining various attributes of different models to form one hybrid model that will enhance the training, extraction, detection, and classification of objects.

In addition to these optimizations, future work will look at expanding the proposed system's ability to diagnose different images, since it was used for only bitewing radiographs from the same dataset. The scope will be expanded to test a variety of different radiographic types and also bitewing radiographs from different datasets.

## Data Availability

The data used to support the findings of the study can be obtained from the corresponding author upon request.

## Additional Points

Deep learning networks require large amount of data to be able to achieve meaningful and effective performance results. Due to the nature of dental images, there is need for hybrid datasets to aid good performance of the networks. There is need of public available datasets for dental images to make deep learning possible.

## Conflicts of Interest

The authors declare that they have no conflicts of interest.

## References

- [1] N. J. Kassebaum, E. Bernabé, M. Dahiya, B. Bhandari, C. J. L. Murray, and W. Marcenes, "Global burden of untreated caries," *Journal of Dental Research*, vol. 94, no. 5, pp. 650–658, 2015.
- [2] F. Casalegno, T. Newton, R. Daher et al., "Caries detection with near-infrared transillumination using deep learning," *Journal of Dental Research*, vol. 98, no. 11, pp. 1227–1233, 2019.

- [3] F. Schwendicke, C. E. Dörfer, P. Schlattmann, L. F. Page, W. M. Thomson, and S. Paris, "Socioeconomic inequality and caries," *Journal of Dental Research*, vol. 94, no. 1, pp. 10–18, 2015.
- [4] M. M. Srivastava, P. Kumar, L. Pradhan, and S. Varadarajan, "Detection of tooth caries in bitewing radiographs using deep learning," 2017, <http://arxiv.org/abs/1711.07312>.
- [5] S. Valizadeh, M. Goodini, S. Ehsani, H. Mohseni, F. Azimi, and H. Bakhshandeh, "Designing of a computer software for detection of approximal caries in posterior teeth," *Iranian Journal of Radiology: A Quarterly Journal Published by the Iranian Radiological Society*, vol. 12, Article ID e16242, 2015.
- [6] H. Nokhbatolfighahae, M. Alikhasi, N. Chiniforush, F. Khoei, N. Safavi, and B. Yaghoob Zadeh, "Evaluation of accuracy of DIAGNOdent in diagnosis of primary and secondary caries in comparison to conventional methods," *Journal of Lasers in Medical Sciences*, vol. 4, pp. 159–67, 2013.
- [7] U. Vural and S. Gökalp, "Diagnostic methods for dental caries used by private dental practitioners in Ankara," *Nigerian Journal of Clinical Practice*, vol. 20, no. 3, pp. 382–387, 2017.
- [8] C. L. Chowdhary and D. P. Acharjya, "Segmentation and feature extraction in medical imaging: a systematic review," *Procedia Computer Science*, vol. 167, pp. 26–36, 2020.
- [9] C. L. Chowdhary and D. P. Acharjya, "Clustering algorithm in possibilistic exponential fuzzy C-mean segmenting medical images," *Journal of Biomimetics, Biomaterials and Biomedical Engineering*, vol. 30, pp. 12–23, 2017.
- [10] R. B. Subramanyam, K. P. Prasad, and B. Anuradha, "Different image segmentation techniques for dental image extraction," *International Journal of Engineering Research in Africa*, vol. 4, pp. 173–177, 2014.
- [11] M. Sezgin and B. Sankur, "Survey over image thresholding techniques and quantitative performance evaluation," *Journal of Electronic Imaging*, vol. 13, pp. 146–166, 2004.
- [12] G. Silva, L. Oliveira, and M. Pithon, "Automatic segmenting teeth in X-ray images: trends, a novel data set, benchmarking and future perspectives," *Expert Systems with Applications*, vol. 107, pp. 15–31, 2018.
- [13] T. Wagner and H. G. Lipinski, "IJBlob: an ImageJ library for connected component analysis and shape analysis," *Journal of Open Research Software*, vol. 1, 2013.
- [14] V. Muneeswaran, P. Nagaraj, S. Godwin, M. Vasundhara, and G. Kalyan, "Codification of dental codes for the cogent recognition of an individual," in *Proceedings of the 2021 5th International Conference on Intelligent Computing and Control Systems (ICICCS)*, pp. 1387–1390, Madurai, India, May 2021.
- [15] M. P. Rani, S. Chopra, and J. Chopra, "A survey of diagnosis of dental image diseases using soft computing techniques," *International Journal for Research in Applied Science & Engineering Technology*, vol. 9, pp. 149–153, 2021.
- [16] S. Minaee, Y. Y. Boykov, F. Porikli, A. J. Plaza, N. Kehtarnavaz, and D. Terzopoulos, "Image segmentation using deep learning: a survey," *IEEE Transactions on Pattern Analysis and Machine Intelligence*, 2021.
- [17] N. S. Punni and S. Agarwal, "Modality specific U-Net variants for biomedical image segmentation: a survey," 2021, <http://arxiv.org/abs/2107.04537>.
- [18] O. P. Singh, A. Singh, G. Srivastava, and N. Kumar, "Image watermarking using soft computing techniques: a comprehensive survey," *Multimedia Tools and Applications*, vol. 80, pp. 1–32, 2020.
- [19] S. S. Chouhan, A. Kaul, and U. P. Singh, "Image segmentation using computational intelligence techniques: review," *Archives of Computational Methods in Engineering*, vol. 26, no. 3, pp. 533–596, 2019.
- [20] V. Chandran, G. S. Nizar, and P. Simon, "Segmentation of dental radiograph images," in *Proceedings of the Third International Conference on Advanced Informatics for Computing Research*, pp. 1–5, Shimla, India, June 2019.
- [21] D. Zhang, Y. Gan, Z. Xia et al., "Molar axis estimation from computed tomography images," in *Proceedings of the 2016 38th Annual International Conference of the IEEE Engineering in Medicine and Biology Society (EMBC)*, pp. 1050–1053, Orlando, FL, USA, August 2016.
- [22] R. K. Devi, A. Banumathi, G. Sangavi, and M. S. Dawood, "A novel region based thresholding for dental cyst extraction in digital dental X-ray images," in *Proceedings of the International Conference On Computational Vision and Bio Inspired Computing*, pp. 1633–1640, Coimbatore, India, September 2018.
- [23] B. Ibragimov and L. Xing, "Segmentation of organs-at-risks in head and neck CT images using convolutional neural networks," *Medical Physics*, vol. 44, no. 2, pp. 547–557, 2017.
- [24] A. E. Rad, M. S. M. Rahim, H. Kolivand, and A. Norouzi, "Automatic computer-aided caries detection from dental x-ray images using intelligent level set," *Multimedia Tools and Applications*, vol. 77, no. 21, pp. 28843–28862, 2018.
- [25] S. Ahmed, K. M. Saifuddin, A. S. Ahmed, A. A. Hossain, and M. T. Iqbal, "Identification and volume estimation of dental caries using CT image," in *Proceedings of the 2017 IEEE International Conference on Telecommunications and Photonics (ICTP)*, pp. 48–51, Dhaka, Bangladesh, December 2017.
- [26] P. H. J. Amorim, T. F. Moraes, J. V. L. Silva, H. Pedrini, and R. B. Ruben, "Reconstruction of panoramic dental images through bézier function optimization," *Frontiers in Bioengineering and Biotechnology*, vol. 8, p. 794, 2020.
- [27] P. L. Lin, P. Y. Huang, P. W. Huang, H. C. Hsu, and C. C. Chen, "Teeth segmentation of dental periapical radiographs based on local singularity analysis," *Computer Methods and Programs in Biomedicine*, vol. 113, no. 2, pp. 433–445, 2014.
- [28] Y. Y. Amer and M. J. Aql, "An efficient segmentation algorithm for panoramic dental images," *Procedia Computer Science*, vol. 65, pp. 718–725, 2015.
- [29] E. H. Said, D. E. M. Nassar, G. Fahmy, and H. H. Ammar, "Teeth segmentation in digitized dental X-ray films using mathematical morphology," *IEEE Transactions on Information Forensics and Security*, vol. 1, no. 2, pp. 178–189, 2006.
- [30] T. Chanwimaluang, S. Sotthivirat, and W. Sinthupinyo, "Automated dental arch detection using computed tomography images," in *Proceedings of the 2008 9th International Conference on Signal Processing*, pp. 737–740, Beijing, China, October 2008.
- [31] S. L. P. Aggarwal, "Data augmentation in dermatology image recognition using machine learning," *Skin Research and Technology*, vol. 25, no. 6, pp. 815–820, 2019.
- [32] S. S. Chouhan, A. Kaul, and U. P. Singh, "Soft computing approaches for image segmentation: a survey," *Multimedia Tools and Applications*, vol. 77, no. 21, pp. 28483–28537, 2018.

### 3.3 Summary

This paper has discussed the segmentation method used. Pre-processing methods that include: augmentation, image enhancement methods and thresholding were discussed and implemented to make sure accurate segmentation is achieved. Thresholding was used to obtain the general outline of teeth, and then component connected analysis by the 8-way clustering method was used. This clustering method was used to group pixels as either dark or bright pixel masks to allow separation of teeth from the background of the whole image. Additionally, edge boundaries of teeth is also a very important part in the segmentation process. Active contours methods were discussed and how they were used for tooth boundaries detection. They were used to finding, count and draw all contours or edge boundaries on the image. From the boundaries detected, unwanted contours were eliminated to remain with just external or big contours that will in turn aid in the next process of caries detection. This elimination of unwanted contours left only specific regions of interest of teeth. This method demonstrated positive results and achieved a very high success rate in segmentation of various dental images in the database.

The next paper will present a caries detection method that will be used on images processed by the active contour method discussed at the end of his chapter. This will then conclude the diagnostic model proposed in this thesis.

# Chapter 4

## Dental Caries Detection

### 4.1 Automatic blob detection for dental caries.

### 4.2 Introduction

This paper discusses how dental caries was detected through the blob detection method to distinguish which regions are carious and those that are not. The presence of dental caries and its diagnosis is possible if potential regions of interest are defined. It is then after which the diagnostic method uses these regions to evaluate whether they are of carious concern or not. This chapter introduces and discusses the edge detector used to locate potential caries, as well as the method for diagnosing the presence of caries in those regions. The feature extraction process starts by removing noise on images from the previous segmentation process. Blob detection algorithm is then used as the edge detection technique to obtain initial positions of suspected caries regions. From all the blobs detected, various blob parameters and filtering techniques are introduced to eliminate false caries blobs, to just remain with detected caries candidates only.

# Automatic Blob Detection for Dental Caries

Vincent Majanga <sup>†</sup> and Serestina Viriri <sup>\*,†</sup> 

School of Mathematics, Statistics and Computer Science, University of KwaZulu-Natal,  
Durban 4000, South Africa; 218081167@stu.ukzn.ac.za

\* Correspondence: viriris@ukzn.ac.za

† These authors contributed equally to this work.

**Abstract:** Dental Caries are one of the most prevalent chronic diseases around the globe. Detecting carious lesions is a challenging task. Conventional computer aided diagnosis and detection methods in the past have heavily relied on the visual inspection of teeth. These methods are only effective on large and clearly visible caries on affected teeth. Conventional methods have been limited in performance due to the complex visual characteristics of dental caries images, which consist of hidden or inaccessible lesions. The early detection of dental caries is an important determinant for treatment and benefits much from the introduction of new tools, such as dental radiography. In this paper, we propose a deep learning-based technique for dental caries detection namely: blob detection. The proposed technique automatically detects hidden and inaccessible dental caries lesions in bitewing radio-graphs. The approach employs data augmentation to increase the number of images in the data set to have a total of 11,114 dental images. Image pre-processing on the data set was through the use of Gaussian blur filters. Image segmentation was handled through thresholding, erosion and dilation morphology, while image boundary detection was achieved through active contours method. Furthermore, the deep learning based network through the sequential model in Keras extracts features from the images through blob detection. Finally, a convexity threshold value of 0.9 is introduced to aid in the classification of caries as either present or not present. The process of detection and classifying dental caries achieved the results of 97% and 96% for the precision and recall values, respectively.

**Keywords:** blob detection; dental caries dataset; deep learning; radiography



**Citation:** Majanga, V.; Viriri, S. Automatic Blob Detection for Dental Caries. *Appl. Sci.* **2021**, *11*, 9232. <https://doi.org/10.3390/app11199232>

Academic Editor: Bruno Chrcanovic

Received: 12 August 2021

Accepted: 28 September 2021

Published: 4 October 2021

**Publisher's Note:** MDPI stays neutral with regard to jurisdictional claims in published maps and institutional affiliations.



**Copyright:** © 2021 by the authors. Licensee MDPI, Basel, Switzerland. This article is an open access article distributed under the terms and conditions of the Creative Commons Attribution (CC BY) license (<https://creativecommons.org/licenses/by/4.0/>).

## 1. Introduction

Caries is the most widespread chronic disease in the world. While there has been a decline recently in rates of large cavity lesions, there are still early lesions that can be identified in most people [1]. Most conventional caries detection methods rely on inspecting teeth visually, and this is effective for large and clearly visible carious lesions as well as those that are partially visible but can be viewed by a handheld mirror [2]. The introduction of dental radiography is to detect hidden or inaccessible lesions that could not be seen through conventional methods. The early detection of dental caries lesions is an important determinant treatment measure and, therefore, a beneficiary of the introduction of new tools [3].

The fastest growing sector in the health care industry is dental services. This involves the prevention, treatment and diagnosis of oral cavity diseases [4]. Most dentists use bite-wing radiographs to aid in finding the location of dental caries. They rely on information from radiographs together with their patient's medical history. Locating dental caries is a challenging task, and sometimes even experienced dentists miss carious lesions when presented with bite-wing radiographs [5]. Traditionally, the detection of dental caries has relied on visual-tactile methods [6]. The sensitivity of visual-tactile methods is limited especially when performed on posterior proximal tooth surfaces. Radiographic methods tend to have high sensitivity but require ionizing radiation [7].

Most of the people who are at risk of dental caries are low-income minorities, socially and economically less privileged, and uneducated people. Furthermore, clinical studies have shown that dental caries are caused or related to dietary changes and risk factors for cardiovascular disease [8]. Some retention and restoration methods have been introduced, proposed and improved to treat dental caries in the past. However, the diagnosis of dental caries has been difficult due to the various anatomical morphologies and different shapes of teeth restorations.

In some teeth, it is difficult to detect caries at an early stage. Many of the carious lesions are detected at an advanced stage. Dental radiography is regarded as the most reliable diagnostic tool for detecting dental caries; however, most of its screening relies on empirical evidence results. The introduction of convolution neural networks in medical imaging analysis has shown excellent performance results. Medical imaging analysis has led to medical segmentation and diagnosis as one of the most important fields for pattern recognition and image processing.

Some deep learning CNN models are used for detection and classification of skin cancer, knee cartilage, diabetic retinopathy, pulmonary tuberculosis and brain tumours among others. These models have shown very high performance accuracy, efficiency and promising clinical applications in various fields. However, there have been very few studies that investigate detection and diagnosis in dentistry based on deep CNN model architectures.

Furthermore, the research on detecting and diagnosis of dental caries is even more limited [9]. Accordingly, our approach presents a technique that evaluates the efficacy of deep learning methods for the detection of dental caries in bite-wing radiographs. We introduce the use of blob detection on bite-wing radiographs to detect dental caries. Blob detection is a mathematical method that detects specific regions in digital or radiographic images. Blobs are regions with notable differences with those in their neighbourhoods.

Blobs are also referred to as regions that are either brighter or darker than their neighbourhood. Blob detectors can be classified as differential methods that are derivative functions based on their position. They can also be classified as the local maxima and minima of the differential method's derivative function. Blobs provide more information about various regions of interest for use for further image processing. With increased interest in medical imaging processing [10] presented a survey of several blob detection methods. We used blob detection to automate dental caries detection, and this will further increase the efficiency and reliability in medical care standards. Details of our approach will be discussed in depth in one section of this research.

Haghanifar et al. [11] presented an automatic diagnosis system for detecting dental cavities in panoramic images. This is done via transfer learning of pre-trained deep learning models to extract relevant features from x-rays and also use a capsule network to draw prediction results. Duong et al. [12] proposed a computational algorithm that automates the recognition of carious lesions on occlusal tooth surfaces in smartphone images through the international caries detection and assessment system (ICDAS).

Jusman et al. [13] presented a study that analyses feature extraction performance of dental caries images using the Gray Level Co-occurrence Matrix (GLCM) algorithm. This method is used to determine pixel and quantization values of the GLCM that is used for an automated classification system for dental caries types. Prados-Privado et al. [14] proposed data extraction on dental images using two reviewers. Most of the included studies employed periapical and bitewing radiography. Image databases ranged from 87–3000 images, with a mean of 669 images. Each study included used a different neural network and different outcome metrics.

Paqué et al. [15] investigated the potential of salivary bacterial and protein markers for evaluating the disease status in healthy individuals with caries. Saliva samples from caries and gingivitis-free individuals ( $n = 18$ ), patients with deep caries lesions ( $n = 38$ ) was collected and analysed for 44 candidate biomarkers namely: selected oral bacteria, growth factors, chemokines and proteolytic enzymes among others. Research by Lee et al. [16]

presented a CNN model using a U-shaped deep CNN (U-Net) for dental caries detection on bitewing radiographs and how the model can improve clinician performance.

## 2. Methods and Techniques

The proposed approach is broken down as shown in Figure 1 and Algorithm 1, and discussed in the subsections that follow.

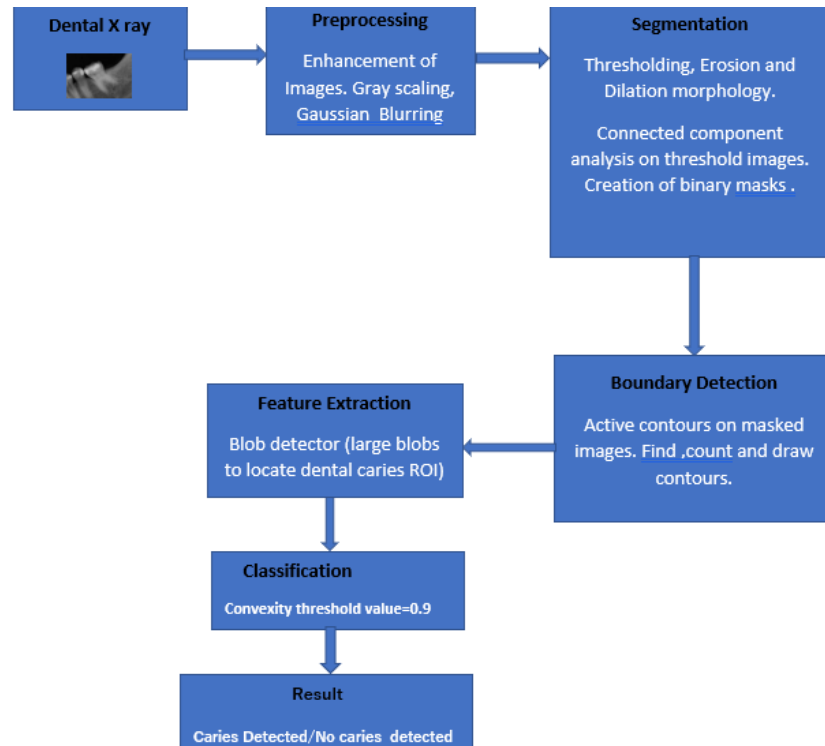


**Figure 1.** System flow diagram.

### 2.1. Pre-Processing of Dental Images

The input images used by this system were 120 dental radiographs, which were then augmented to produce 11,114 images sufficient for the deep learning process. The augmentation process involved the rotation, scaling and resizing of the images. Additionally, these images were pre-processed, which included contrast and brightness adjustment and scaling to compensate for the non-uniformity from image illumination. These sub processes were performed via pre-processing techniques that included gray image scaling and blurring as seen in Figure 2.

### 2.2. Segmentation of Images

Segmentation involves image thresholding to convert blurred source images to several binary images and masks. Thereafter, erosion and dilation morphology was used to diminish foreground features while accentuating background features, respectively, as shown in Figure 2. Additionally, the eight-way kernel was used to combine darker or brighter pixel regions on the image into a final caries lesion mask. The detection of these darker or brighter regions was influenced by the (LoG) Laplacian of Gaussian approach, which is a convolution kernel of the form:

$$LoG = \frac{x^2 + y^2 - 2\sigma^2}{\sigma^4} e^{-\frac{x^2+y^2}{2\sigma^2}} \quad (1)$$

where  $\sigma$  is the width of the kernel. The masking procedure increases segmentation accuracy. Further, image edge segmentation is handled via active contours method to detect tooth

edge boundaries. This aids easier isolation of the caries lesion region from the surrounding normal skin. From the segmented caries lesion, there still exists other blobs that are not carious. To overcome this issue, we found only the biggest blobs in the segmented image, and these are dental caries, as in Figure 3.



**Figure 2.** First Row: Original Gaussian blurred image. Second Row: Images after Erosion morphology. Third Row: Images after Dilation morphology. Fourth Row: Masked threshold image after connected component analysis via the eight-way kernel clustering method.



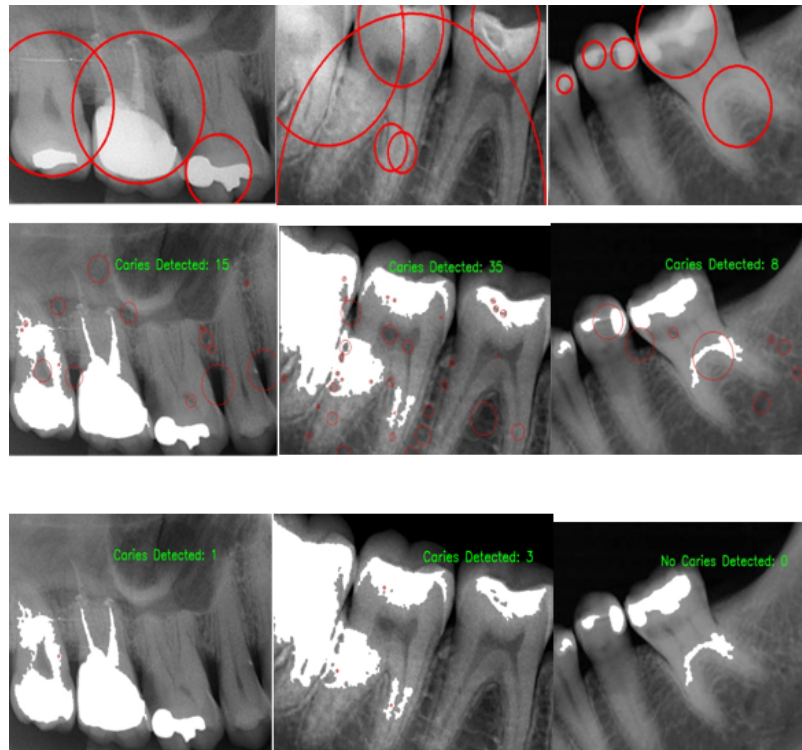


**Figure 3.** First Row: Teeth boundary detection via active contours method. Second Row: All blobs detected on masked images. Third Row: Caries detected blobs on masked images.

### 2.3. Feature Extraction

#### 2.3.1. Noise Reduction

Before the process of feature extraction starts, it is important to remove noise and retain edge information on images. This post-processing step is achieved by the use of edge-preventing smoothing Gaussian filters [17], that has a Gaussian distribution with mean  $\mu$  and standard deviation  $\sigma$ . The Gaussian filter values are calculated by averaging centre's of neighbourhood pixels with a certain range  $[\mu - 2\sigma, \mu + 2\sigma]$ . The  $M$  number of the centre's neighbour pixels within the given range is then calculated.

The centre pixel's intensity value is replaced by the calculated filter values when the number  $M$  of the centre's neighbour pixels within the range is greater than a specific threshold  $K$ , or the average value of the neighbour pixel when the above condition is not met. Some edge information is removed if a high value of threshold  $K$  value is used. In our experiments,  $K$  the value was set at 3 with a  $3 \times 3$  kernel to remove unwanted noise in our masked images before extracting the needed features.

#### 2.3.2. Caries Candidate Detection

Geometric features are the most important extraction features to look for when detecting caries on dental radiographs. Geometric features on images are enhanced through the adoption of Hessian analysis [18]. Hessian analysis technique computes the second derivatives along 3D directions by convoluting the given image with derivatives of the Gaussian kernel [19]. The Hessian analysis matrix is defined as:

$$H_{\sigma}(x, y, z) = \begin{pmatrix} I_{xx} & I_{xy} & I_{xz} \\ I_{yx} & I_{yy} & I_{yz} \\ I_{zx} & I_{zy} & I_{zz} \end{pmatrix} \quad (2)$$

where  $\sigma$  is the standard deviation of the Gaussian distribution and  $I_{ij}$  is the second deviation along  $i$ th and  $j$ th direction. The standard deviation  $\sigma$  could be used to control the radius

of blob-like structures. Eigen values that indicate three orthogonal directions, and Eigen vectors that indicate degrees of curvature along the given directions can be used to solve the hessian matrix at each pixel. Therefore, the likelihood of blobs together with the magnitude of pixel's Eigen values can be formulated as:

$$R_B = \frac{|\lambda_1|}{\sqrt{|\lambda_2||\lambda_3|}} \quad (3)$$

$$M = \sqrt{\sum_{n=1}^3 \lambda_n^2} \quad (4)$$

where  $R_B$  and  $M$  represent the likelihood of blobs and the magnitude of pixel's Eigen values, respectively. Generally, the magnitude of Eigen values of objects are larger than that of the background. Blobs can be enhanced further using the formula:

$$B_{\sigma}(\lambda_p) = \begin{cases} (1 - e^{-\frac{R_B}{2\alpha}}), & \text{if } \lambda_1 > 0, \lambda_2 > 0, \text{ and } \lambda_3 > 0 \\ 0, & \text{otherwise} \end{cases} \quad (5)$$

where  $\lambda_p$  indicates Eigen values at position  $p = (x, y, z)$  and  $\alpha$  and  $\beta$  refer to sensitivity parameters of  $R_B$  and  $M$ , respectively. In our approach, the sensitivity parameter was set at 0.3 to control the number of blobs detected in the darker regions. The condition  $\lambda_1 > 0, \lambda_2 > 0, \text{ and } \lambda_3 > 0$  is used to enhance only dark objects. Furthermore, carious lesions of different sizes can be detected, by adjusting the formula above as:

$$\text{Blobness}(\lambda_p) = \max_{\sigma_{\min} \leq (\sigma) \leq \sigma_{\max}} B_{\sigma}(\lambda_p) \quad (6)$$

where  $\sigma_{\min}$  is the minimum scale and  $\sigma_{\max}$  the maximum scale of carious lesions.

### 2.3.3. Caries Candidate Selection

From setting the blobness sensitivity parameters, many redundant non-caries candidates and actual caries candidates were detected. If all the caries candidates were used to extract features and estimate the likelihood of caries, processing would take a long time. Additionally, a long processing time leads to poor performance of the CAD system, and this is because of the high frequency of false positives (FPs). Therefore, caries candidate selection is adopted to eliminate FPs from carious candidates. High blobness values indicate the candidate has caries, while those with lower blobness values are non-caries candidates. Therefore, maximum and mean blobness values of caries candidates were used to eliminate false positives. The formulas are defined as:

$$\text{Blobness}_{\text{mean}}(T) = \frac{\sum_{p \in T} \text{Blobness}(\lambda_p)}{N_T} \quad (7)$$

$$\text{Blobness}_{\text{max}}(T) = \max_{p \in T} \text{Blobness}(\lambda_p) \quad (8)$$

where  $T$  refers to a caries candidate with  $N_T$  voxels and  $p$  a voxel that belongs to the caries candidate. The size of blobs was also used as a feature in selecting caries candidates. Size feature is used because the caries candidate detection based on Hessian analysis is sensitive to intensity variations and leads it to detect many small regions including edge spaces of teeth as caries candidates. These edge spaces and small regions are not part of true caries lesions and their size can be used to eliminate many false positives from among the caries candidates as seen in Figure 3. The linear regression model [20] is applied to eliminate false positives from among caries candidates. The caries selection function  $L_s(T)$  is defined as:

$$Z(T) = \beta_0 + \sum_{i=1}^{N_f} \beta_i x_i \quad (9)$$

$$L_s(T) = \frac{1}{1 + e^{-Z(T)}} \quad (10)$$

where  $N_f$  is the number of features,  $x_i$  the feature value,  $\beta_0$  is the constant coefficient, and  $\beta_i$  is the corresponding coefficient estimated by the linear regression model. Lastly, the criteria used for caries selection is expressed as:

$$L_s(T) \geq THresh \quad (11)$$

where  $THresh$  is the threshold used to determine the remaining caries candidates after eliminating false positives. The detected regions remain as dental caries when values estimated by the caries selection model was equal or greater than threshold. Those values less than the threshold given were removed. In our experiments, the convexity threshold value was set at 0.9 to detect dental caries. After the caries candidate selection, false positives were eliminated, and only carious candidates remain, which are now classified as “Dental Caries Detected”.

---

**Algorithm 1** Proposed Model for Dental Image Segmentation.

---

```

1: procedure ENCODER( $Y$ ) ▷  $Y : y_i$  is an input image with dimension (L, H).
2:   Initialization:  $Feature_i = y_0$ ;
3:   for ( $i = 0 : N - 1$ ) do
4:      $AugmentedFeature_i = DataAugmentation(Feature_i)$ ;
5:      $GrayScalingFeature_i = GrayScaling(AugmentedFeature_i)$ ;
6:      $FilteringFeature_i = GuassainBlurFiltering(GrayScalingFeature_i)$ ;
7:   end for
8: end procedure
9: procedure PROCEDURE ENHANCEMENT( $FilteringFeature_i$ ) ▷ It is the output of the preprocessing procedure
10:  for ( $j = 0 : M - 1$ ) do
11:     $ErisonFeature_i = ErisonMorophology(FilteringFeature_i)$ ;
12:     $DialtionFeature_i = DialtionMorophology(ErisonFeature_i)$ ;
13:  end for
14: end procedure
15: procedure PROCEDURE SEGMENTATION( $DialtionFeature_i$ ) ▷ It is the output of the enhancement procedure
16:  for ( $s = 0 : L - 1$ ) do
17:     $ThresholdingFeature_i = Thresholding(DialtionFeature_i)$ ;
18:     $ConnectedFeature_i = ConnectedComponentFeature(ThresholdingFeature_i)$ ;
19:  end for
20: end procedure
21: procedure PROCEDURE FEATUREEXTRACTION( $ConnectedFeature_i$ ) ▷ It is the output of the segmentation procedure
22:  for ( $r = 0 : K - 1$ ) do
23:     $Feature_i = FeatureExtraction(ConnectedFeature_i)$ ;
24:     $Segmented Image Feature = Feature_i$ ; ▷ Final Segmented Output Display.
25:  end for
26: end procedure

```

---

### 3. Results and Discussion

Experimental results from the proposed approach are based on the analysis of the caries candidate detection process. Experiments were carried out on 11,114 bitewing X-ray images of the augmented dental dataset. The dataset was split into 10,090 training set images and 1024 test images. In order to process the data set, several individual stages were used to analyse the dataset, as have been discussed in the previous sections of this work. Figure 1 shows an overview of the processing stages that include: preprocessing, segmentation and feature extraction.

Additionally, performance evaluation of the proposed approach was based on its ability to detect and locate dental caries on test data images. A Gaussian filter was used to reduce noise on the images before introducing a convexity threshold value to eliminate false positives regions from actual detected caries candidates. Figure 4 shows the caries detection algorithm's identification of caries locations on Gaussian filtered images before false positives are eliminated. Figure 5, shows the identification of dental caries locations remaining after introducing a convexity threshold value of 1.0 that eliminates false positives.

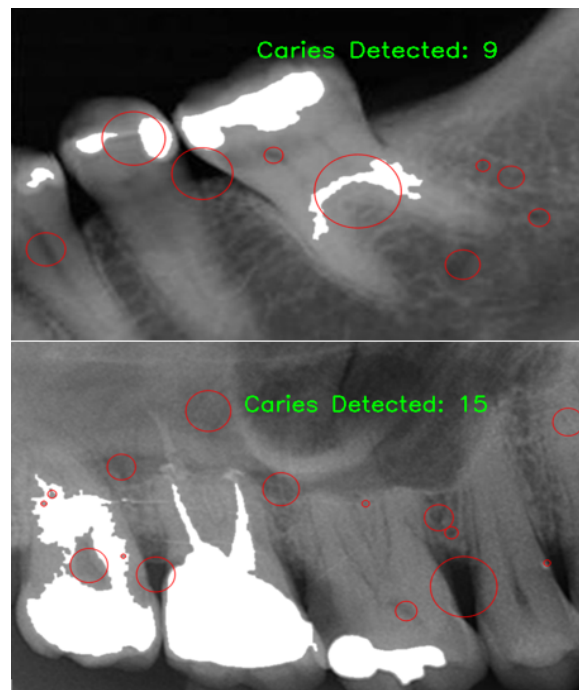


**Figure 4.** Gaussian filtered images of all caries detected regions, including false positives.

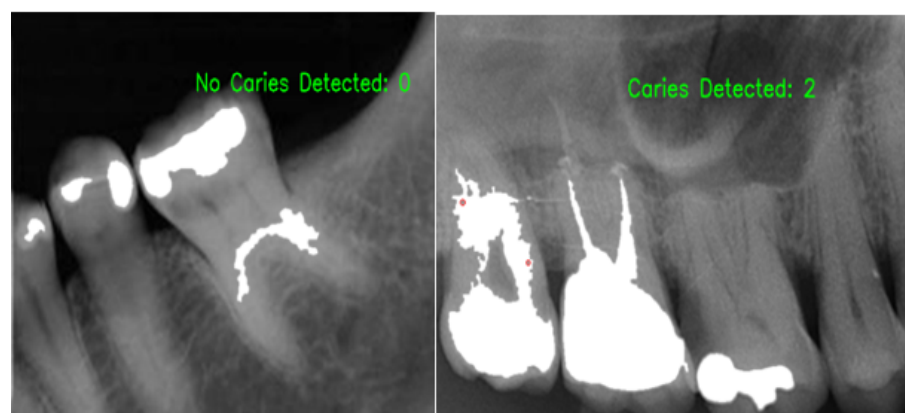


**Figure 5.** Images of dental caries detected after eliminating false positives through the use of the convexity threshold.

The results comparison was performed against different caries detection diagnostic methods to determine if the results fell within acceptable limits or not. The caries detection diagnostic methods compared against include textural classification as discussed by [21], dental classification for periapical radiographs by [22] and caries detection through a

supervised learning model proposed by [23] for panoramic images. The comparison of our proposed method with other detection techniques is shown in Table 1.

**Table 1.** Comparison of various caries detection methods.

Detection Methods	Dataset Images	Accuracy
Caries detection in panoramic images [23]	1392	98.0%
Dental classification for periapical images [22]	78	82.5%
Textural classification of digital images [21]	64	96.88%
PaxNet [11]	470	86.05%
ICDAS [12]	620	92.37%
GLCM [13]	240	80%
Deep learning [16]	304	64.14%
<b>Proposed approach</b>	<b>11,114</b>	<b>97.0%</b>

Our proposed method achieved better accuracy than the others with the introduction of blob detection on dental radiographs. Despite our results falling within the acceptable range of a novel approach, [23] enjoyed marginally higher results, and this is attributed to various reasons. Some reasons include differences in the database analysed, where our approach used bitewing radiographs while [23] used panoramic radiographs. Another reason is attributed to the errors experienced when analysing bitewing radiographs, namely exposure errors and image augmentation anomalies.

#### *Limitations*

Most of the existing systems dwell on the segmentation of caries and not on caries detection. The reluctance from healthcare experts to invest in computer aided systems (CAD) systems is due to the high number of false positive results. There is a need to improve existing systems, and one way to do so is by the introduction of automatic blob detection technique. Blob detection has been used in other fields of medical imaging but has not seen substantive use in the field of dental imaging.

#### **4. Conclusions**

There is a huge potential for use of dental radiography and, in particular, for work focused on caries detection. Blob detection was used in this research to detect all caries candidates, which also included false positives. The use of image analysis techniques was encouraged to filter out detected unwanted regions, such as edges from the caries regions. A threshold property value was then introduced to aid in the elimination of false positives from the selected regions to leave the detected caries candidates. The proposed caries detection method was able to administer favourable results compared to other detection models with an accuracy of 97%.

The introduction of blob detection offers a more robust and automatic way to detect caries on dental radiographs compared to other detection methods. The proposed approach presents an avenue for future research using unsupervised models from its impressive success rate with supervised models. More dental radiographic images are needed to improve the training and learning process to produce even better results. Figure 6 shows both the training and validation accuracy graphs of the proposed method. Weight regularization methods are also encouraged to reduce overfitting.

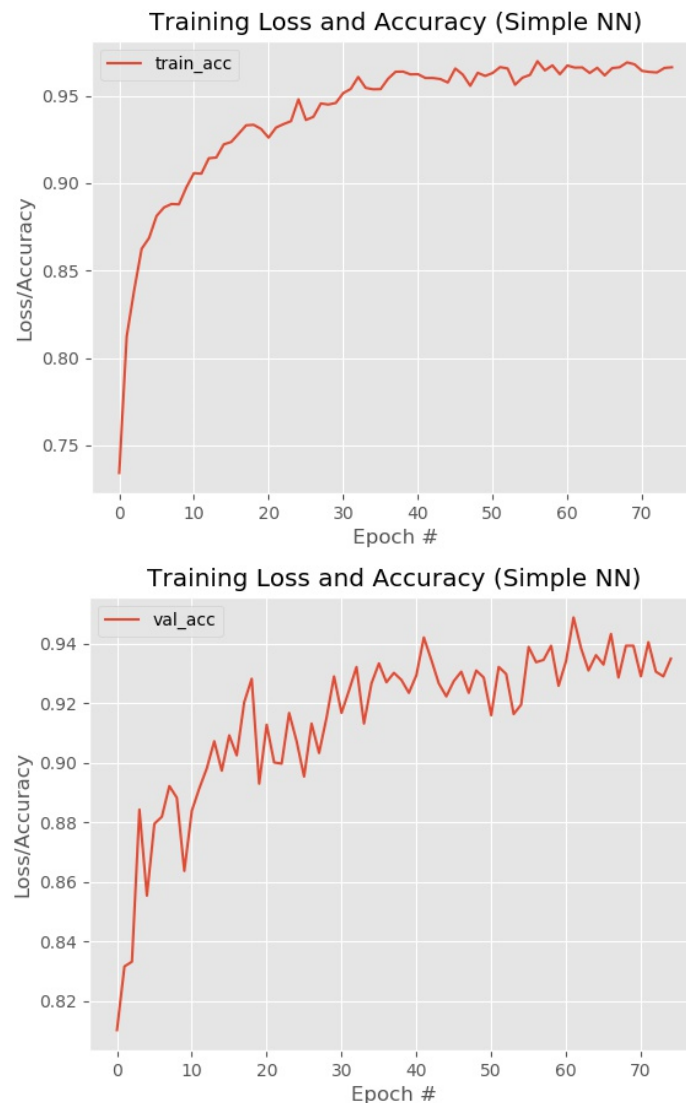


**Figure 6.** Training and validation accuracy graph curves for the proposed method.

## 5. Future Works

From our survey, various techniques, methods and approaches were discussed that point towards the segmentation and detection of dental images. Various works that stem from the industry and academia have been mentioned and discussed regarding existing algorithms, segmentation and detection methods and also various protocols for evaluating performance. There are issues and encouraging future perspectives of study that have resulted from our discussions, which are highlighted as:

- **Data availability and reliability.** Deep learning networks require large amount of data to achieve meaningful and effective performance results. Due to the nature of dental images, there is need for hybrid datasets to aid good performance of the networks. There is need of public available datasets for dental images to make deep learning in the field possible. Data augmentation is also a good method to obtain more images for dental datasets.
- **Data standardization.** Many methods discussed are handling the pre-processing step through manual methods, such as cropping the region of interest on an image. These methods contribute to the loss of some key details from the images. Some networks end up dividing a whole image into subregions, and this slows down the learning



process of one subregion after the other. There are methods like down-sampling, which might lead to the deletion of important details and this seem to have been due to limitations in computational power. Deep learning approaches have seen increased learning on whole images rather than manual manipulation of images at the pre-processing stage, in order to obtain more general and accurate results.

- **Weight Regularization Methods.** Deep learning networks can also be improved by introducing weight regularization to improve their performance. The regularization of weights involves optimization of model hyper-parameters, such as the learning rate and the dropout rate. Basically, weight regularization methods are introduced into networks for parameter optimization.
- **Hybrid approaches.** Deep networks can also be enhanced by combining several models or methods to form hybrid networks that will improve overall evaluation performance. The combination can be in any stage of the model, for instance combining two pre-processing techniques to come with a single one to enhance image quality. This combination can also be handled by joining various attributes of different models to form one hybrid model that will enhance the training, extraction, detection and classification of objects.

**Author Contributions:** Contributions: Conceptualization, V.M. and S.V.; methodology, V.M.; formal analysis, V.M. and S.V.; investigation, V.M.; resources, S.V.; writing original draft preparation, V.M.; writing review and editing, S.V.; supervision, S.V. Both authors have read and agreed to the published version of the manuscript.

**Funding:** This research received no external funding.

**Institutional Review Board Statement:** Not applicable.

**Informed Consent Statement:** Informed consent was obtained from all subjects involved in the study.

**Data Availability Statement:** Data available in publicly accessible repositories.

**Conflicts of Interest:** The authors declare no conflict of interest.

## References

1. Kassebaum, N.; Bernabé, E.; Dahiya, M.; Bhandari, B.; Murray, C.; Marcenes, W. Global burden of untreated caries: A systematic review and metaregression. *J. Dent. Res.* **2015**, *94*, 650–658. [\[CrossRef\]](#) [\[PubMed\]](#)
2. Casalegno, F.; Newton, T.; Daher, R.; Abdelaziz, M.; Lodi-Rizzini, A.; Schürmann, F.; Krejci, I.; Markram, H. Caries detection with near-infrared transillumination using deep learning. *J. Dent. Res.* **2019**, *98*, 1227–1233. [\[CrossRef\]](#) [\[PubMed\]](#)
3. Schwendicke, F.; Dörfer, C.; Schlattmann, P.; Page, L.F.; Thomson, W.; Paris, S. Socioeconomic inequality and caries: A systematic review and meta-analysis. *J. Dent. Res.* **2015**, *94*, 10–18. [\[CrossRef\]](#) [\[PubMed\]](#)
4. Srivastava, M.M.; Kumar, P.; Pradhan, L.; Varadarajan, S. Detection of tooth caries in bitewing radiographs using deep learning. *arXiv* **2017**, arXiv:1711.07312.
5. Valizadeh, S.; Goodini, M.; Ehsani, S.; Mohseni, H.; Azimi, F.; Bakhshandeh, H. Designing of a computer software for detection of approximal caries in posterior teeth. *Iran. J. Radiol.* **2015**, *12*, e16242. [\[CrossRef\]](#)
6. Nokhbatolfoghahaie, H.; Alikhasi, M.; Chiniforush, N.; Khoei, F.; Safavi, N.; Zadeh, B.Y. Evaluation of accuracy of DIAGNOdent in diagnosis of primary and secondary caries in comparison to conventional methods. *J. Lasers Med. Sci.* **2013**, *4*, 159. [\[PubMed\]](#)
7. Vural, U.; Gökalp, S. Diagnostic methods for dental caries used by private dental practitioners in Ankara. *Niger. J. Clin. Pract.* **2017**, *20*, 382–387. [\[CrossRef\]](#) [\[PubMed\]](#)
8. Watt, R.G.; Tsakos, G.; De Oliveira, C.; Hamer, M. Tooth Loss and Cardiovascular Disease Mortality Risk—Results from the Scottish Health Survey. *PLoS ONE* **2012**, *7*, e30797. [\[CrossRef\]](#) [\[PubMed\]](#)
9. Lee, J.-H.; Kim, D.-H.; Jeong, S.-N.; Choi, S.-H. Detection and diagnosis of dental caries using a deep learning-based convolutional neural network algorithm. *J. Dent.* **2018**, *77*, 106–111. [\[CrossRef\]](#) [\[PubMed\]](#)
10. Han, K.T.M.; Uyyanonvara, B. A Survey of Blob Detection Algorithms for Biomedical Images. In Proceedings of the 2016 7th International Conference of Information and Communication Technology for Embedded Systems (IC-ICTES), Bangkok, Thailand, 20–22 March 2016; pp. 57–60.
11. Haghani, A.; Majdabadi, M.M.; Ko, S.B. Paxnet: Dental caries detection in panoramic X-ray using ensemble transfer learning and capsule classifier. *arXiv* **2020**, arXiv:2012.13666.
12. Duong, D.L.; Kabir, M.H.; Kuo, R.F. Automated caries detection with smartphone color photography using machine learning. *Health Inf. J.* **2021**, *27*. [\[CrossRef\]](#)

13. Jusman, Y.; Tamarena, R.I.; Puspita, S.; Saleh, E.; Kanafiah, S.N.A.M. Analysis of Features Extraction Performance to Differentiate of Dental Caries Types Using Gray Level Co-occurrence Matrix Algorithm. In Proceedings of the 2020 10th IEEE International Conference on Control System, Computing and Engineering (ICCSCE), Penang, Malaysia, 21–22 August 2020; pp. 148–152.
14. Prados-Privado, M.; García Villalón, J.; Martínez-Martínez, C.H.; Ivorra, C.; Prados-Frutos, J.C. Dental Caries Diagnosis and Detection Using Neural Networks: A Systematic Review. *J. Clin. Med.* **2020**, *9*, 3579. [[CrossRef](#)] [[PubMed](#)]
15. Paqué, P.N.; Herz, C.; Wiedemeier, D.B.; Mitsakakis, K.; Attin, T.; Bao, K.; Belibasakis, G.N.; Hays, J.P.; Jenzer, J.S.; Kaman, W.E.; et al. Salivary Biomarkers for Dental Caries Detection and Personalized Monitoring. *J. Personal. Med.* **2021**, *11*, 235. [[CrossRef](#)] [[PubMed](#)]
16. Lee, S.; Oh, S.I.; Jo, J.; Kang, S.; Shin, Y.; Park, J.W. Deep Learning for Early Dental Caries Detection in Bitewing Radiographs. *Sci. Rep.* **2021**, *11*, 16087.
17. Lee, J.-S. Digital image smoothing and the sigma filter. *Comput. Vis. Graph. Image Process.* **1983**, *24*, 255–269. [[CrossRef](#)]
18. Vos, P.C.; Barentsz, J.O.; Karssemeijer, N.; Huisman, H. Automatic computer-aided detection of prostate cancer based on multiparametric magnetic resonance image analysis. *Phys. Med. Biol.* **2012**, *57*, 1527–1542. [[CrossRef](#)] [[PubMed](#)]
19. Moon, W.K.; Shen, Y.-W.; Bae, M.S.; Huang, C.-S.; Chen, J.-H.; Chang, R.-F. Computer-Aided Tumor Detection Based on Multi-Scale Blob Detection Algorithm in Automated Breast Ultrasound Images. *IEEE Trans. Med. Imaging* **2013**, *32*, 1191–1200. [[CrossRef](#)]
20. Hosmer, D.W.; Lemeshow, S. *Applied Logistic Regression*; John Wiley & Sons, Inc.: New York, NY, USA, 2000.
21. Geetha, V.; Aprameya, K.S. Textural analysis based classification of digital X-ray images for dental caries diagnosis. *Int. J. Eng. Manuf.* **2019**, *9*, 44–45.
22. Tangel, M.L.; Fatichah, C.; Yan, F.; Betancourt, J.P.; Widyanto, M.R.; Dong, F.; Hirota, K. Dental classification for periapical radiograph based on multiple fuzzy attribute. In Proceedings of the 2013 Joint IFSA World Congress and NAFIPS Annual Meeting (IFSA/NAFIPS), Edmonton, AB, Canada, 24–28 June 2013; pp. 304–309.
23. Oliveira, J.P.R.D. Caries Detection in Panoramic Dental X-ray Images. Doctoral Dissertation, Universidade da Beira Interior, Covilhã, Portugal, 2009.



## 4.3 Summary

This paper discusses the proposed caries diagnostic approach. The Gaussian filter was used to remove noise from images that were earlier segmented via the active contour method in the previous segmentation chapter. After the filtering step, a blob detection technique was introduced to detect all blobs on the images. Later on, a convexity threshold value is introduced to eliminate false positive caries blobs to be left with true positive caries blobs. Therefore, we are classifying these remaining blobs as detected dental caries on the image. The next chapter will discuss results of both the segmentation and detection method, and compare their results against current systems.

## Chapter 5

# Experimental Results and Discussion

### 5.1 Introduction

Performance evaluation of the overall method proposed in this thesis is based on the analysis and success rates from both the segmentation and caries diagnosis processes. It is also important to understand the nature of the dataset analyzed to achieve these results. Results from different existing segmentation methods are readily available, and are therefore compared to those of the proposed method. In order to determine the performance of a caries diagnostics method, comparisons are needed to be made against correct detection rates of existing systems' ability to diagnose dental caries. The performance of the proposed method was measured by its ability to locate known caries, and any predictions it made with regard to caries which had not been previously identified were considered as false positives.

## 5.2 Dataset

Given the low number of image data available for this thesis, it is difficult for deep learning networks to derive intelligent decisions. These networks need huge amounts of data to be able to achieve good performance, and thus data augmentation is very important. Image augmentation is achieved through artificially creating training images by multiple processing steps namely: random shifts, shear and flips. Data augmentation was initially popularized by [12] in order to make simulation more feasible and simple. In this proposed method, 120 dental bitewing images available were subjected to data augmentation. Image data augmentation techniques such as rotation, horizontal and vertical shifts and flips, zoom, and increased brightness were used to generate a final dataset of 11,148 images. These generated images are subdivided into, 10090 training images and 1058 test images in the dataset. The images are in JPG format and the test images are used as the ground truths used for the testing phase. These augmented bitewing radiographic images had image dimensions of 748 pixels in width, 512 pixels in height, and gray scale levels on  $[0, 255]$  scale. Further, the testing images represented a variety selection of teeth that include: molars, incisors, canines and wisdom teeth. Figure. 5.1 show images from the original set and images after augmentation has been carried out.

## 5.3 Caries Detection Framework

A caries detection framework was proposed as the best way of handling and processing the dental radiographs in the augmented dataset. Individual stages in the framework have already been discussed in detail in previously chapters, but the overview is shown by Figure 5.2 and how they relate with each other.



Images in original dataset



Augmented images

Figure 5.1: Images in the original dataset, images in the generated dataset after augmentation.

## 5.4 Segmentation Results

The success rate of the segmentation methods covered in this research is from separating individual teeth from different jaw regions on an image. The success rate of the

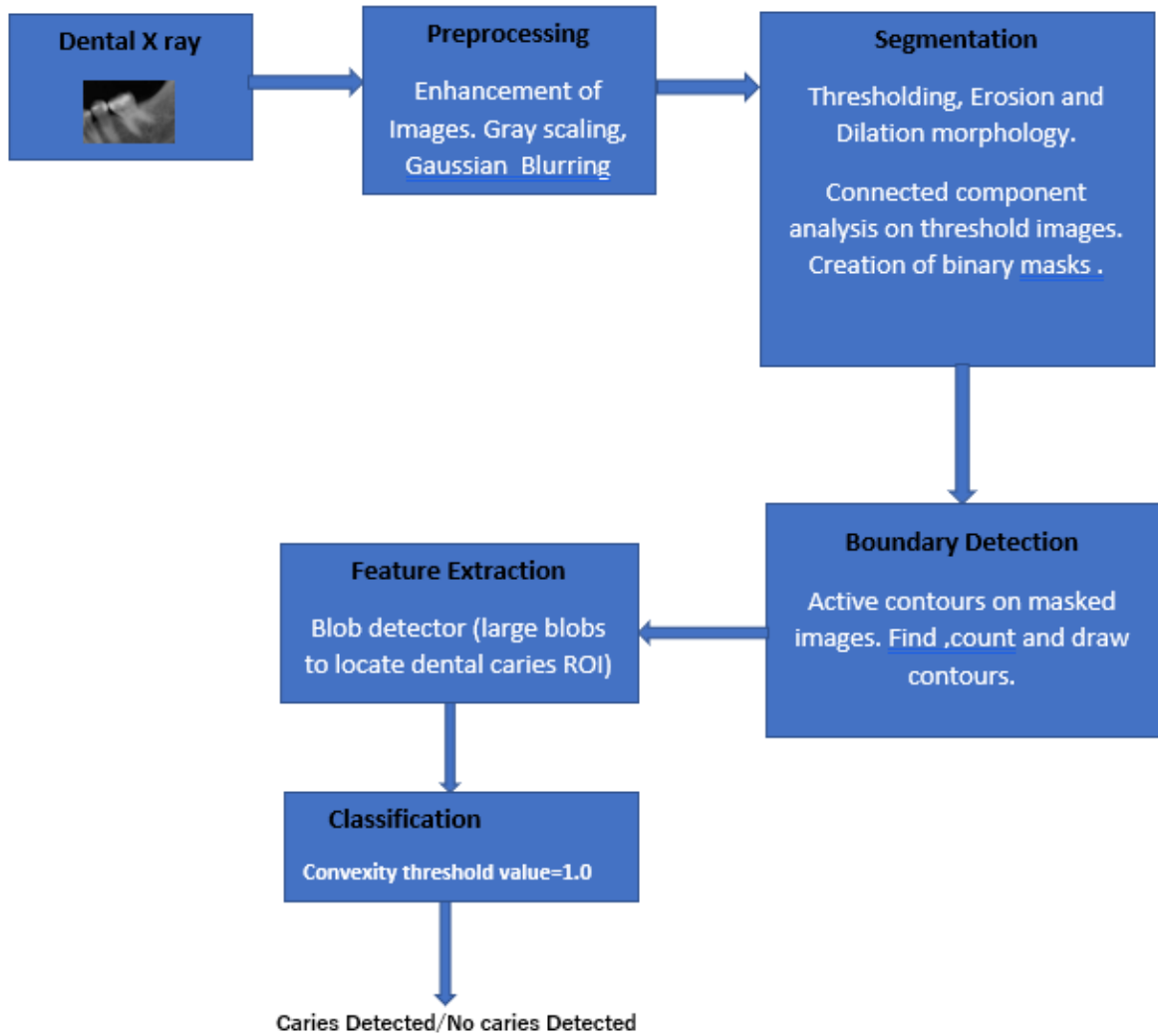


Figure 5.2: An overview of the caries detection framework.

segmentation method is measured as to how it clearly shows tooth edge boundaries, and individual teeth on images throughout the whole dataset. Teeth separation is correctly considered if the separation did not cause division of the teeth. Teeth which were already partial as a result of being at the edge of the radiograph are considered correctly separated if no further partiality was caused. Teeth that were not correctly segmented were either as a result of poor image contrast, where enhancement techniques could not salvage a distinction between teeth and non-teeth structures. The

deep learning process of the segmentation method was optimized through the use of dropout to give better results. Dropout is simply dropping off units in the network that are not necessary for the processing stage. It should be noted that the proposed segmentation method after optimization exhibited better results compared to other existing implementations. Table 5.1 provides a comparison of the proposed method to other implementations of the segmentation process. Results got from the proposed segmentation method indicate a noticeable improvement on existing models. Figure. 5.3 show some image examples of the segmentation results.

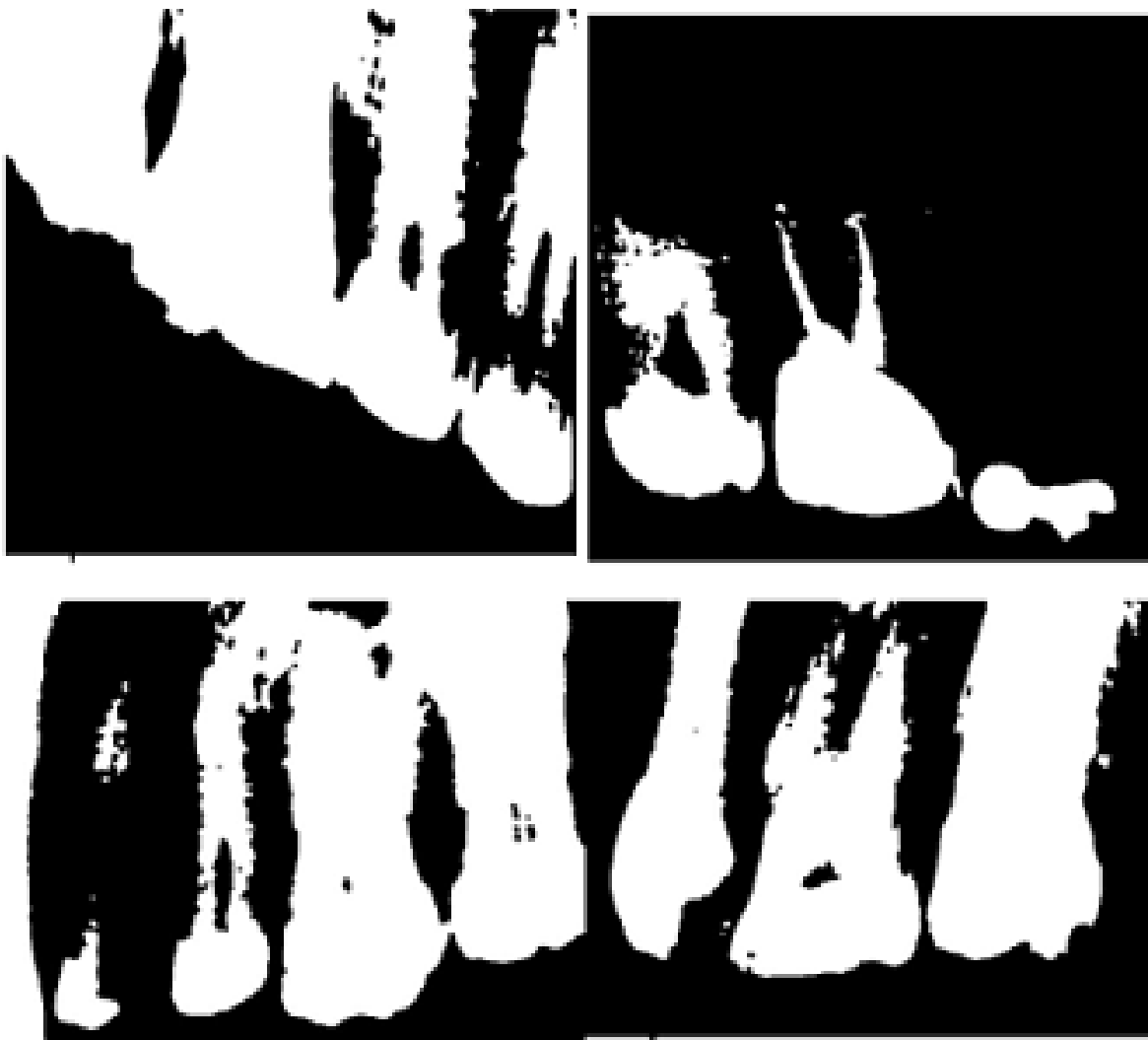


Figure 5.3: Examples of the segmentation results in the dataset.

Table 5.1: Overall comparison of Segmentation Methods.

Methods	Accuracy
Segmentation methods evaluation [24]	77.23%
Unsupervised Caries Detection [23]	87.5%
Brain Tumor Segmentation using DCNN [11]	85.0%
<b>Proposed Segmentation Method</b>	<b>91.31%</b>

## 5.5 Caries Detection Results

Experimental results elicited from the proposed approach are based purely on analysis of the caries candidate detection process. Experiments were carried out on test data of 11,114 bitewing X-ray images of the augmented dental dataset. The dataset was split into, 10090 training set images and 1024 test images. Performance evaluation results are based on the ability of the detection approach to detect and locate dental caries on test data images. Since there was no available ground truth data, thus, test data was used to evaluate the success rate of the detection method. A Gaussian filter was used on images as shown by Figure 5.4 to reduce noise on the and retain edge information. After processing the images, the blob detection method was used to identify and locate both locations of identified caries and locations of false positive regions. All these detected regions are shown in Figure 5.5. These incorrectly identified regions defined as false positive regions need to be eliminated to remain with correctly identified caries regions. A convexity threshold value of 1.0 is introduced to eliminate false positive regions from correctly identified carious regions. Figure ?? show correctly identified dental caries, which are classified either as "Caries Detected" or "No Caries".





Figure 5.4: Examples of Gaussian filtered images.

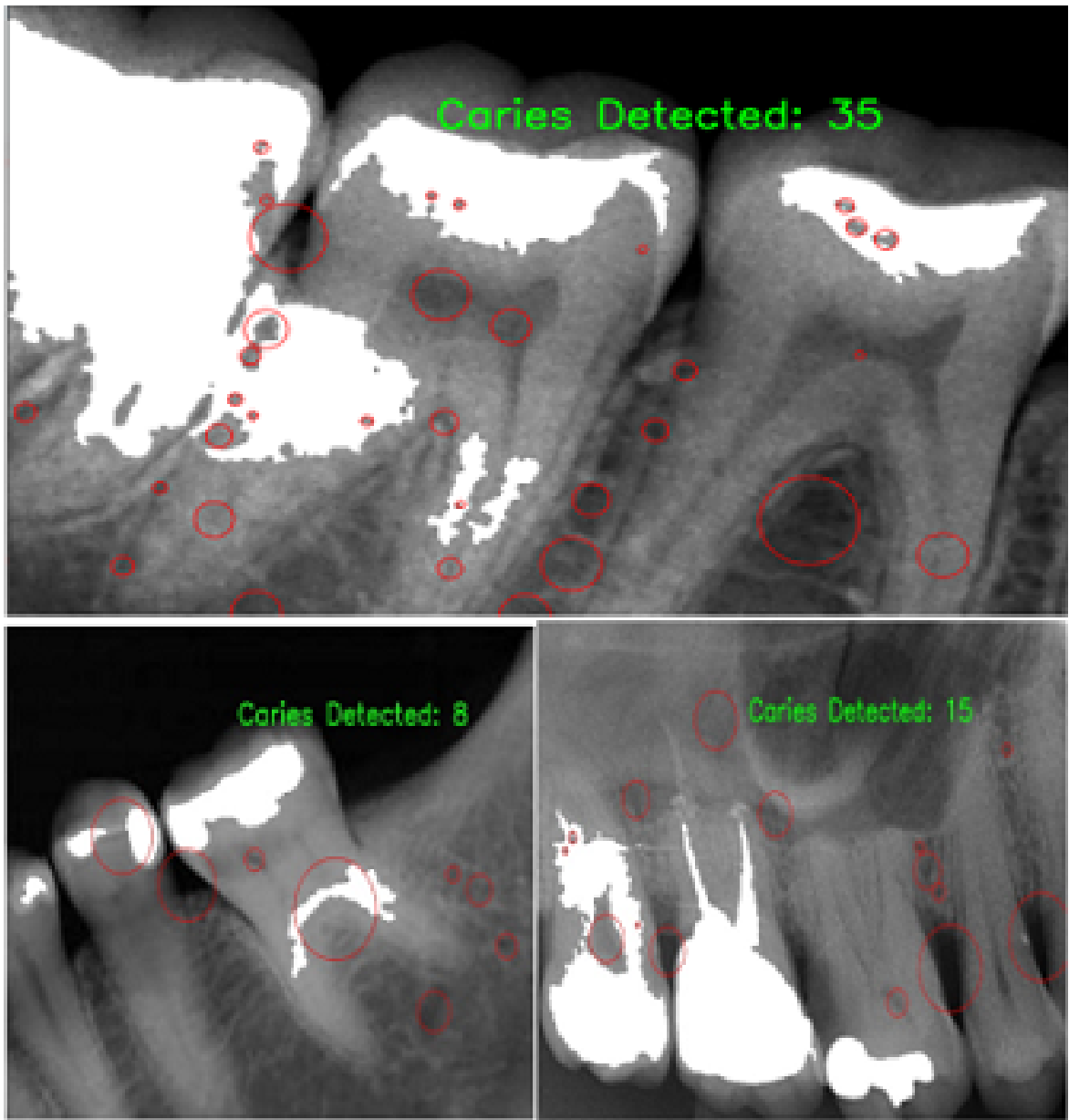


Figure 5.5: Examples of all detected caries blobs

Results comparison was done against other different caries detection diagnostic methods, to determine if the results fell within acceptable limits or not. The caries detection diagnostic methods compared against include textural classification as dis-

cussed by [8], dental classification for periapical radiographs by [31], and caries detection through a supervised learning model proposed by [21] for panoramic images. The comparison of the proposed method with other detection techniques is shown in Table 5.2.

The proposed method achieves better accuracy results than others with its introduction of blob detection on dental radiographs. Despite these results falling within the acceptable range of a novel approach, [21] enjoys marginally higher results and this is attributed to various reasons. Some reasons are due to differences in the database analyzed, where our approach used bitewing radiographs while [21] used panoramic radiographs. Another reason is attributed to errors experienced when analyzing bitewing radiographs, namely: exposure errors and image augmentation anomalies.

Table 5.2: Comparison of caries detection methods.

Detection Methods	Accuracy
Caries detection in panoramic images [21]	98.0%
Dental classification for periapical images [31]	82.5%
Textural classification of digital images [8]	93.61%
<b>Proposed approach</b>	<b>97.0%</b>

## 5.6 Conclusion

This chapter discussed the dataset and its augmentation, the caries detection framework, segmentation and caries detection results. The dataset comprised non-perfect

images due to the augmentation process. The caries detection framework was discussed to give an overview of all the previous processes combined to reach the final results. The results obtained from the framework were presented and compared to existing models. The results showed that the proposed framework performed favourably compared to the existing methods. The next chapter will delve into implications of the results discussed in this chapter and give more in depth conclusions. The next chapter will also look at future work done to enhance the caries diagnosis framework described in this chapter.

# Chapter 6

## Conclusion and Future Work

### 6.1 Conclusion

There is a huge potential for use of dental radiography, and especially work focused on caries detection. Most of the existing systems dwell much on segmentation of caries and not on caries detection. The reluctance from healthcare experts to invest in computer aided systems (CAD) systems is due to the high number of false positive results witnessed from them. There is a need to improve existing systems, and one way to do so is by the introduction of automatic blob detection technique. Blob detection has been used in other fields of medical imaging, but has not seen substantive use in the field of dental imaging. The use of such image analysis techniques to determine the presence of caries aims to create a system that takes a human diagnostic approach, whereby dental caries are diagnosed based on visual interpretation of teeth.

In this research work, a supervised deep learning model for caries detection was proposed. The model is implemented through a segmentation method to separate dental radiographs into individual teeth combined with a boundary detection method to determine tooth edge boundaries for caries analysis, and finally a diagnostic method

that accesses these boundaries using image analysis techniques. The segmentation method was implemented through existing pre-processing techniques in order to obtain threshold images ready for edge boundary detection. These techniques included: data augmentation, morphology operations, filtering. The edge boundary detection was handled by combination of thresholding and an active contour model. Finally, the diagnostic method was handled by Gaussian filters for noise reduction, blob detection and convexity threshold for caries detection.

The proposed segmentation method was compared against existing models and its results proved favourable. The new method showed improved performance because of the combined aspect of thresholding to separate individual teeth, while active contours model to locate edge boundaries. The proposed caries detection method was able to obtain favourable results compared to other existing detection methods, with a correct diagnosis rate of 97%. Therefore, it can be concluded that the proposed framework described in this thesis provides a new approach to both the problems of tooth segmentation and dental caries detection. The segmentation method proposed offers a robust way for determining both individual teeth separation and edge boundary detection, which makes it easier for both supervised and unsupervised learning models to correctly process teeth in the dataset. The success rate of the proposed caries detection method on a supervised model provides a potential avenue for future work using unsupervised models, thus leading to even better results.

## **6.2 Future Work**

Image analysis has been used by the proposed caries detection model in this thesis to determine presence of dental caries in dental radiographs. The final results depend heavily on the quality of the image by the time it reaches the diagnostic method. Optimization of the model at several key processes, such as the use of dropout at the

segmentation stage, could improve the final result and future work will look at how to implement such optimizations. The dataset that was used was relatively noise free, thus minimal preprocessing needed to be implemented for noise removal. The dataset had few images for processing and there was need to add more images through various processing methods, that will aid deep learning by the model.

There are a series of encouraging future perspectives of study that may see improvement in dental segmentation and detection of dental caries. Among them are:

- **Data Availability and Reliability.** Deep learning networks require large amount of data to be able to achieve meaningful and effective performance results. Due to the nature of dental images, there is need for hybrid datasets to aid good performance of the networks. There is need of public available datasets for dental images to make deep learning possible.
- **Data Standardization.** Many methods discussed in this research are handling image pre-processing via manual methods, such as, cropping regions of interest on an image. These methods contribute to loss of some key details from the images. Some networks end up dividing a whole image into subregions and this ends up slowing down the learning process that occurs one subregion after the other. Other methods such as down-sampling lead to deletion of important image details, and this is due to limitations in computational power. Deep learning approaches have seen and increased in learning of whole images rather than the manual manipulation of images via pre-processing, to get more general and accurate results.
- **Weight Regularization Methods.** Deep learning methods and networks can also be improved by the introduction of weight regularization to improve their performance. The regularization of weights involves optimization of model hy-

perparameters such as the learning rate and the dropout rate. Basically, weight regularization methods are introduced into networks for parameter optimization.

- **Hybrid Approaches.** Deep learning methods can be further improved by combining several models or techniques to form hybrid ones that will eventually improve the overall evaluation performance. The combination can be at any stage of the model, for instance combining two or more pre-processing techniques to come up with a single step to enhance image quality. The combination can also be handled by joining various attributes of different models to form one hybrid model that will enhance the training, extraction, detection and classification of objects.

In addition to these optimizations, future work will look at expanding the proposed system's ability to diagnose different images, since it is currently used for only testing bitewing radiographs from the same dataset. The scope will be expanded to test a variety of different radiographic types, and also bitewing radiographs from different datasets.



# Bibliography

- [1] ZZ Akarslan, M Akdevelioglu, K Gungor, and H Erten. A comparison of the diagnostic accuracy of bitewing, periapical, unfiltered and filtered digital panoramic images for approximal caries detection in posterior teeth. *Dentomaxillofacial Radiology*, 37(8):458–463, 2008.
- [2] Greene Vardiman Black. Mottled teeth: an endemic developmental imperfection of the enamel of the teeth heretofore unknown in the literature of dentistry. *Dental Cosmos*, 58:129–156, 1916.
- [3] Greene Vardiman Black. *The pathology of the hard tissues of the teeth*, volume 1. Medico-Dental Publishing Company, 1917.
- [4] Greene Vardiman Black. *Operative dentistry*, volume 2. Medico-Dental Publishing Company, 1955.
- [5] William H Bowen, Downen Birkhed, L Granath, and WD McHugh. Dental caries: Dietary and microbiology factors. *Systemized prevention of oral disease: Theory and practice*, pages 19–41, 1986.
- [6] H Trendley Dean, Francis A Arnold Jr, Philip Jay, and John W Knutson. Studies on mass control of dental caries through fluoridation of the public water supply. *Public Health Reports (1896-1970)*, pages 1403–1408, 1950.

- [7] Margherita Fontana and Domenick T Zero. Assessing patients' caries risk. *The Journal of the American Dental Association*, 137(9):1231–1239, 2006.
- [8] V Geetha and KS Aprameya. Textural analysis based classification of digital x-ray images for dental caries diagnosis. *Int J Eng Manuf (IJEM)*., 9(3):44–45, 2019.
- [9] Susan O Griffin, E Oong, W Kohn, Brani Vidakovic, BF Gooch, and CDC Dental Sealant Systematic Review Work Group. The effectiveness of sealants in managing caries lesions. *Journal of dental research*, 87(2):169–174, 2008.
- [10] JOSEPH HEAD. A study of saliva and its action on tooth enamel in reference to its hardening and softening. *Journal of the American Medical Association*, 59(24):2118–2122, 1912.
- [11] Saddam Hussain, Syed Muhammad Anwar, and Muhammad Majid. Brain tumor segmentation using cascaded deep convolutional neural network. In *2017 39th Annual International Conference of the IEEE Engineering in Medicine and Biology Society (EMBC)*, pages 1998–2001. IEEE, 2017.
- [12] Zeshan Hussain, Francisco Gimenez, Darvin Yi, and Daniel Rubin. Differential data augmentation techniques for medical imaging classification tasks. In *AMIA Annual Symposium Proceedings*, volume 2017, page 979. American Medical Informatics Association, 2017.
- [13] Theodore Koulourides et al. Implications of remineralization in the treatment of dental caries. 1986.
- [14] ID Mandel and S Wotman. The salivary secretions in health and disease. *Oral sciences reviews*, (8):25, 1976.
- [15] Frederick S McKay. The relation of mottled enamel to caries. *The Journal of the American Dental Association (1922)*, 15(8):1429–1437, 1928.

- [16] Willoughby D Miller. The presence of bacterial plaques on the surface of teeth and their significance. *Dent Cosmos*, 44:425–446, 1902.
- [17] Jack Mirza and Guy Robertson. Vital guide to dental implants. *Vital*, 6(1):19–22, 2008.
- [18] Mahvash NAVAZesh. How can oral health care providers determine if patients have dry mouth? *The Journal of the american dental association*, 134(5):613–618, 2003.
- [19] Michael G Newman, Henry Takei, Perry R Klokkevold, and Fermin A Carranza. *Carranza’s clinical periodontology*. Elsevier health sciences, 2011.
- [20] Hanieh Nokhbatolfoghahaie, Marzieh Alikhasi, Nasim Chiniforush, Farzaneh Khoei, Nassimeh Safavi, and Behnoush Yaghoub Zadeh. Evaluation of accuracy of diagnodent in diagnosis of primary and secondary caries in comparison to conventional methods. *Journal of lasers in medical sciences*, 4(4):159, 2013.
- [21] João Paulo Ribeiro de Oliveira. *Caries detection in panoramic dental X-ray images*. PhD thesis, 2009.
- [22] World Health Organization et al. Sugars and dental caries. Technical report, World Health Organization, 2017.
- [23] Darren Osterloh and Serestina Viriri. Unsupervised caries detection in non-standardized bitewing dental x-rays. In *International Symposium on Visual Computing*, pages 649–658. Springer, 2016.
- [24] Abdolvahab Ehsani Rad, Mohd Shafry Mohd Rahim, Amjad Rehman, Ayman Altameem, and Tanzila Saba. Evaluation of current dental radiographs segmentation approaches in computer-aided applications. *IETE Technical Review*, 30(3):210–222, 2013.

- [25] Howard R Raper. Practical clinical preventive dentistry based upon periodic roentgen-ray examinations. *The Journal of the American Dental Association* (1922), 12(9):1084–1100, 1925.
- [26] E Reich, A Lussi, and E Newbrun. Caries-risk assessment. *International dental journal*, 49(1):15–26, 1999.
- [27] F Schwendicke, CE Dörfer, P Schlattmann, L Foster Page, WM Thomson, and S Paris. Socioeconomic inequality and caries: a systematic review and meta-analysis. *Journal of dental research*, 94(1):10–18, 2015.
- [28] Furqan Shaukat, Gulistan Raja, and Alejandro F Frangi. Computer-aided detection of lung nodules: a review. *Journal of Medical Imaging*, 6(2):020901, 2019.
- [29] Muktabh Mayank Srivastava, Pratyush Kumar, Lalit Pradhan, and Srikrishna Varadarajan. Detection of tooth caries in bitewing radiographs using deep learning. *arXiv preprint arXiv:1711.07312*, 2017.
- [30] Robert M Stephan. Intra-oral hydrogen-ion concentrations associated with dental caries activity. *Journal of dental research*, 23(4):257–266, 1944.
- [31] Martin L Tangel, Chastine Fatichah, Fei Yan, Janet P Betancourt, M Rahmat Widianto, Fangyan Dong, and Kaoru Hirota. Dental classification for periapical radiograph based on multiple fuzzy attribute. In *2013 Joint IFSA World Congress and NAFIPS Annual Meeting (IFSA/NAFIPS)*, pages 304–309. IEEE, 2013.
- [32] Shubhangi Vinayak Tikhe, Anjali Milind Naik, Sadashiv D Bhide, T Saravanan, and KP Kaliyamurthie. Algorithm to identify enamel caries and interproximal caries using dental digital radiographs. In *2016 IEEE 6th International Conference on Advanced Computing (IACC)*, pages 225–228. IEEE, 2016.

- [33] Solmaz Valizadeh, Mostafa Goodini, Sara Ehsani, Hadis Mohseni, Fateme Azimi, and Hooman Bakhshandeh. Designing of a computer software for detection of approximal caries in posterior teeth. *Iranian Journal of Radiology*, 12(4), 2015.
- [34] UK Vural and S Gökalp. Diagnostic methods for dental caries used by private dental practitioners in ankara. *Nigerian Journal of Clinical Practice*, 20(3):382–387, 2017.
- [35] Anne Waugh and Allison Grant. *Ross & Wilson Anatomy and physiology in health and illness E-book*. Elsevier Health Sciences, 2014.
- [36] Robert L Weiss and Albert H Trithart. Between-meal eating habits and dental caries experience in preschool children. *American Journal of Public Health and the Nations Health*, 50(8):1097–1104, 1960.
- [37] Ann Wenzel. Bitewing and digital bitewing radiography for detection of caries lesions. *Journal of dental research*, 83(1\_suppl):72–75, 2004.
- [38] Domenick T Zero, Margherita Fontana, E Angeles Martínez-Mier, Andréa Ferreira-Zandoná, Masatoshi Ando, Carlos González-Cabezas, and Stephen Bayne. The biology, prevention, diagnosis and treatment of dental caries: scientific advances in the united states. *The Journal of the American Dental Association*, 140:25S–34S, 2009.